UNIVERSIDADE FEDERAL DE PERNAMBUCO

CENTRO DE CIÊNCIAS BIOLÓGICAS

REDE NORDESTE DE BIOTECNOLOGIA

ANA CAROLINA MATOS DA SILVA DIAS

DESENVOLVIMENTO DE PLATAFORMAS SENSORAS PARA DETECÇÃO ELETROQUÍMICA DO ANTÍGENO NS1 DO VÍRUS DA DENGUE

Recife

2015

ANA CAROLINA MATOS DA SILVA DIAS

DESENVOLVIMENTO DE PLATAFORMAS SENSORAS PARA DETECÇÃO ELETROQUÍMICA DO ANTÍGENO NS1 DO VÍRUS DA DENGUE

Tese apresentada ao Programa de Pós-Graduação em Biotecnologia da Rede Nordeste de Biotecnologia, Universidade Federal de Pernambuco, como parte dos requisitos exigidos para obtenção do título de Doutor em Biotecnologia.

Orientadora: Profa. Dra. Rosa A. Fireman Dutra

Recife

2015

Catalogação na fonte
Elaine Barroso
CRB 1728

Dias, Ana Carolina Matos da Silva
Desenvolvimento de plataformas sensoras para detecção eletroquímica do antígeno NS1 do vírus da dengue/ Ana Carolina Matos da Silva Dias– Recife: O Autor, 2016.

133 folhas : il., fig., tab.
Orientadora: Rosa A. Fireman Dutra
Tese (doutorado) – Universidade Federal de Pernambuco.
Centro de Ciências Biológicas. Biotecnologia, 2016.

Inclui referências, apêndices e anexos

1. Dengue 2. Nanopartículas 3. Biossensores I. Dutra, Rosa A. Fireman (orientadora) II. Título

616.91852 CDD (22.ed.) UFPE/CCB-2016-044

ANA CAROLINA MATOS DA SILVA DIAS

DESENVOLVIMENTO DE PLATAFORMAS SENSORAS PARA DETECÇÃO ELETROQUÍMICA DO ANTÍGENO NS1 DO VÍRUS DA DENGUE

APROVADA EM 06/05/2015

Banca Examinadora:

Prof.ª Dr.ª Rosa Amália Fireman Dutra

(Depto. de Engenharia Biomédica, UFPE) – 1ª Examinadora.

Prof.ª Dr.ª Maria Tereza dos Santos Correia

(Depto. de Bioquímica, UFPE) – 2ª Examinadora.

Prof.ª Drª. Marli Tenório Cordeiro

(Centro de Pesquisas Aggeu Magalhães) – 3ª Examinadora.

Prof.ª Dr.ª Madalena Carneiro da Cunha Areias

(Depto. de Química, UFPE) – 4ª Examinadora.

Prof. Dr. Ranilson de Souza Bezerra

(Depto. de Bioquímica, UFPE) – 5º Examinador.

Prof.ª Dr.ª Patrícia Maria Guedes Paiva

(Depto. de Bioquímica, UFPE) – Membro suplente.

Prof.ª Dr.ª Adriana Fontes

(Depto. de Biofísica, UFPE) – Membro suplente.

Recife

2015

Aos meus pais Airton e Gerlane e irmãs Amanda e Elaine

por todo amor, carinho e dedicação...

Ao meu marido Marcelo pelo amor, companheirismo e incentivo...

... dedico.

AGRADECIMENTOS

A Deus, por ter me guiado e iluminado meu caminho para que eu alcançasse mais um objetivo em minha vida e pela força para superar os obstáculos encontrados nesta caminhada.

À professora e orientadora Rosa Fireman Dutra, pela confiança, orientação e dedicação dispensados desde o início da minha carreira científica.

Aos colegas do Laboratório de Pesquisa em Diagnóstico (LAPED), com os quais foram divididos os últimos anos de aprendizado, pela contribuição de acrescentar conhecimentos a este trabalho e pelos momentos de descontração e apoio.

Aos professores e funcionários da RENORBIO, que contribuíram para a formação do meu caráter e conduta científica.

À Fundação de Amparo à Ciência e Tecnologia do Estado de Pernambuco (FACEPE) e ao Conselho Nacional de Desenvolvimento Científico e Tecnológico (CNPq), pelo apoio financeiro.

Aos funcionários do Centro de Tecnologias Estratégicas do Nordeste (CETENE), pela cooperação na realização de serviços técnicos de microscopia eletrônica, espectroscopia por infravermelho, entre outros.

“Nenhuma luta haverá jamais de me embrutecer, nenhum cotidiano será tão pesado a ponto de me esmagar, nenhuma carga me fará baixar a cabeça. Quero ser diferente, eu sou, e se não for, me farei.”

(Caio Fernando Abreu)

RESUMO

A infecção pelo vírus dengue (DENV) é uma das doenças tropicais mais negligenciadas e de maior importância de saúde pública no mundo. Novos métodos de diagnóstico da doença têm sido estudados através da detecção da proteína NS1 do DENV. O antígeno NS1 é um importante marcador precoce da fase aguda da dengue, secretado em altas concentrações pelo vírus no sangue de pessoas infectadas logo nos primeiros dias, porém, não é muito utilizado na rotina laboratorial para diagnóstico da doença devido ao alto custo dos ensaios. A presente tese descreve o desenvolvimento de duas plataformas sensoras eletroquímicas baseadas em eletrodos impressos (EIs) modificados com nanomateriais para detecção do antígeno NS1 do DENV. Os EIs foram confeccionados utilizando-se a impressão de tinta de carbono sobre o polietileno tereftalato (PET), suporte para impressão dos moldes. Inicialmente, foram estudados os efeitos de nanotubos de carbono e sua contribuição na transferência de elétrons, condutividade e aumento de área eletroativa da plataforma sensora. O estudo foi baseado na incorporação de nanotubos de carbono funcionalizados com grupos carboxílicos à tinta de carbono. Para detecção do NS1, um imunoensaio do tipo "sanduíche" foi realizado, no qual a captura específica do NS1 pôde ser avaliada através das reações redox da enzima peroxidase conjugada ao anticorpo. Uma faixa linear entre 0,04 μg/mL e 2 μg/mL de NS1 foi obtida, indicando boa performance analítica do imunossensor, com coeficiente de correlação linear de 0,996 ($p<0.0001$, $n=8$) e limite de detecção de 0,012 μg/mL de NS1. Posteriormente, foi investigada a contribuição de nanopartículas metálicas no desenvolvimento de sensores eletroquímicos livres de marcação. Foram utilizadas nanopartículas de ouro (NPsAu) funcionalizadas com grupos amina para a imobilização covalente de anticorpos. Na síntese das NPsAu, foi utilizado o polietilenoimina como agente redutor e funcionalizante para promover uma ligação amida com o anticorpo anti-NS1. O imunossensor desenvolvido mostrou curva de calibração com faixa de concentração linear entre 0,1 μg/mL e 2 μg/mL de NS1 ($r = 0,995$, $p<0.0001$, $n=7$) e limite de detecção de 0,03 μg/mL de NS1. A contribuição dos nanomateriais para as plataformas sensoras desenvolvidas mostrou-se efetiva na sensibilidade analítica, devido ao aumento de área eletroativa e maior quantidade de anticorpos imobilizados. A aplicação destes nanomateriais nos imunossensores proporciona novas alternativas de diagnóstico para detecção da proteína NS1 do DENV.

Palavras-chave: eletrodo impresso, nanotubos de carbono, nanopartículas de ouro, dengue, antígeno NS1.

ABSTRACT

Infection by Dengue Virus (DENV) is one of the most neglected tropical diseases and of higher importance of public health worldwide. New methods of diagnosis of the disease have been studied through the detection of NS1 protein of DENV. NS1 antigen is an important early marker of acute dengue infection secreted in high concentrations by the virus in the blood of infected people in first days, however it is not widely used in the laboratory routine for diagnosis of the disease due to high cost of assays. The present thesis describes the development of two electrochemical sensor platforms based on screen-printed electrodes (SPEs) modified with nanomaterials for detection of NS1 antigen of DENV. SPEs were prepared using carbon ink printing on the polyethylene terephthalate (PET), support for molds printing. Initially, the effects of carbon nanotubes and their contribution to the electron transfer, conductivity and increase of electroactive area of the sensor platform were studied. The study was based on the incorporation of carbon nanotubes functionalized with carboxylic groups to the carbon ink. For NS1 detection, a sandwich-type immunoassay was carried out, wherein the specific capture of NS1 may be assessed by redox reactions of peroxidase enzyme conjugated to the antibody. A linear range between 0.04 μg/mL and 2 μg/mL NS1 was obtained, indicating good analytical performance of the immunosensor, with linear correlation coefficient of 0.996 ($p<0.0001$, $n=8$) and limit of detection of 0.012 μg/mL NS1. Subsequently, the contribution of metal nanoparticles in the development of label-free electrochemical sensors was investigated. Gold nanoparticles (AuNPs) functionalized with amine groups were used for covalent immobilization of antibodies. In the synthesis of AuNPs, polyethyleneimine was used as a reducing and functionalizing agent to promote an amide bond with anti-NS1 antibody. The developed immunosensor showed calibration curve with linear concentration range between 0.1 μg/mL and 2 μg/mL NS1 ($r = 0.995$, $p<0.0001$, $n = 7$) and limit of detection of 0.03 μg/mL NS1. The contribution of nanomaterials for the sensor platforms developed proved effective in the analytical sensitivity due to the increase of electroactive area and larger amount of immobilized biomolecules. The application of these nanomaterials in immunosensors provides new alternatives of diagnosis for detection of NS1 protein of DENV.

Keywords: screen-printed electrode, carbon nanotubes, gold nanoparticles, dengue, NS1 antigen.

LISTA DE ILUSTRAÇÕES

Figura 1 - Ilustração do mosquito transmissor da dengue no Brasil, *Aedes aegypti*..... 17
Figura 2 - Número médio de casos de dengue nos trinta países/territórios mais endêmicos reportados para OMS, 2004-2010. 19
Figura 3 - Número de casos de dengue no Brasil de 1990 a 2012. 20
Figura 4 - Ficha de investigação de dengue para notificação dos casos da doença no Brasil. 21
Figura 5 - Genoma do vírus dengue. 23
Figura 6 - Representação esquemática do período de detecção, após início dos sintomas, do antígeno NS1 e dos anticorpos IgM e IgG, na infecção primária e na infecção secundária da dengue..... 24
Figura 7 - Representação esquemática dos componentes de um biossensor..... 27
Figura 8 – (a) Ilustração esquemática da estrutura de um anticorpo em forma de Y, onde DV = domínio variável, DC = domínio constante, $F(ab')_2$ = fragmentos de ligação ao antígeno e Fc = fragmento de não ligação ao antígeno; (b) estrutura tridimensional do anticorpo. 28
Figura 9 – Estrutura do PEI ramificado. 33
Figura 10 - Nanopartículas de ouro com diferentes tamanhos, variando de 5 a 100 nm. ... 36
Figura 11 - Esquema ilustrativo das rotas de síntese de nanopartículas de ouro: *top down* e *bottom up*..... 37
Figura 12 - Esquema básico de uma célula eletroquímica tri-eletródica: (a) eletrodo de referência Ag/AgCl (KCl Sat.), (b) eletrodo impresso de carbono como eletrodo de trabalho e (c) eletrodo auxiliar de platina..... 39
Figura 13 - Representação gráfica de um típico voltamograma cíclico de um sistema reversível obtido pela técnica de VC, onde Epa = potencial de pico anódico, Epc = potencial de pico catódico, Ipa = corrente de pico anódico e Ipc = corrente de pico catódico. 41
Figura 14 - Voltametria de onda quadrada: (1) forma de aplicação do potencial e (2) voltamogramas esquemáticos de um sistema reversível. 42

LISTA DE ABREVIATURAS, SIGLAS E SÍMBOLOS

AFM – Microscopia de força atômica, do inglês "*Atomic Force Microscopy*"

ATR – Refletância total atenuada, do inglês "*Attenuated Total Reflectance*"

DC – Domínio constante

DENV – Vírus dengue, do inglês "*Dengue Virus*"

DLS – Espalhamento dinâmico de luz, do inglês "*Dynamic Light Scattering*"

DNA – Ácido desoxirribonucleico, do inglês "*Deoxyribonucleic acid*"

DRX – Difração de raios X

DV – Domínio variável

EDC – 1-etil-3-(dimetilaminopropil) carbodiimida

EIs – Eletrodos impressos, do inglês "*Screen-printed electrodes*" (SPE)

ELISA – Ensaio imunoenzimático, do inglês "*Enzyme-Linked Immunosorbent Assay*"

FTIR – Espectroscopia no infravermelho por transformada de Fourier, do inglês "*Fourier Transform Infrared Spectroscopy*"

Ig – Imunoglobulina

IgA – Imunoglobulina A

IgD – Imunoglobulina D

IgE – Imunoglobulina E

IgG – Imunoglobulina G

IgM – Imunoglobulina M

IUPAC – União Internacional de Química Pura e Aplicada, do inglês "*International Union of Pure and Applied Chemistry"*

kb – Kilobases

kDa – Kilo Daltons

MET – Microscopia eletrônica de transmissão

MEV – Microscopia eletrônica de varredura

MWCNTs – Nanotubos de carbono de múltiplas paredes, do inglês "*Multi-Walled Carbon Nanotubes*"

μm – Micrômetros

NHS – N-hidroxissuccinimida

nm – Nanômetros

NPsAu – Nanopartículas de ouro

NS1 – Não estrutural 1, do inglês *"Nonstructural 1"*

NS2 – Não estrutural 2, do inglês *"Nonstructural 2"*

NS3 – Não estrutural 3, do inglês *"Nonstructural 3"*

NS4 – Não estrutural 4, do inglês *"Nonstructural 4"*

NS5 – Não estrutural 5, do inglês *"Nonstructural 5"*

NTCs – Nanotubos de carbono

OMS – Organização Mundial de Saúde

PET – Politereftalato de etila

PCR – Reação em Cadeia da Polimerase, do inglês "*Polymerase Chain Reaction"*

PEI – Polietilenoimina

RNA – Ácido ribonucleico, do inglês "*Ribonucleic acid*"

RT-PCR – Reação em Cadeia de Polimerase via Transcriptase Reversa

SINAN – Sistema de Informação de Agravos de Notificação

SWCNTs – Nanotubos de carbono de parede simples, do inglês "*Single-Walled Carbon Nanotubes*"

UV-vis – Espectroscopia no ultravioleta visível

VC – Voltametria cíclica

VOQ – Voltametria de onda quadrada

vs. – Versus

SUMÁRIO

1 INTRODUÇÃO 14
2 REVISÃO DE LITERATURA 17
2.1 Dengue 17
2.1.1 Dados epidemiológicos 18
2.1.2 Agente etiológico 22
2.1.3 Diagnóstico laboratorial 23
2.2 Biossensores 26
2.3 Imunossensores 27
2.3.1 Imunossensores para diagnóstico de dengue 29
2.4 Construção e caracterização de plataformas sensoras 30
2.4.1 Preparação de eletrodos 30
2.4.1.1 Limpeza eletródica 32
2.4.1.2 Funcionalização de superfícies e imobilização de anticorpos 32
2.4.1.3 Emprego de filmes poliméricos 33
2.4.1.4 Uso de Nanomateriais 34
2.4.1.4.1 Nanotubos de carbono 34
2.4.1.4.2 Nanopartículas de ouro 35
2.4.2 Caracterização eletroquímica 38
2.4.2.1 Sistema eletroquímico 38
2.4.2.2 Técnicas eletroquímicas 39
2.4.3 Caracterização estrutural 43
2.4.4 Caracterização morfológica 44
3 OBJETIVOS 46
3.1 Objetivo geral 46
3.2 Objetivos específicos 46
4 MANUSCRITOS 47
4.1 Manuscrito 1 47
4.2 Manuscrito 2 54
5 CONCLUSÕES 79
6 REFERÊNCIAS 80
7 APÊNDICES 96

7.1 Apêndice A – Artigo publicado, ao longo do Doutorado, no periódico *Optics Express*, com fator de impacto de 3,525. 96
7.2 Apêndice B – Artigo publicado, ao longo do Doutorado, no periódico *Talanta*, com fator de impacto 3,511. 105
7.3 Apêndice C – Artigo publicado, ao longo do Doutorado, no periódico *Journal of Chemical Technology and Biotechnology*, com fator de impacto 2,494. 111
8 ANEXOS 118
Anexo A – Normas para publicação no periódico *Colloids and Surfaces B: Biointerfaces*, fator de impacto 4.287. 118

1 INTRODUÇÃO

A infecção pelo vírus dengue (DENV) constitui-se numa das doenças tropicais mais negligenciadas e de maior importância para saúde pública no mundo (LINARES et al., 2013). É uma doença de amplo espectro clínico, incluindo desde formas brandas até quadros graves, causada por diferentes sorotipos do vírus pertencente ao gênero *Flavivirus*, família *Flaviviridae* (MINISTÉRIO DA SAÚDE$_a$, 2005).

As epidemias da doença geram uma grande carga econômica devido aos gastos com hospitalização, assistência médica, medidas de prevenção e controle do vetor, entre outros (OMS, 2012). Sendo assim, a detecção precoce da fase aguda é crucial para o manejo clínico do paciente. As principais técnicas utilizadas para o diagnóstico de dengue são: isolamento do vírus em cultura de células, detecção do RNA viral usando Reação em Cadeia da Polimerase (PCR, do inglês *Polymerase Chain Reaction*), exames sorológicos para detecção de anticorpos IgM e IgG e detecção de antígenos virais, como, por exemplo, o antígeno NS1. O isolamento do vírus é utilizado como "padrão ouro" para o diagnóstico e sorotipagem das infecções pelo DENV, mas este método é demorado e trabalhoso, não sendo conveniente para determinação rápida em surtos ou semi-surtos epidêmicos. Os kits comerciais de imunoensaio para diagnóstico sorológico de dengue exigem longos tempos de ensaio (na ordem de algumas horas) e processamento da amostra (incluindo extensas lavagens e etapas de incubação), além da medida ser realizada de modo indireto (LAPPHRA et al., 2008) e de não fornecer um diagnóstico precoce, já que é necessário esperar até o quinto dia ou mais de início da febre para detectar os anticorpos (VAZQUEZ et al., 2010). O teste de PCR é considerado hoje o método mais sensível, porém, apresenta um alto custo e difícil manejo, sobretudo em surtos epidêmicos, quando há necessidade de inquéritos em locais remotos. Um método de diagnóstico que pode equilibrar o custo e a especificidade do teste é a detecção do antígeno NS1 do DENV. A proteína não-estrutural 1 (NS1) é um importante marcador para o diagnóstico da doença na fase aguda, encontrada em altas concentrações no sangue de pacientes infectados (ALCON et al., 2002).

Alguns imunossensores para diagnóstico de dengue através da detecção da proteína NS1 do vírus já são descritos na literatura. Os métodos de detecção são variados, incluindo sensores piezoelétricos, ópticos (CAMARA et al., 2013) e

eletroquímicos. Cavalcanti et al. (2012) descreveram um imunossensor eletroquímico baseado em eletrodo de filme de ouro obtido de CDs (*compact disk*) graváveis (CDtrodo) para detecção do NS1. O imunossensor mostrou uma resposta linear de 1 a 100 ng/mL de NS1. Silva et al. (2014_a) desenvolveram um imunoeletrodo nanoestruturado empregando nanotubos de carbono e polialilamina para detecção da proteína NS1 do DENV. O sensor apresentou um limite de detecção de 0,035 μg/mL NS1, que é bem menor que a concentração encontrada no sangue do paciente nos primeiros dias da doença.

No desenvolvimento de imunossensores eletroquímicos, a tecnologia dos eletrodos impressos (EIs) tem atendido à demanda do mercado oferecendo um completo sistema de eletrodos projetados com grande simplicidade e economia (BERGAMINI, OLIVEIRA; ZANONI, 2005). Essa tecnologia constitui uma ferramenta de custo reduzido, metodologia simplificada, passível de portabilidade e com capacidade de produção em massa (WANG et al., 2008). O método de confecção dos EIs baseia-se na deposição de tintas sobre substratos inertes, sendo bastante adequada para produção em massa de eletrodos descartáveis (FANJUL-BOLADO et al., 2008). Os EIs podem ser modificados através da imobilização da biomolécula na sua superfície ou misturando a tinta com a biomolécula, a fim de melhorar a resposta eletroquímica para o analito de interesse (HART et al., 2004; BERGAMINI; OLIVEIRA; ZANONI, 2005).

Com o intuito de aperfeiçoar esses dispositivos, a modificação dos EIs com nanomateriais tem sido bastante estudada (FANJUL-BOLADO et al., 2007). Dentre os vários tipos de nanomateriais, os nanotubos de carbono (NTCs) e as nanopartículas de ouro (NPsAu) têm recebido especial atenção devido às suas propriedades químicas, eletrônicas e mecânicas, que os tornam potencialmente úteis em diversas aplicações (JEYKUMARI; NARAYANAN, 2009). Os nanotubos possuem alta condutividade elétrica, estrutura única, força mecânica significativa e boa estabilidade química (YANG et al., 2010). As NPsAu também têm sido aplicadas para preparar eletrodos modificados por apresentarem propriedades como facilidade de síntese, controle do tamanho, facilidade de modificação química da sua superfície, excelente condutividade eletrônica e estabilidade química e elevada relação superfície/volume (COSTA, 2012; YANG et al., 2011; WANG et al., 2014). Quando aplicados em sensores eletroquímicos, os NTCs e as NPsAu são capazes de melhorar a reatividade eletroquímica de importantes espécies eletroativas e aumentar a área superficial do eletrodo, permitindo uma maior quantidade de biomoléculas imobilizadas e,

consequentemente, uma maior sensibilidade do método de detecção (SILVA et al., 2014_b).

Nesta Tese, são apresentados dois imunossensores eletroquímicos baseados na tecnologia de EIs modificados com nanomateriais (nanotubos de carbono e nanopartículas de ouro) para detecção do antígeno NS1 do DENV. Nas plataformas sensoras desenvolvidas, os anticorpos anti-NS1 foram imobilizados na superfície eletródica de modo orientado, facilitando seu reconhecimento pelo antígeno, porém, a resposta foi obtida através de dois sistemas diferentes (marcado e não-marcado). Os processos de preparação, caracterização e desenvolvimento das plataformas sensoras são descritos neste trabalho visando contribuir com o desenvolvimento de novas metodologias para detecção do antígeno NS1 do DENV.

2 REVISÃO DE LITERATURA

2.1 Dengue

A dengue é classificada hoje como a arbovirose mais importante do mundo, segundo a Organização Mundial de Saúde (OMS, 2012). É uma doença infecciosa aguda de gravidade variável, causada por um arbovírus do gênero *Flavivirus* (MINISTÉRIO DA SAÚDE, 2005_a).

O *Aedes aegypti* (Figura 1) é o principal vetor de dengue no mundo, porém, os mosquitos *Aedes albopictus* e *Aedes polynesiensis* podem atuar como vetores em algumas localidades. O *Aedes albopictus*, vetor de manutenção da dengue na Ásia, já se encontra presente nas Américas, com ampla dispersão no Brasil, mas até o momento não foi associado à transmissão da dengue nas Américas (MINISTÉRIO DA SAÚDE, 2005_a; BARBOSA, RODRIGUES &CABRAL, 2010). É considerado um vetor em potencial na transmissão da dengue na Ásia e no Pacífico, cujo habitat natural são os meios silvestres. Já o *Aedes aegypti* é principalmente encontrado em áreas tropicais e subtropicais do mundo, inclusive no Brasil, pois as condições do meio ambiente favorecem seu desenvolvimento e proliferação (TAUIL, 2002). O mosquito é doméstico e antropofílico, com aparência inofensiva, mede menos de um centímetro e seu corpo e pernas possuem a cor café ou preta com listras brancas. Utiliza-se preferencialmente de depósitos artificiais de água parada para colocar seus ovos e possui atividade hematofágica diurna, sendo assim, ele costuma picar nas primeiras horas da manhã e nas últimas da tarde, evitando o sol forte, mas, mesmo nas horas quentes, ele pode atacar à sombra, dentro ou fora de casa (OLIVEIRA, 2012).

Figura 1 - Ilustração do mosquito transmissor da dengue no Brasil, *Aedes aegypti*.

Fonte: MUHAMMAD MAHDI KARIM (www.micro2macro.net).

A dengue pode apresentar um amplo espectro de manifestações clínicas, incluindo desde quadros oligossintomáticos, podendo mostrar-se com sintomas clássicos, até formas hemorrágicas (SOUZA, 2008). A primeira manifestação é a febre, geralmente alta (39 a 40ºC) de início abrupto, associada à cefaleia, adinamia, mialgias, artralgias, dor retro-orbitária, com presença ou não de exantema e/ou prurido. Anorexia, náuseas, vômitos e diarreia podem ser observados por dois a seis dias. Alguns pacientes podem evoluir para formas graves da doença e passam a apresentar sinais de alarme da dengue, como o surgimento de manifestações hemorrágicas espontâneas e plaquetopenia (plaquetas <100.000/mm^3) (MINISTÉRIO DA SAÚDE, 2005_b).

A partir de janeiro de 2014, O Ministério da Saúde passou a utilizar a nova classificação da dengue, determinada pela OMS desde 2009. As denominações dengue clássico, febre hemorrágica do dengue (Grau I, II, III e IV), dengue com complicação e síndrome de choque do dengue deixaram de ser utilizadas. Atualmente, são usadas as seguintes denominações: dengue, dengue com sinais de alarme e dengue grave. Essa nova denominação se mostrou mais sensível para captar os casos graves e, com isso, deverá contribuir para melhorar o diagnóstico e estadiamento/manejo dos pacientes, para uma possível redução da letalidade por dengue e uma maior aproximação entre vigilância epidemiológica e assistência (MINISTÉRIO DA SAÚDE, 2014).

2.1.1 Dados epidemiológicos

A dengue é uma grande preocupação para a saúde pública nas regiões tropicais e subtropicais do mundo. Nos últimos cinquenta anos, a dengue se propagou de nove para cem países e sua incidência mundial aumentou trinta vezes, convertendo-se na doença viral transmitida por mosquito de mais rápida propagação (OMS, 2012).

A OMS estima que 50-100 milhões de infecções por dengue ocorram a cada ano. Atualmente, quase metade da população mundial vive em países onde a dengue é endêmica, e mais de 390 milhões de pessoas no mundo padecem da doença a cada ano, quando, há meio século, só foram registrados 15 mil casos em nove países do sudeste asiático. A taxa de letalidade varia entre os países, mas pode ser tão elevada quanto 10-15% em alguns e menor que 1% em outros (NUNES, 2011). A Figura 2 demonstra o número médio de casos de dengue nos países mais endêmicos, entre os anos de 2004 e 2010.

Figura 2 - Número médio de casos de dengue nos trinta países/territórios mais endêmicos reportados para OMS, 2004-2010.

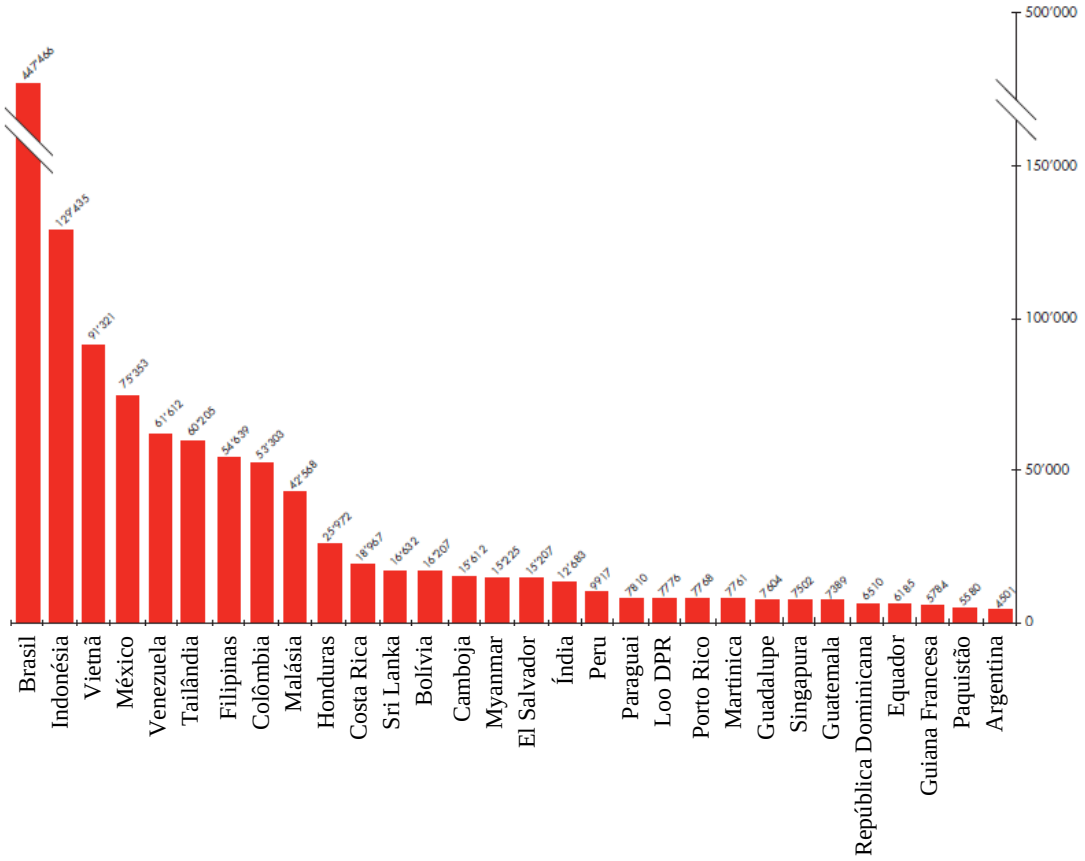

Fonte: OMS, 2012.

Durante quase sessenta anos (1923 a 1981), o Brasil não apresentou registro de casos de dengue em seu território, porém, em 1976, o *Aedes aegypti* foi reintroduzido no país devido a falhas na vigilância epidemiológica e mudanças sociais e ambientais decorrentes da urbanização acelerada dessa época (ZARA, 2012).

O DENV-1, que causou grandes epidemias nas Américas na década de 70, foi reintroduzido no Brasil em 1981-82 em Boa Vista (RR), juntamente com o DENV-4. Contudo, a epidemia foi limitada. Por outro lado, em 1986, 1990 e 2002 os DENV-1, DENV-2 e DENV-3, respectivamente, foram introduzidos no estado do Rio de Janeiro, sendo responsáveis por grandes epidemias que se espalharam para outros estados do Brasil (NOGUEIRA, ARAÚJO & SCHATZMAYR, 2007; TEIXEIRA et al., 2009).

Mais recentemente, o DENV-4 foi detectado em algumas cidades do Brasil. Infelizmente, a reintrodução do DENV-4 era esperada pela vigilância epidemiológica brasileira, pois, países fronteiriços como a Venezuela e a Colômbia possuem grande circulação de DENV-4 (FIGUEIREDO et al., 2008).

Segundo o Ministério da Saúde (2014$_a$), na última década foram registrados cerca de cinco milhões de casos de dengue no Brasil, com cerca de oitocentas mortes, sendo quase um milhão de casos somente no ano de 2010. Em 2013, o número foi quase três vezes maior que o número de casos em 2012. A Região Sudeste concentra o maior número de casos (63,6% do total). Em seguida, vêm as regiões Centro-Oeste (18,4%), Nordeste (9,9%), Sul (4,8%) e Norte (3,3%). A Figura 3 mostra o número de casos de dengue no Brasil entre o período de 1990 a 2012.

Figura 3 - Número de casos de dengue no Brasil de 1990 a 2012.

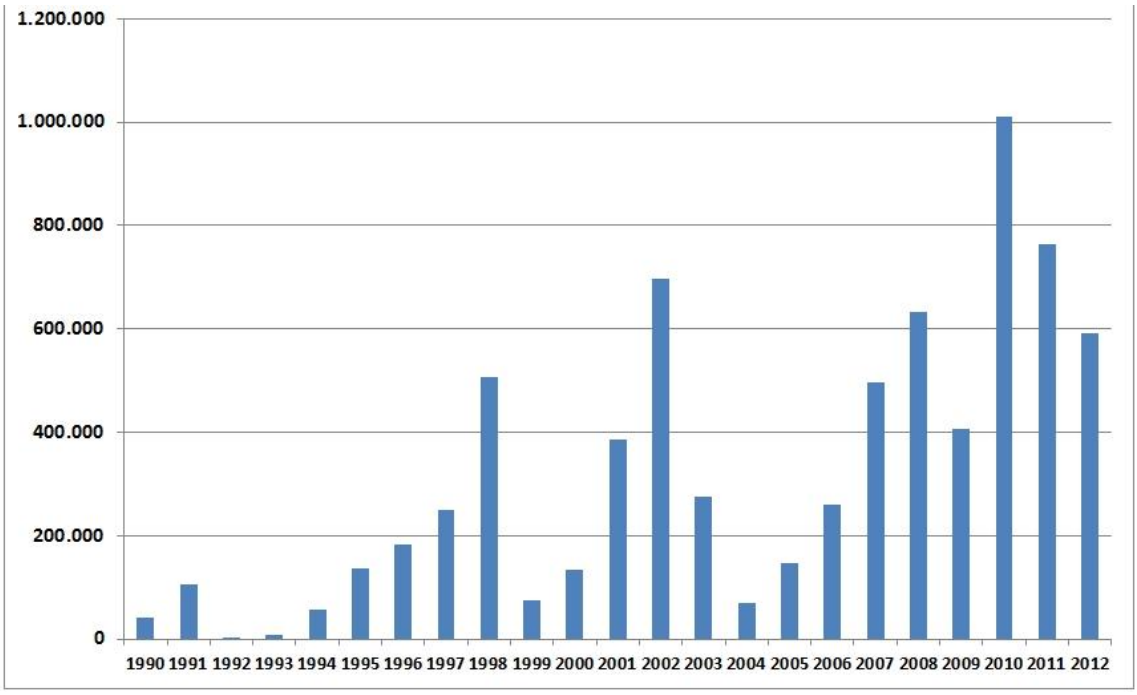

Fonte: http://portal.saude.gov.br/portal/arquivos/pdf/dados_dengue_classica_2012_at032013

Há vários fatores apontados como responsáveis pelo ressurgimento de epidemias e pela expansão geográfica de dengue nas últimas décadas. Entre eles, estão: crescimento populacional descontrolado, urbanização desordenada, meios de transporte mais rápidos, maior atividade de viajantes carreadores de vírus, deficiência de saneamento, aumento de lixo e coleta inadequada de resíduos sólidos, mudanças climáticas, facilidade de adaptação das populações de mosquitos transmissores que leva a um aumento da dispersão e densidade vetorial, falhas no combate aos mosquitos, velocidade de circulação e replicação viral, hiperendemicidade, ausência de vacina e, por fim, desestruturação da saúde pública nos últimos 30 anos (BELARMINO, 2013).

As notificações e análises epidemiológicas dos casos de dengue no Brasil são feitas hoje com base na nova classificação da OMS, por intermédio do Sistema de Informação de Agravos de Notificação (SINAN), através do preenchimento da ficha de investigação de dengue (Figura 4) (MINISTÉRIO DA SAÚDE, 2014_b).

Figura 4 - Ficha de investigação de dengue para notificação dos casos da doença no Brasil.

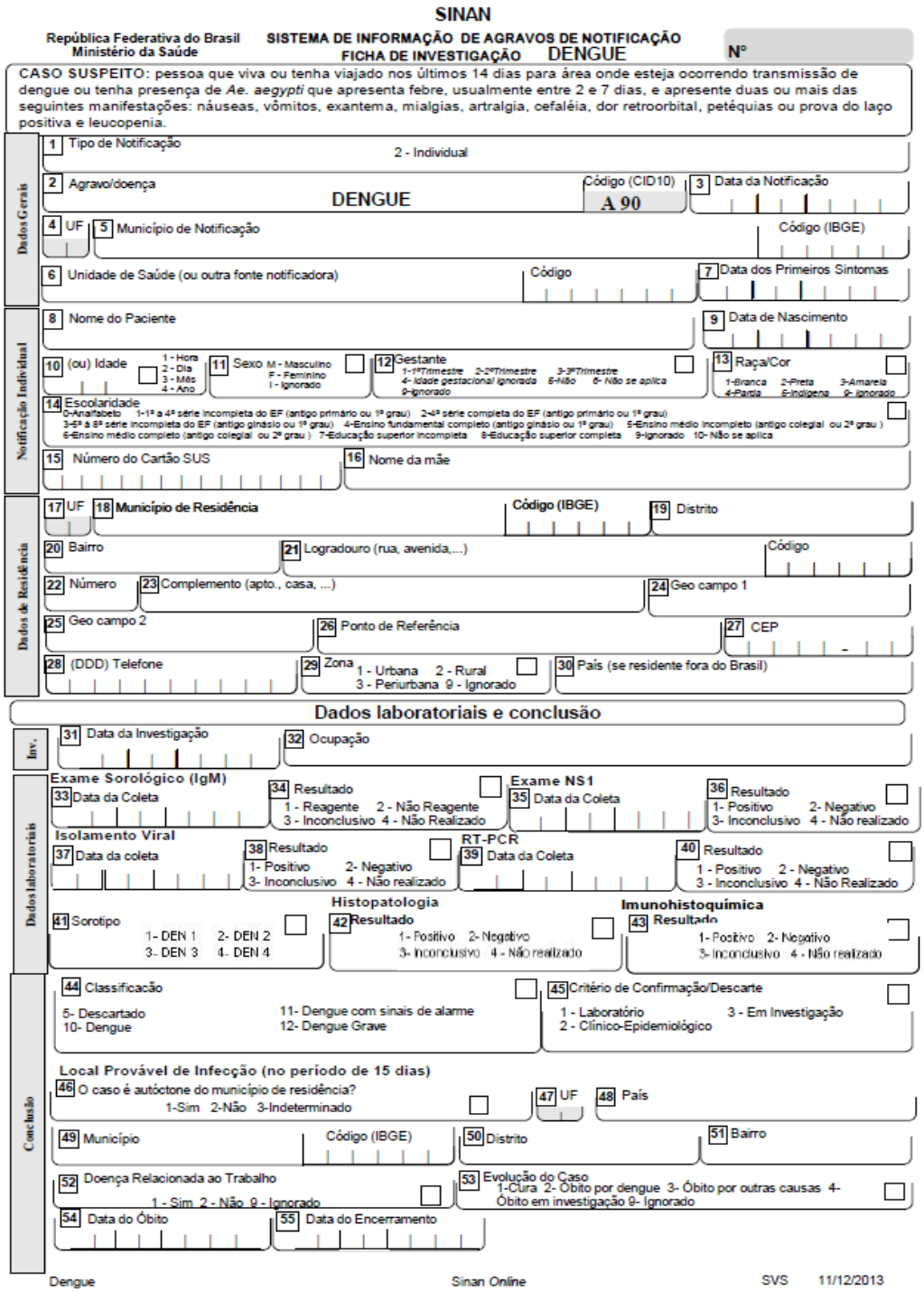

Fonte: http://dtr2004.saude.gov.br/sinanweb/

2.1.2 Agente etiológico

A dengue é causada por quatro sorotipos do vírus dengue (DENV-1, DENV-2, DENV-3 e DENV-4) pertencentes ao gênero *Flavivirus*, da família *Flaviviridae*. Recentemente, foi identificado um novo tipo do vírus que, até então, está relacionado apenas com um único surto que ocorreu em 2007 na Malásia (NORMILE, 2013). Segundo Rothman (2011), os sorotipos do vírus são relacionados geneticamente e antigenicamente, causando as mesmas manifestações clínicas.

Indivíduos que são infectados por um sorotipo do DENV (infecção primária) tornam-se imunes ao mesmo, porém, não aos outros tipos que restam. Portanto, o mesmo indivíduo pode ser infectado por outro sorotipo do DENV, adquirindo uma infecção secundária, cujo risco de desenvolver a forma grave da doença é muito maior (VERHAGEN & GROOT, 2014).

O vírus fica incubado no organismo de dois a quinze dias (com médias de cinco a sete dias), apenas após esse período é que surgirão os primeiros sintomas da doença. O período em que o mosquito pode ser contaminado ao picar um humano infectado vai desde um dia antes de aparecer a febre no homem até seis dias depois da manifestação desta (NUNES, 2011).

O DENV é composto por uma fita única de RNA de 11 kb de comprimento e apresenta-se como uma partícula esférica, com diâmetro de 40-50 nm, recoberta por um envelope de lipopolissacarídeo (GUZMAN et al., 2010). O genoma do vírus (Figura 5) contém o código de três proteínas estruturais (capsídeo [C], proteína da membrana [M] e glicoproteína do envelope viral [E]) e sete outras proteínas não estruturais (NS1, NS2a, NS2b, NS3, NS4a, NS4b e NS5) (SINGHI, KISSOON & BANSAL, 2007). As três proteínas estruturais localizam-se no capsídeo viral, sendo a proteína C responsável pela forma esférica da partícula viral, e a proteína M, juntamente com a proteína E, forma o revestimento externo dessa partícula. A glicoproteína E também é responsável pela ligação às células hospedeiras e pelo reconhecimento de anticorpos específicos. Entre as proteínas não estruturais, a NS1 é uma das mais conservadas, o que parece importante para manter a viabilidade do vírus. A NS1 contribui na replicação do RNA viral e se expressa na superfície das células infectadas. Durante a fase aguda da infecção pelo DENV, a NS1 pode ser encontrada intracelularmente nas organelas ou secretada na fase fluida, alcançando a circulação periférica (YOUNG et al., 2000). A glicoproteína

NS1 (46 kDa) é expressa em duas formas: uma forma ancorada na membrana e uma forma secretada (LINDENBACH & RICE, 2003).

Figura 5 - Genoma do vírus dengue.

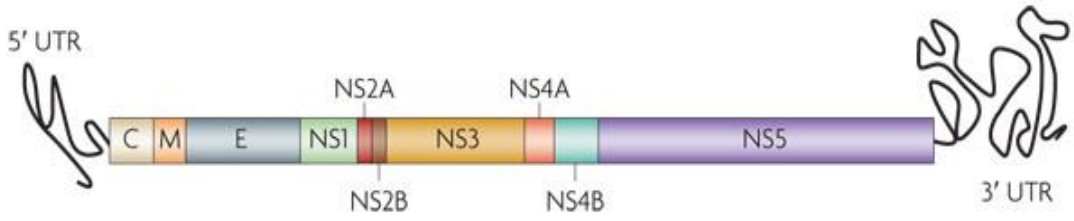

Fonte: GUZMAN et al., 2010.

2.1.3 Diagnóstico laboratorial

O diagnóstico rápido e preciso da dengue é primordial para detecção precoce de casos graves, diagnóstico diferencial com outras doenças infecciosas e triagem clínica dos pacientes (PHUONG et al., 2009). Os testes rápidos aceleram o diagnóstico específico, facilitando as ações de atividades de vigilância e auxiliando no controle de surtos (OMS, 2009).

O diagnóstico da doença pode ser realizado através do isolamento do vírus em cultura de células (YAMADA et al., 2002), da detecção do RNA viral usando PCR (Reação em Cadeia de Polimerase) (NAJIOULLAH, VIRON & CÉSAIRE, 2014), de exames sorológicos (RIVETZ et al., 2009) e pela detecção de antígenos virais (AHMED & BROOR, 2014). A escolha do método de diagnóstico depende da finalidade para a qual o teste é feito (por exemplo, diagnóstico clínico, levantamento epidemiológico, desenvolvimento de vacinas), o tipo de instalações laboratoriais e conhecimentos técnicos disponíveis, o custo e o tempo da coleta da amostra.

Após o início da doença, o vírus pode ser detectado no soro, no plasma e nas células circulantes por quatro a cinco dias (Figura 6). Nessa fase, o isolamento do vírus e a detecção por ácidos nucleicos ou antígenos podem ser usados no diagnóstico da infecção. Após o final da fase aguda, a sorologia é o método de escolha para o diagnóstico (HALSTEAD, 2007; BUCHY et al., 2007). A resposta do anticorpo à infecção ocorre de acordo com a imunidade do paciente. Quando a infecção ocorre em pacientes que não foram infectados antes, o paciente desenvolve uma resposta primária

caracterizada por um lento aumento de anticorpos específicos. As imunoglobulinas M (anticorpos IgM) são as primeiras imunoglobulinas a aparecerem. Esses anticorpos são detectáveis em 50% dos pacientes por três a cinco dias após o início da doença, aumentando para 80% no quinto dia, e 99% no décimo. Os níveis de IgM atingem um pico cerca de duas semanas após o início dos sintomas e então declinam geralmente a níveis indetectáveis por dois a três meses. Os níveis das imunoglobulinas G (anticorpos IgG) geralmente são detectados em baixas concentrações no final da primeira semana da doença, aumentando lentamente, e permanecem detectáveis após vários meses (OMS, 2009).

Figura 6 - Representação esquemática do período de detecção, após início dos sintomas, do antígeno NS1 e dos anticorpos IgM e IgG, na infecção primária e na infecção secundária da dengue.

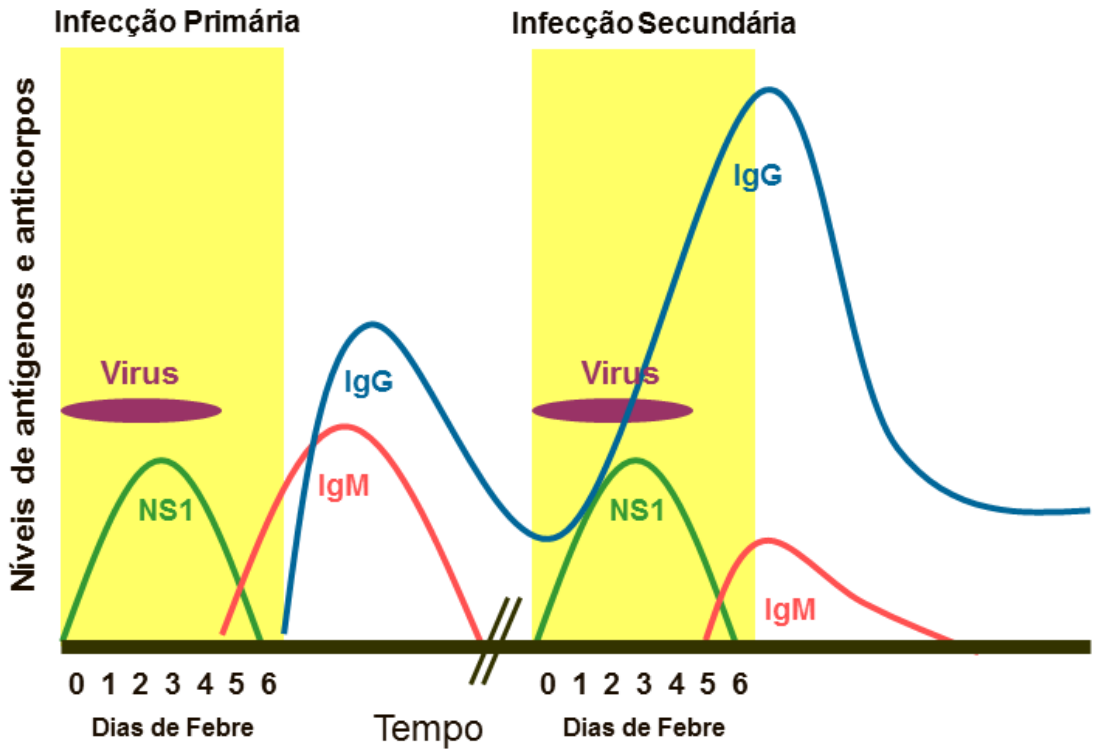

Fonte: CDC.

O diagnóstico através do isolamento do vírus é um método bastante confiável e sensível, porém, requer laboratório especializado para cultura de células, tem um longo tempo de duração (mais de uma semana, podendo demorar até 30 dias), não sendo útil para diagnóstico rápido dos pacientes, e tem menor sensibilidade quando comparado com os métodos moleculares (HUNSPERGER et al., 2014). A detecção do RNA viral

através da RT-PCR também permite o diagnóstico precoce durante a fase febril. No entanto, o procedimento da técnica é complicado; além disso, o resultado não é imediato, dificultando seu uso rotineiro nos laboratórios de diagnóstico clínico (AHMED; BROOR, 2014).

Imunoensaios para detecção de anticorpos IgG e IgM contra o vírus dengue são comumente usados para diagnóstico da infecção em laboratórios de rotina; dentre eles, destacam-se a detecção de anticorpos IgM através do MAC-ELISA e o ELISA-IgG indireto (SHU; HUANG, 2004). O MAC-ELISA tornou-se o método mais utilizado em razão da facilidade de execução, podendo ser processado um número elevado de amostras, com um significativo número de casos confirmados em uma única coleta de soro (SOUZA, 2008). No entanto, uma das limitações destas técnicas é a variação do limite de detecção durante a fase aguda da doença, além da sua vulnerabilidade a reações cruzadas causadas por anticorpos contra flavivírus relacionados, como o vírus do Oeste do Nilo, da encefalite viral e da febre amarela (SCHILLING et al., 2004; HUHTAMO et al., 2010).

Os métodos de diagnóstico baseados na detecção do antígeno NS1 do DENV são capazes de identificar a doença na fase aguda, de modo rápido e confiável (ZHANG et al., 2014). O Antígeno NS1 está presente nos quatro sorotipos do DENV, circula em altas concentrações no sangue, tanto na infecção primária quanto na secundária, podendo ser detectado a partir do 1º dia do surgimento da febre e pode ficar circulante por até nove dias após o aparecimento dos sintomas. Portanto, sua detecção contribui decisivamente para o diagnóstico/tratamento imediato, prevenindo a evolução para formas mais graves da doença (SOUZA, 2008). O diagnóstico precoce, graças à detecção do antígeno NS1 do DENV, permite uma melhora considerável no cuidado do paciente, possibilitando também um tratamento apropriado antecipadamente, evitando sérias complicações e ajudando a limitar a disseminação da doença (KUMARASAMY et al., 2007; MCBRIDE, 2009).

Recentemente, diferentes métodos de detecção do antígeno NS1 têm sido desenvolvidos. Entre os principais disponíveis no mercado, estão os kits de ELISA *Panbio® Dengue Early ELISA*, *Standard Diagnostics Dengue NS1 Ag ELISA* e *Bio-Rad™ Platelia Dengue NS1 Ag-ELISA* (ZHANG et al., 2014). Esses kits de ELISA são usados para detectar antígenos NS1 no soro do paciente, permitindo o diagnóstico precoce da dengue, porém são testes para uso em laboratório que demandam técnicos qualificados e não permitem uma resposta em tempo real. Portanto, faz-se necessário o

incentivo ao desenvolvimento de novas tecnologias para o diagnóstico da infecção por DENV, com o objetivo de diminuir o tempo de execução e os custos do ensaio, sem perder a especificidade e a sensibilidade dos métodos convencionais.

2.2 Biossensores

O primeiro biossensor, demonstrado por CLARK e LYONS (1962), foi produzido para determinação da glicose. A tecnologia desse trabalho foi transferida e desenvolvida pela *Yellow Springs Instrument Company* levando ao lançamento comercial do primeiro biossensor de glicose em 1975 (YELLOW SPRINGS INSTRUMENT COMPANY, 2012). Desde então, várias formas de biossensores para glicose foram desenvolvidas (RICCI; PALLESCHI, 2005), assim como muitas outras tecnologias de dispositivos (ARYA; DATTA; MALHOTRA, 2008; SILVA et al., 2013; JAHANSHAHI et al., 2014;).

Nos últimos anos, os biossensores têm mostrado um grande potencial para aplicações na área de medicina (HASAN et al., 2014). A sua utilização traz uma série de vantagens. Primeiro, os biossensores são altamente sensíveis, pois, as biomoléculas frequentemente possuem uma elevada afinidade pelos seus alvos. Em segundo lugar, o reconhecimento biológico normalmente é bastante seletivo; como exemplo, tem-se o sistema chave-fechadura da enzima e seu substrato (NEWMAN; SETFORD, 2006). Em terceiro lugar, devido ao desenvolvimento da moderna indústria eletrônica, tem sido relativamente fácil desenvolver dispositivos biossensores baratos, integrados e prontos para o uso. Os biossensores melhoram a capacidade de detectar diversas biomoléculas, como antígenos, anticorpos e enzimas, sendo particularmente úteis para pequenas clínicas e, principalmente, para análises *point-of-care* (SONG; XU; FAN, 2006).

De acordo com a definição proposta pela União Internacional de Química Pura e Aplicada (IUPAC), um biossensor é um dispositivo integrado capaz de fornecer uma informação analítica específica quantitativa ou qualitativa através do uso de um elemento de reconhecimento biológico que está em contato direto com o elemento transdutor (Figura 7) (OSMA; STOYTCHEVA, 2014). O biorreceptor é o elemento biológico imobilizado (por exemplo, enzima, sonda de DNA, anticorpo) que é reconhecido pelo analito (por exemplo, substrato da enzima, DNA complementar, antígeno). O transdutor é usado para converter o sinal (bio)químico resultante da

interação do analito com o biorreceptor em um sinal elétrico. A intensidade do sinal gerado é diretamente ou inversamente proporcional à concentração do analito. Transdutores eletroquímicos são frequentemente usados no desenvolvimento de biossensores. Esses sistemas oferecem algumas vantagens, como baixo custo, simples design e pequena dimensão (AHMET; AHLATCIOĞLU; İPEK, 2012).

Figura 7 - Representação esquemática dos componentes de um biossensor.

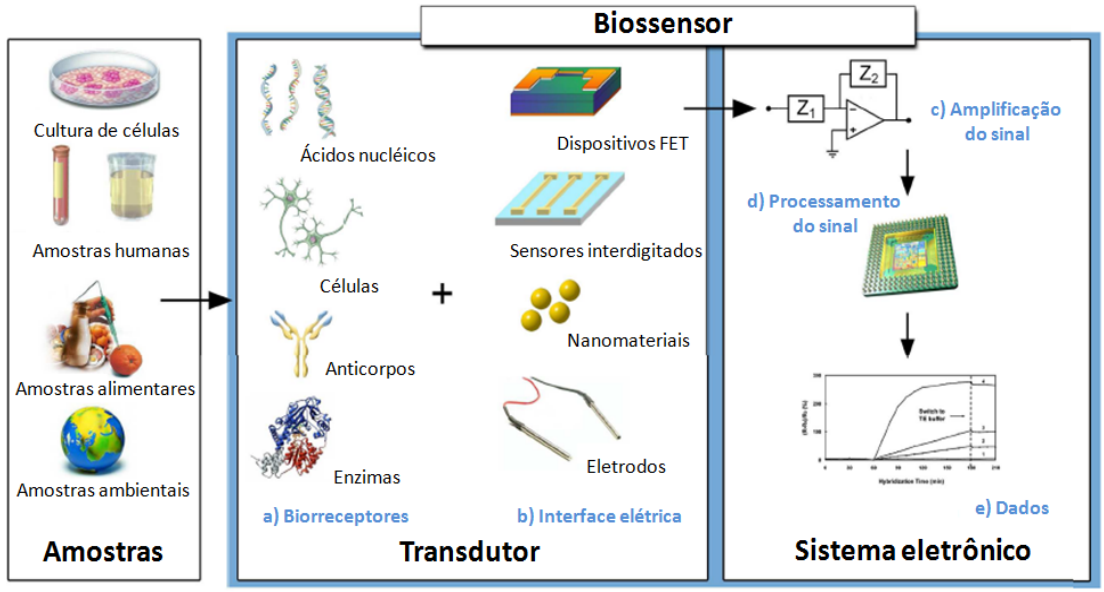

Fonte: GRIESHABER et al., 2008.

2.3 Imunossensores

Os biossensores aplicados aos imunoensaios são denominados de imunossensores. Eles são baseados na especificidade entre antígenos e anticorpos, que são imobilizados na superfície sensora, com o objetivo de detectar seletivamente a concentração do respectivo alvo (YUAN; CHAI; TANG, 2007).

Os anticorpos são uma família de glicoproteínas conhecidas como imunoglobulinas (Ig). Existem geralmente cinco classes distintas de glicoproteínas (IgA, IgG, IgM, IgD e IgE), sendo a IgG a classe mais abundante (aproximadamente 70%) e mais frequentemente utilizada em técnicas imunoanalíticas (ZHANG; JU; WANG, 2008).

Como mostrado na Figura 8, a IgG é uma molécula em forma de “Y” baseada em dois tipos distintos de cadeias polipeptídicas. O peso molecular da cadeia menor (leve) é de aproximadamente 25 kDa, enquanto que o da cadeia maior (pesada) é de

aproximadamente 50 kDa. Em cada molécula de IgG, existem duas cadeias leves e duas cadeias pesadas unidas por pontes dissulfeto. Cada cadeia leve tem um domínio variável (DV) e um domínio constante (DC), enquanto cada cadeia pesada consiste de um domínio variável e três constantes. Os DVs, em ambos os tipos de cadeia, são as regiões mais importantes no que diz respeito à interação de ligação antígeno-anticorpo. Em geral, a molécula de anticorpo pode ser dividida em dois fragmentos principais: o fragmento de não-ligação ao antígeno, denominado Fc, e o fragmento de ligação ao antígeno, F(ab) (2 fragmentos) (ZHANG, JU & WANG, 2008). As porções F(ab) possuem grupos amino que interagem com o sítio de ligação do antígeno. Já as extremidades da porção Fc possuem grupamentos carboxílicos que são utilizados para permitir uma imobilização orientada dos anticorpos à superfície sensora deixando os sítios de ligação ao antígeno livres (RICCARDI, COSTA & YAMANAKA, 2002).

Figura 8 – (a) Ilustração esquemática da estrutura de um anticorpo em forma de Y, onde DV = domínio variável, DC = domínio constante, $F(ab')_2$ = fragmentos de ligação ao antígeno e Fc = fragmento de não ligação ao antígeno; (b) estrutura tridimensional do anticorpo.

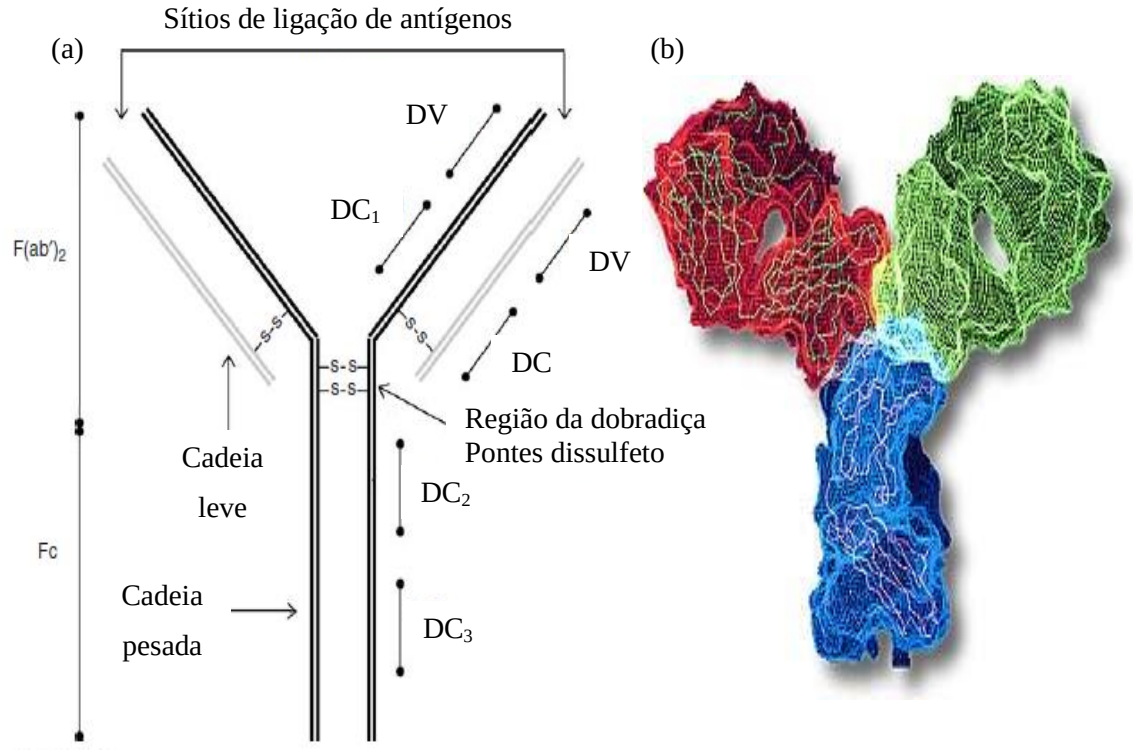

Fonte: (a) Adaptada de ZHANG; JU; WANG, 2008; (b) http://updates.clltopics.org/wp-content/uploads/2009/10/Ofatumumab.JPG

A fim de facilitar a ligação dos anticorpos à superfície sensora, os grupamentos carboxílicos terminais dos anticorpos podem ser ativados com uma mistura de 1-etil-3-

(3-dimetilamino propil) carbodiimida (EDC) e N-hidroxisuccinimida (NHS). O EDC reage com o grupo carboxílico dos anticorpos para formar um intermediário amino-reativo o-acilisoureia. A adição do NHS estabiliza o intermediário amino-reativo, que aumenta a eficiência de reações de acoplamento mediadas pelo EDC. Assim, a ativação in situ dos anticorpos deixa a porção Fc terminada com um NHS-éster, que é susceptível ao ataque nucleofílico dos grupos amina na superfície do eletrodo para formar uma ligação amida estável (PEI et al., 2010). A ligação pelo terminal Fc do anticorpo melhora a sensibilidade e seletividade de imunossensor devido à imobilização orientada dos anticorpos (RICCARDI; COSTA; YAMANAKA, 2002).

Os imunossensores podem ser classificados de acordo com o uso de marcadores conjugados aos anticorpos ou antígenos como marcados ou não-marcados (*label-free*). A maioria dos imunossensores marcados descritos na literatura exploram o princípio dos imunoensaios competitivos e do tipo "sanduíche" utilizando enzimas, fluoróforos e nanopartículas como marcadores. Apesar de seletivo, este método implica em maiores custos operacionais, incluindo aumento das etapas de processamento da amostra (RAPP; GRUHL; LÄNGE, 2010). Nos ensaios *label-free*, a resposta do imunossensor é obtida diretamente após o evento de biorreconhecimento. Neste tipo de ensaio, a interação antígeno-anticorpo na superfície sensora pode ser obtida através do monitoramento de mudanças nas propriedades elétricas da plataforma sensora (BACKMAN et al., 2005).

2.3.1 Imunossensores para diagnóstico de dengue

Alguns imunossensores para dengue utilizando diferentes métodos de detecção estão descritos na literatura. Camara et al. (2013) descreveram um sensor de fibra óptica baseado na ressonância de plásmon de superfície localizado utilizando nanopartículas de ouro imobilizadas na extremidade da fibra. O sensor foi capaz de detectar antígenos NS1 em diferentes concentrações, com um limite de quantificação de 0,074 μg/mL. Silva et al. (2014_b) desenvolveram um imunossensor eletroquímico baseado em eletrodo impresso de carbono modificado com tiofeno para diagnóstico precoce de dengue. O sensor apresentou uma faixa linear nas concentrações de 0,05 a 0,6 μg/mL de NS1 (r=0,991), com limite de detecção de 0,015 μg/mL. Nos dois trabalhos, o nível de NS1 detectado está dentro da faixa encontrada nos soros dos pacientes com dengue. No

entanto, ainda se faz necessário o uso de novas tecnologias no desenvolvimento de dispositivos sensores portáteis, de menor custo e rápida resposta para uso no diagnóstico precoce da dengue na fase aguda.

2.4 Construção e caracterização de plataformas sensoras

O desenvolvimento de plataformas sensoras é um processo minucioso que envolve as seguintes etapas: confecção dos eletrodos, limpeza da superfície eletródica, funcionalização da superfície e imobilização de biomoléculas. Cada uma dessas etapas deve ser devidamente caracterizada para padronização dos parâmetros e, consequentemente, melhor desempenho do biossensor.

A caracterização é uma importante etapa no processo de construção do biossensor e pode ser classificada em: eletroquímica, estrutural ou morfológica. As técnicas utilizadas para caracterização da plataforma sensora são ferramentas valiosas para o controle de qualidade, bem como para a avaliação das diferentes etapas e parâmetros do biossensor.

2.4.1 Preparação de eletrodos

A escolha do material para o eletrodo de trabalho, cuja superfície sofrerá a modificação, é um aspecto muito importante para preparação do sensor. Esta matriz deve apresentar características eletroquímicas apropriadas e também ser adequada para o método de imobilização selecionado (VIEIRA, 2007). A importância da escolha do material do eletrodo de trabalho também se deve ao fato de que as respostas obtidas estão relacionadas com reações redox que ocorrem na superfície ou interface eletrodo-solução. Desta forma, o analito de interesse pode interagir com a superfície eletródica, resultando numa transferência de elétrons. Entretanto, se a transferência for muito lenta, não ocorrer ou ocorrer em valores de potencial fora da janela de potencial do eletrodo, é possível realizar uma modificação na superfície eletródica a fim de melhorar a resposta final, onde o analito irá interagir diretamente com o agente modificante (GALLI et al., 2006).

Diversos materiais podem ser utilizados na preparação do eletrodo de trabalho, tais como: ouro, prata, mercúrio, grafite, carbono vítreo, nanotubos de carbono,

nanofios de ouro, nanopartículas de ouro, nanopartículas de óxido metálico, pasta de carbono, entre outros (FERREIRA et al., 2013).

A construção de eletrodos à base de carbono tem recebido cada vez mais atenção devido às características atrativas do carbono, tais como versatilidade, baixo custo e uma ampla janela de potencial. Via de regra, eles possuem um menor custo, são mecanicamente estáveis e estão disponíveis em uma variedade de formas, tais como carbono vítreo, pasta de carbono, fibras de carbono, diamante dopado, grafite pirolítico, carbono vítreo reticulado, fulerenos, nanotubos de carbono, entre outros (MARTINS, 2005). O eletrodo de carbono, na sua forma mais simples, é bom condutor de eletricidade. Os materiais de carbono formam ligações covalentes fortes com alguns modificadores de superfície favorecendo o desenvolvimento de eletrodos modificados (CARIDADE, 2008).

A tecnologia de EIs é uma técnica amplamente utilizada, confiável e bem estabelecida para fabricação de sensores eletroquímicos, que permite o desenvolvimento de dispositivos miniaturizados, portáteis e sensíveis (HAYAT; MARTY, 2014). É um método atraente para a produção em massa de sensores, apresentando como vantagens: flexibilidade no design, automação no processo, portabilidade, boa reprodutibilidade, uma grande variedade de materiais e custos reduzidos (ALONSO-LOMILLO et al., 2009; FANJUL-BOLADO et al., 2007).

Os EIs são preparados através da deposição de tintas na superfície do substrato (vidro, plástico ou cerâmica) na forma de finos filmes. Sua flexibilidade deve-se ao seu elevado número de possíveis modificações. Diferentes tintas podem ser usadas para se obter eletrodos de diferentes dimensões e formas (AHMET; AHLATCIOĞLU; İPEK, 2012). Tintas de carbono ou metálicas (platina, ouro e prata) têm sido comumente utilizadas como filme condutor na fabricação de EIs. Em particular, as tintas de carbono têm se destacado devido às suas características atrativas citadas acima (USLU & OZKAN, 2007; ZHANG et al., 2011). As tintas de carbono, em geral, são compostas por partículas de grafite, polímeros aglutinantes e outros aditivos. Diferenças na sua composição (tipo, tamanho e carga das partículas de grafite), impressão, condições de cura e pré-tratamentos podem afetar a transferência de elétrons e o desempenho analítico dos EIs (GORNALL; COLLYER; HIGSON, 2009). Estudos realizados por Wang et al. (1998) demonstraram que a composição e a preparação dos eletrodos utilizando diferentes tintas comerciais de carbono têm profunda influência sobre o comportamento eletroquímico dos sensores impressos.

2.4.1.1 Limpeza eletródica

Uma variedade de procedimentos mecânicos e químicos de limpeza de superfície de eletrodos tem sido descrita na literatura. Eles diferem de acordo com o material eletródico e com o tipo de molécula que vai ser imobilizada na superfície. Os procedimentos mais comumente utilizados são: pré-anodização (CUI et al., 2001), limpeza com solução piranha (H_2O_2:H_2SO_4 na proporção 1:3), tratamento eletroquímico (ALONSO-LOMILLO et al., 2009) e polimento mecânico com lixa apropriada e alumina (SILVA et al., 2010). Esses métodos de limpeza são aplicados na superfície do eletrodo com o objetivo de diminuir a sua rugosidade ou de ativar a superfície (WEI et al., 2007).

Assim como os demais eletrodos, principalmente os de platina e de ouro, os eletrodos de carbono também apresentam problemas de adsorção em suas superfícies, oriundos dos processos eletródicos que resultam na passivação do eletrodo e, consequentemente, no decréscimo do sinal analítico. Para contornar este problema, muitos pesquisadores sugerem a aplicação de pulsos de potenciais (positivos e/ou negativos), de maneira a eliminar o material indesejável da superfície do eletrodo. Além disso, o tratamento eletroquímico prévio pode atuar no desempenho do eletrodo de modo a favorecer, por exemplo, a transferência de elétrons das espécies envolvidas (FELIX, 2009).

2.4.1.2 Funcionalização de superfícies e imobilização de anticorpos

Para permitir a construção de imunossensores com alta sensibilidade e especificidade, é essencial uma incorporação estável dos elementos de reconhecimento e esta tem sido uma etapa crítica no desenvolvimento destes dispositivos analíticos. Isso porque os anticorpos ou antígenos, quando imobilizados, precisam reter a maior parte de sua atividade biológica, para que o imunossensor possa apresentar sensibilidade significativa para o composto alvo (CHEN; DONG, 2003). Uma característica desejável do método de imobilização escolhido é que ele resulte em um anticorpo imobilizado que seja orientado com o mínimo de impedimento estérico para interagir favoravelmente com seu antígeno alvo, ou seja, com as porções F(ab) livres. Evidentemente, esta característica tem uma influência direta sobre o nível de sensibilidade do imunossensor

(FOWLER et al., 2008). Além disso, uma eficiente imobilização do material biológico também garante uma maior estabilidade ao imunossensor.

Para fornecer uma matriz de imobilização de anticorpos adequada, as superfícies eletródicas podem ser funcionalizadas com diferentes modificadores. A funcionalização é caracterizada pela modificação química da superfície, proporcionando condições ótimas para a ancoragem dos anticorpos (SRIVASTAVA et al., 2014).

2.4.1.3 Emprego de filmes poliméricos

A funcionalização da superfície eletródica pode ser realizada através da deposição de filmes poliméricos ou do crescimento de cadeias poliméricas sobre a superfície do eletrodo. Devido à grande variedade das características dos polímeros, suas propriedades podem ser exploradas conforme o interesse (SRIVASTAVA et al., 2014).

Os filmes poliméricos geralmente contêm grupos funcionais que podem ser utilizados para imobilizar biomoléculas via grupo funcional específico, podendo ser hidroxilas (-OH), carbonilas (-C=O), carboxilas (-COOH) e aminas primárias ($-NH_2$) (TUNCAGIL et al., 2009). Dentre os polímeros mais estudados para aplicação em biossensores, estão: polipirrol, politiofeno, polianilina, polialilamina e polietilenoimina (PEI).

O PEI é um polieletrólito catiônico rico em amina (Figura 9), com valor de pKa= 5,5, altamente ramificado com grande densidade de cargas, que contém grupos amina primários, secundários e terciários, aproximadamente na proporção 25/50/25, respectivamente (NOSSER, 2013). Além de ser utilizado para funcionalização da superfície eletródica, o PEI pode ser usado engenhosamente tanto como um agente funcional como um agente redutor e protetor para formação de nanopartículas de ouro (ZHU et al., 2013).

Figura 9 – Estrutura do PEI ramificado.

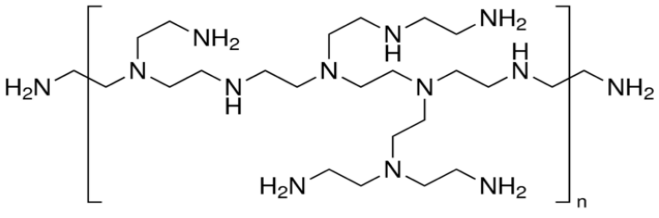

Fonte: http://www.sigmaaldrich.com/catalog/product/aldrich/408727?lang=pt&region=BR

A funcionalização de nanopartículas utilizando o PEI é facilitada pela sua capacidade de formar complexos com polieletrólitos catiônicos e íons metálicos. Esses polímeros agem como agente controlador de tamanho e conferem grande estabilidade aos nanocompósitos (JAHAN et al., 2014). Outra vantagem da utilização do PEI é a obtenção de grupos funcionais na superfície das nanopartículas através da síntese em uma única etapa. O PEI forma um escudo carregado positivamente ao redor das NPsAu prevenindo sua agregação em solução e fornecendo uma ligação para ancorar as nanopartículas sobre a superfície do eletrodo (FRASCA et al., 2012).

2.4.1.4 Uso de Nanomateriais

A descoberta de novos nanomateriais abre diversos caminhos no campo do desenvolvimento dos sensores eletroquímicos. A aplicação dos nanomateriais integrados à superfície dos eletrodos tem possibilitado o desenvolvimento de sensores mais sensíveis e reprodutíveis (KERMAN et al., 2008). Esses materiais promovem o aumento da área reativa e da transferência de elétrons, diminuem o potencial de trabalho do sensor, podendo, consequentemente, contribuir para uma maior estabilidade do elemento biológico (JUBETE et al., 2009). Recentemente, vários tipos de materiais, incluindo nanopartículas metálicas, nanopartículas semicondutoras e NTCs, têm sido utilizados em sensores eletroquímicos (LIU; LIN, 2007).

2.4.1.4.1 Nanotubos de carbono

Os NTCs foram sintetizados pela primeira vez por Sumio Iijima, em 1991, e despertaram grande interesse nos mais diversos ramos da ciência. Eles são formados pelo enrolamento de folhas de grafeno formando um cilindro, podendo ser classificados em duas categorias: nanotubos de carbono de parede simples (SWCNTs, do inglês: *Single-Walled Carbon Nanotubes*) ou nanotubos de carbono de múltiplas paredes (MWCNTs, do inglês: *Multi-Walled Carbon Nanotubes*) (IJIMA, 2002).

Os MWCNTs são constituídos de vários cilindros concêntricos de folhas de grafeno, com cerca de 3,4 Å de espaçamento entre as camadas. MWCNTs geralmente têm 2 – 100 nm de diâmetro, já a única folha de grafeno do SWCNT tem cerca de 0,2 – 2 nm de diâmetro. O comprimento dos nanotubos pode variar de micrômetros a centímetros (JEYKUMARI; NARAYANAN, 2009).

As propriedades dos NTCs como, por exemplo, alta área específica, flexibilidade e elevadas resistência mecânica e condutividade térmica, permitiram supor uma variada gama de aplicações desde o armazenamento de energia e hidrogênio até aplicações médicas (OLIVEIRA, 2009). No entanto, eles requerem funcionalização orgânica para aumentar sua solubilidade em solventes orgânicos e compatibilidade com polímeros orgânicos (CHANG; LIU, 2010). A funcionalização de NTCs através de suas paredes, pontas ou por encapsulamento tem sido vista como uma forma de explorar o seu potencial na nanotecnologia. Os nanotubos funcionalizados podem ter propriedades eletrônicas e mecânicas que são substancialmente diferentes dos nanotubos não funcionalizados e este fenômeno é explorado para uso em sensores, dispositivos eletrônicos e eletromecânicos em escala nanométrica devido à sua grande resistência e flexibilidade mecânica (SOUZA FILHO; FAGAN, 2007).

Os NTCs possuem excelentes propriedades para aplicação em superfícies sensoras, tais como: aumento da área eletroativa da superfície eletródica e da reatividade eletroquímica de importantes espécies eletroativas e, por meio disso, facilitam as reações de transferência de elétrons envolvendo proteínas e superfícies previamente funcionalizadas (KIM et al., 2006). Superfícies nanoestruturadas apresentam excelente condutividade elétrica e acentuada propriedade eletrocatalítica. Tais características podem aumentar a cinética de transferência de elétrons ao eletrodo, bem como melhorar a reprodutibilidade e a sensibilidade do imunossensor (YÁÑEZ-SEDEÑO et al., 2010).

2.4.1.4.2 Nanopartículas de ouro

Com o desenvolvimento da nanotecnologia, a utilização de NPsAu na medicina, principalmente em estudos envolvendo diagnósticos, tem crescido rapidamente nos últimos anos. Na área de imunossensores, as NPsAu têm sido aplicadas para preparar eletrodos modificados por apresentarem propriedades únicas, tais como biocompatibilidade, síntese relativamente simples, controle do tamanho das nanopartículas, facilidade de modificação química da sua superfície, excelente condutividade eletrônica e estabilidade química e elevada relação superfície/volume (COSTA, 2012; YANG et al., 2011; WANG et al., 2014).

As propriedades físicas e químicas das NPsAu são dependentes de fatores como forma, composição, tamanho e natureza da sua superfície. A alteração do tamanho, por

exemplo, é responsável por mudanças consideráveis nas propriedades fundamentais do ouro, como a cor, portanto, as NPsAu podem assumir diferentes cores conforme seu tamanho (Figura 10). Quando estão em solução, as NPsAu apresentam intensa coloração avermelhada, vinho ou arroxeada, contrastando com o ouro metálico amarelo (COSTA, 2012). Diante dessas variáveis, o desenvolvimento de diferentes métodos de síntese e modificação da superfície das nanopartículas são etapas determinantes para o sucesso da sua aplicação.

Figura 10 - Nanopartículas de ouro com diferentes tamanhos, variando de 5 a 100 nm.

Fonte: http://nanocomposix.com/collections/gold-spheres.

Para obtenção de nanopartículas, podem ser utilizadas duas rotas de síntese: *top down* e *bottom up* (Figura 11). Os métodos *top down* envolvem a manipulação do ouro em escala macro, no qual, através de processos físicos, as partículas são quebradas até que estejam em escala nanométrica, porém, são procedimentos limitados em relação ao controle do tamanho e da forma das NPsAu, assim como posterior funcionalização. Em contraste, os métodos *bottom up* são mais simples e possibilitam maior controle sobre o processo (controle de tamanho e forma das NPsAu, material monocristalino e possibilidade de obtenção de partículas em escala de tamanho muito inferior que na rota *top down)*. Na síntese *bottom up*, as NPsAu são originadas a partir de precursores moleculares ou atômicos e a redução desses precursores pode ser biológica, química ou física (GORUP, 2010; OLTEANU et al., 2013). A redução biológica é considerada uma síntese verde e resulta em NPsAu estáveis, mas elas não são uniformes e são sintetizadas de forma relativamente lenta (VETCHINKINA et al., 2013).

Figura 11 - Esquema ilustrativo das rotas de síntese de nanopartículas de ouro: *top down* e *bottom up*.

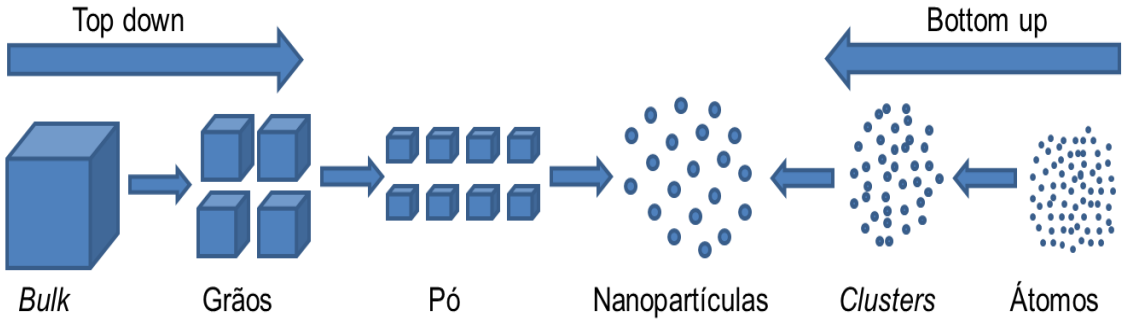

Fonte: Adaptado de GORUP, 2010.

Um exemplo simples e bastante utilizado de síntese de NPsAu, através do processo *bottom up*, é a redução química de uma solução de ácido tetracloroáurico ($HAuCl_4$) com citrato de sódio ou borohidreto de sódio (TURKEVICH; STEVENSON; HILLIER, 1951; FRENS, 1971) em meios aquosos e orgânicos, embora existam métodos mais precisos e avançados (REDDY, 2006). Na síntese por redução química, após a dissolução do $HAuCl_4$, a solução é rapidamente agitada enquanto um agente redutor é adicionado. Isso faz com que íons Au(III) sejam reduzidos a Au(0). À medida que mais e mais íons formam átomos de ouro, a solução se torna supersaturada, e o ouro gradualmente começa a precipitar na forma de subpartículas nanométricas. O restante dos átomos de ouro que se formam mantém as partículas existentes, e se a solução for agitada vigorosamente o suficiente, as partículas serão bastante uniformes em tamanho. Soluções coloidais de NPsAu preparadas por redução com citrato e borohidreto de sódio têm uma coloração vermelho-vinho. Soluções de nanobastões de ouro coloidal têm uma cor azul com diferentes propriedades ópticas (REDDY, 2006). Para evitar que ocorra agregação de partículas, um agente estabilizante, que adere à superfície das nanopartículas, é geralmente adicionado (POPIOLSKI, 2011).

Como as NPsAu tendem a ser instáveis em solução, precauções para evitar a agregação ou precipitação têm resultado no uso de moléculas orgânicas ou polímeros como agentes estabilizantes, que não só evitam a agregação, mas também resultam em nanopartículas estabilizadas e funcionalizadas (ZHAO et al., 2008; JAHAN; MANSOOR; KANWAL, 2014). O uso de espécies estabilizantes poliméricas na síntese de NPsAu tem inspirado estudos de diferentes rotas de síntese para ligar os polímeros às nanopartículas metálicas.

A síntese e funcionalização de NPsAu são facilmente realizadas e têm sido utilizadas em várias aplicações. Geralmente, os grupos funcionais –NH ou –SH de moléculas orgânicas são conhecidos por se ligarem à superfície das NPsAu. A modificação química das superfícies das NPsAu fornece uma eficiente plataforma para melhorar a imobilização de biomoléculas, sejam elas DNA, anticorpos ou enzimas (BRONDANI et al., 2013).

2.4.2 Caracterização eletroquímica

A caracterização eletroquímica baseia-se nos fenômenos associados à transferência de elétrons que ocorre na interface entre a superfície do eletrodo de trabalho e a camada fina de solução adjacente a essa superfície (BRETT; BRETT, 1993). Os métodos eletroanalíticos fazem uso de propriedades elétricas mensuráveis (corrente elétrica, diferenças de potencial, acúmulo interfaciais de carga, entre outros) a partir de fenômenos nos quais uma espécie redox interage física e/ou quimicamente com demais componentes do meio. Tais interações são observadas quando se aplicam perturbações controladas ao sistema através do uso de variáveis que medem as propriedades eletroquímicas (PACHECO et al., 2013).

A caracterização eletroquímica é realizada através do uso de um potenciostato e da célula eletroquímica, empregando uma gama variada de técnicas, tais como voltametria cíclica (VC) e voltametria de onda quadrada (VOQ), voltametria de pulso diferencial e voltametria linear.

2.4.2.1 Sistema eletroquímico

O sistema eletroquímico é composto pelos seguintes componentes: um potenciostato e uma célula eletroquímica.

O potenciostato requer uma célula eletroquímica com três eletrodos: um eletrodo de trabalho, um eletrodo de referência (prata/cloreto de prata - Ag/AgCl ou calomelano saturado - Hg_2Cl_2/Hg) e um eletrodo auxiliar (fio de platina). Esses eletrodos são conectados ao potenciostato e imersos em uma célula eletroquímica contendo a solução da espécie eletroativa de interesse com um excesso de um eletrólito inerte (eletrólito suporte), responsável por garantir o controle difusional das espécies (GANDRA et al., 2004). O eletrodo de referência mantém o potencial do eletrodo de trabalho estável com

o tempo e temperatura, não sendo alterado por pequenas perturbações do sistema, ou seja, pela passagem de corrente. O eletrodo auxiliar estabelece uma conexão com a solução eletrolítica, enquanto o eletrodo de trabalho funciona como elemento transdutor da reação bioquímica (GRIESHABER et al., 2008). O material do eletrodo, a modificação da sua superfície e sua dimensão afetam a capacidade de detecção do sensor. Na Figura 12, pode ser visto um esquema ilustrativo de uma célula eletroquímica composta por três tipos de eletrodos: eletrodo de trabalho, eletrodo de referência e eletrodo auxiliar ou contra-eletrodo (AHMET; AHLATCIOĞLU; İPEK, 2012).

Figura 12 - Esquema básico de uma célula eletroquímica tri-eletródica: (a) eletrodo de referência Ag/AgCl (KCl Sat.), (b) eletrodo impresso de carbono como eletrodo de trabalho e (c) eletrodo auxiliar de platina.

Fonte: SILVA, B. V. M., 2012.

2.4.2.2 Técnicas eletroquímicas

As técnicas eletroquímicas encontram aplicações em diversos campos desde a pesquisa básica até a análise de rotina. Os métodos eletroquímicos possibilitam o estabelecimento de relações diretas entre a concentração do analito e algumas propriedades elétricas, como corrente, potencial, condutividade, resistência e carga elétrica. Como as medidas destas propriedades são facilmente acessíveis experimentalmente, as técnicas eletroquímicas são adequadas para quantificação de espécies de interesse nas diferentes áreas de estudo (SOUZA; MACHADO; AVACA, 2003).

Essas técnicas necessitam de equipamento e eletrodos apropriados, sendo o equipamento referido o potenciostato, que tem a função de controlar o potencial aplicado ao eletrodo de trabalho e permitir a medição da corrente que passa por este (GANDRA et al., 2004).

O comportamento eletroquímico do eletrodo é investigado através do estudo da reação de transferência de elétrons na superfície eletródica utilizando-se uma solução de Ferricianeto/Ferrocianeto de potássio como par de sonda redox.

Neste trabalho, as técnicas eletroquímicas de VC e VOQ foram empregadas para caracterização eletroquímica do imunossensor.

A voltametria é uma técnica eletroanalítica que se baseia nos fenômenos que ocorrem na interface entre a superfície do eletrodo de trabalho e a camada fina de solução adjacente a essa superfície (GANDRA et al., 2004). Essa técnica é classificada como dinâmica, pois a célula eletroquímica é operada na presença de corrente elétrica ($i > 0$) que, por sua vez, é medida em função da aplicação controlada de um potencial. Assim, nessa técnica, as informações sobre o analito são obtidas por meio da medição da magnitude da corrente elétrica que surge entre o eletrodo de trabalho e o eletrodo auxiliar ao se aplicar uma diferença de potencial entre o eletrodo de trabalho e o eletrodo de referência (PACHECO et al., 2013).

Na técnica de VC, o potencial é linearmente variado com o tempo, partindo de um valor inicial até atingir um potencial final. Neste ponto, a varredura é invertida até atingir o seu ponto de partida novamente. Como resultado, obtém-se um registro de corrente em função da variação do potencial, denominado voltamograma cíclico (Figura 13). Os processos redox que acontecem no eletrodo são representados tanto por correntes de picos anódicos (Ipa) e catódicos (Ipc) quanto por potenciais de picos anódicos (Epa) e catódicos (Epc) (KOZAN, 2007).

A técnica de VC pode ser utilizada para caracterização de estudos de modificação da superfície sensora, detalhando importantes informações do sistema, tais como potencial de oxidação e redução da espécie, número de elétrons transferidos, reversibilidade da reação, coeficiente de difusão, etc (BRETT; BRETT, 1993).

Figura 13 - Representação gráfica de um típico voltamograma cíclico de um sistema reversível obtido pela técnica de VC, onde Epa = potencial de pico anódico, Epc = potencial de pico catódico, Ipa = corrente de pico anódico e Ipc = corrente de pico catódico.

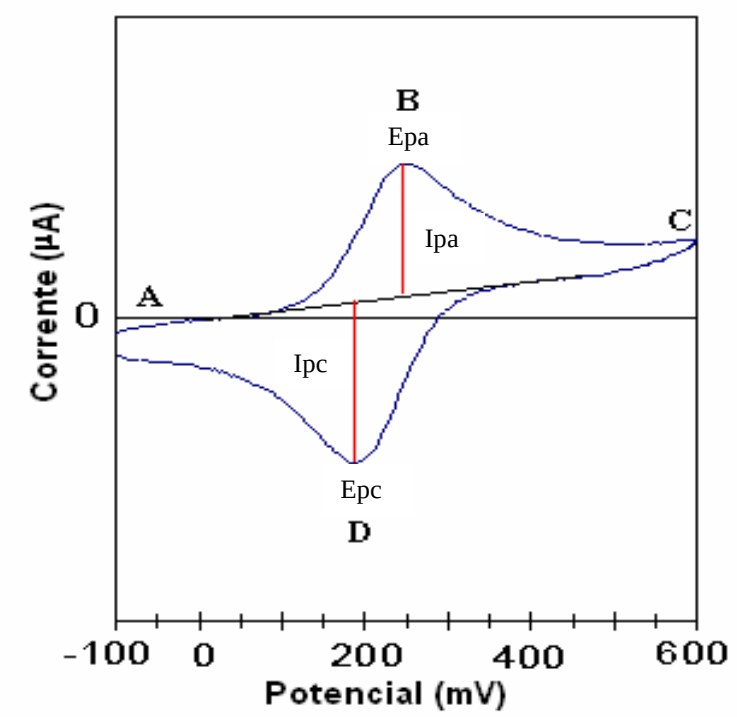

Fonte: Adaptada de PATACAS, 2007.

Para uma reação reversível, ou seja, uma reação que ocorre com velocidade suficientemente alta para estabelecer um equilíbrio dinâmico na interface, as Ipa e Ipc são aproximadamente iguais em valor absoluto, a Ip varia linearmente com a raiz quadrada da velocidade de varredura ($v^{1/2}$), a diferença entre os Ep é aproximadamente 59 mV / *n* e Ep é independente da velocidade de varredura (v). Já em sistemas irreversíveis observa-se uma completa ausência de picos de óxido-redução reversos e deslocamentos do Ep em relação à velocidade de varredura (BRETT; BRETT, 1993; BARD; FAULKNER, 2001). A 25ºC, a corrente de pico é dada pela Equação de Randles-Sevcik:

$$i_p = 2{,}69 \text{ X } 10^5 \, n^{3/2} \, A \, D^{1/2} \, C \, v^{1/2}$$

onde i_p = corrente de pico, n = número de elétrons adicionados ou removidos, A = área do eletrodo (cm^2), D = coeficiente de difusão ($cm^2 \, s^{-1}$), C = concentração (mol cm^{-3}) e v = velocidade de varredura (V s^{-1}) (BARD & FAULKNER, 2001).

Na VC, ao variar o potencial de trabalho, a contribuição da corrente capacitiva torna-se significativa, não distinguível da corrente faradaica da reação, em altas velocidades, o que inviabiliza a análise. Assim, a introdução das técnicas voltamétricas

de onda quadrada e pulso diferencial na área eletroanalítica tem como objetivo minimizar a influência das correntes capacitivas em sistemas voltamétricos baseados na medida de corrente faradaica (BARKER; JENKINS, 1952; BARKER; GARDNER, 1960).

A voltametria de onda quadrada, do inglês *Square Wave Voltammetry*, tem recebido crescente atenção como uma técnica voltamétrica rápida e sensível para análises quantitativas de rotina. É considerada uma técnica voltamétrica de pulso onde a forma do pico de corrente resultante é proveniente da sobreposição de pulsos de potencial de altura *a* (amplitude de pulsos), a uma escada de potenciais de largura *ΔEs* (incremento de varredura de potenciais) e duração *2t* (período). As medidas de corrente são feitas no final dos pulsos diretos e reversos e o sinal obtido, após derivação, é dado como uma intensidade da corrente resultante, apresentando excelente sensibilidade e alta rejeição a correntes capacitivas. O pico voltamétrico resultante apresenta posição, largura e altura características do tipo de sistema redox avaliado (SOUZA et al., 2004). A Figura 14 apresenta a forma de aplicação do potencial da VOQ e os voltamogramas esquemáticos de um processo redox de um sistema reversível.

Figura 14 - Voltametria de onda quadrada: (1) forma de aplicação do potencial e (2) voltamogramas esquemáticos de um sistema reversível.

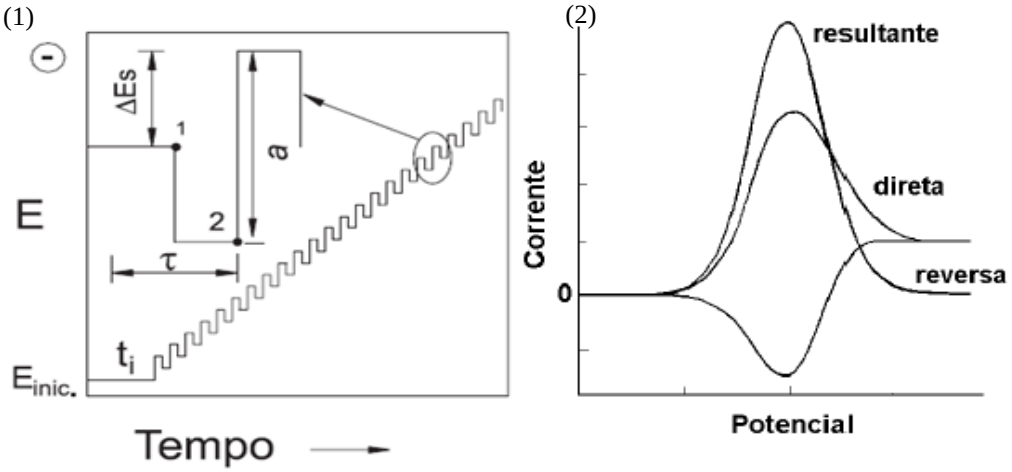

Fonte: SOUZA; MACHADO; AVACA, 2003.

Do ponto de vista prático, a maior vantagem da VOQ é a possibilidade de se obter correntes de pico bem definidas em experimentos executados em alta velocidade de varredura, melhorando, assim, a sensibilidade da técnica. Além disto, por tratar-se de uma técnica de pulso, a corrente faradaica pode ser coletada em um intervalo de tempo

adequado para que a contribuição da corrente capacitiva tenha se minimizado. Uma outra vantagem apresentada pela VOQ é a redução no ruído de fundo por meio de varreduras repetitivas. Além disso, ainda é possível, pela observação dos sinais das varreduras direta e inversa, se obter as informações análogas àquelas obtidas utilizando-se a VC, porém, com uma sensibilidade maior devido à minimização da contribuição da corrente capacitiva (SOUZA; MACHADO; AVACA, 2003).

2.4.3 Caracterização estrutural

Uma variedade de técnicas pode ser utilizada para caracterizar a estrutura e morfologia dos nanomateriais. As mais utilizadas são: espectroscopia no infravermelho por transformada de Fourier (do inglês, Fourier Transform InfraRed Spectroscopy, FTIR), difração de raios X (DRX), espectroscopia no ultravioleta visível (UV-vis), microscopia de força atômica (AFM), microscopia eletrônica de varredura (MEV) e microscopia eletrônica de transmissão (MET).

A espectroscopia no infravermelho por transformada de Fourier (FTIR) é uma técnica óptica utilizada para análise química de nanomateriais ou superfícies nanoestruturadas, que tem como princípio a detecção da radiação absorvida pelas ligações moleculares de diferentes materiais. A radiação infravermelha, ao incidir numa molécula, provoca a excitação dos seus grupos químicos em modos vibracionais. Assim, quando a energia radiante corresponde ao mesmo nível energético vibracional da molécula em análise, a luz é absorvida (GRIFFITHS; HASETH, 2007; ALBERT; ALBERT; QUACK, 2011). Cada molécula possui um espectro de absorção único, como uma impressão digital. A partir do conhecimento da localização das bandas de absorção de cada grupo funcional ou elemento, é possível caracterizar as amostras e, se conhecida a intensidade das bandas, determinar a concentração dos seus constituintes (SMITH, 1998). O espectrômetro no infravermelho por transformada de Fourier é constituído por uma fonte de radiação na região do infravermelho, um interferômetro com um espelho móvel, um detector, um conversor analógico/digital e um computador. A luz da fonte do espectrofotômetro incide sobre o interferômetro, que separa a mesma em dois feixes, um incide sobre um espelho fixo e outro incide sobre um espelho móvel. Os feixes de luz refletidos pelo espelho móvel e fixo se sobrepõem. Este feixe de luz sobreposto passa pela amostra incidindo no detector. O espectro detectado não pode ser diretamente interpretado, necessitando ser reconstruído por aplicação da transformada de Fourier. Os

dados tratados representam a relação da absorbância (ou transmitância) da ligação dos grupos químicos vs. a frequência ou número de onda. Dependendo da amostra, o espectro pode ser medido em modo de transmitância ou de refletância (FOSCHINI, 2009).

2.4.4 Caracterização morfológica

A AFM é uma técnica bastante útil para caracterização morfológica de diferentes superfícies sensoras. Este método tem com princípio básico a análise de medidas de deflexões obtidas através de varreduras da superfície de uma amostra com um cantilever acoplado a uma ponteira na sua extremidade. As análises por AFM permitem a obtenção de imagens em duas e três dimensões das superfícies estudadas. Como vantagem adicional, não requer a preparação das amostras através do recobrimento por materiais condutores, permitindo a análise de amostras biológicas sem perda das suas propriedades (MORITA; WIESENDANGER; MEYER, 2002).

Outra técnica muito utilizada para análise morfológica é a MEV. O microscópio eletrônico de varredura é um aparelho que pode fornecer rapidamente informações sobre a morfologia e identificação de elementos químicos de uma amostra sólida. As imagens obtidas por MEV são decorrentes do efeito de espalhamento de um feixe de elétrons incidente sobre a superfície a ser varrida. Ao colidir com a superfície amostrada, os elétrons retroespalhados e secundários são captados por uma câmera para exibição da imagem. A principal razão de sua utilidade é a alta resolução que pode ser obtida quando as amostras são observadas; valores da ordem de 2 a 5 nm são geralmente apresentados por instrumentos comerciais, enquanto instrumentos de pesquisa avançada são capazes de alcançar uma resolução menor que 1 nm. Outra característica importante da MEV é a aparência tridimensional da imagem das amostras, resultado direto da grande profundidade de campo. Permite, também, o exame em pequenos aumentos e com grande profundidade de foco, o que é extremamente útil, pois a imagem eletrônica complementa a informação dada pela imagem óptica (DEDAVID; GOMES; MACHADO, 2007).

Diferentemente da MEV, na MET é possível a observação direta de estruturas, formando imagens a níveis atômicos. O funcionamento do microscópio eletrônico de transmissão ocorre da seguinte forma: um feixe de elétrons atravessa a amostra sofrendo diversos tipos de espalhamento que dependem das características do material. Imagens

de campo claro são formadas por elétrons que sofrem pouco desvio, enquanto as de campo escuro são formadas por elétrons difratados pelos planos cristalinos do material (REIMER, 1997).

3 OBJETIVOS

3.1 Objetivo geral

Desenvolver plataformas sensoras, utilizando a tecnologia do eletrodo impresso, visando à detecção da proteína NS1 do vírus dengue.

3.2 Objetivos específicos

- Desenvolver eletrodos descartáveis como plataformas sensoras visando à aplicação em sensores para imunoensaio;
- Padronizar os eletrodos impressos quanto à área da superfície eletródica e aos componentes do compósito, com a finalidade de obter melhores estabilidade, reprodutibilidade e resposta amperométrica;
- Imobilizar anticorpos anti-NS1 de modo irreversível na superfície eletródica de carbono;
- Caracterizar a superfície nanoestruturada através de microscopia eletrônica de varredura, microscopia de força atômica, microscopia eletrônica de transmissão e espectroscopia no infravermelho por transformada de Fourier;
- Desenvolver um imunossensor empregando técnicas eletroquímicas para a detecção de antígeno NS1 do DENV na fase aguda da infecção;
- Estabelecer curva de calibração para detecção do antígeno NS1 do DENV em amostras biológicas;

4 MANUSCRITOS

4.1 Manuscrito 1

Manuscrito publicado no periódico *Biosensors and Bioelectronics*, fator de impacto 6.451:

A sensor tip based on carbon nanotube-ink printed electrode for the dengue virus NS1 protein

Ana Carolina M. S. Dias[a], Sérgio L. R. Gomes-Filho[a], Mízia M. S. Silva[a], Rosa F. Dutra[a]*

[a] *Biomedical Engineering Laboratory, Department of Biomedical Engineering, Federal University of Pernambuco, Av. Prof. Moraes Rego, 1235, 50670-901, Recife, Brazil*.

Biosensors and Bioelectronics 44 (2013) 216–221

Contents lists available at SciVerse ScienceDirect

Biosensors and Bioelectronics

journal homepage: www.elsevier.com/locate/bios

A sensor tip based on carbon nanotube-ink printed electrode for the dengue virus NS1 protein

Ana Carolina M.S. Dias, Sérgio L.R. Gomes-Filho, Mízia M.S. Silva, Rosa F. Dutra *

Biomedical Engineering Laboratory, Federal University of Pernambuco, Av. Prof. Moraes Rego, 1235, Campus da Saúde, 50670-901 Recife, Brazil

ARTICLE INFO

Article history:
Received 5 November 2012
Received in revised form
18 December 2012
Accepted 18 December 2012
Available online 2 January 2013

Keywords:
Immunosensor
Screen-printed electrode
Carbon nanotubes
Dengue virus
NS1

ABSTRACT

An immunosensor for the non-structural protein 1 (NS1) of the dengue virus based on carbon nanotube-screen printed electrodes (CNT-SPE) was successfully developed. A homogeneous mixture containing carboxylated carbon nanotubes was dispersed in carbon ink to prepare a screen printed working electrode. Anti-NS1 antibodies were covalently linked to CNT-SPE by an ethylenediamine film strategy. Amperometrical responses were generated at −0.5 V vs. Ag/AgCl by hydrogen peroxide reaction with peroxidase (HRP) conjugated to the anti-NS1. An excellent detection limit (in the order of 12 ng mL^{-1}) and a sensitivity of 85.59 μA mM^{-1} cm^{-2} were achieved permitting dengue diagnostic according to the clinical range required. The matrix effect, as well as the performance of the assays, was successfully evaluated using spiked blood serum sample obtaining excellent recovery values in the results. Carbon nanotubes incorporated to the carbon ink improved the reproducibility and sensitivity of the CNT-SPE immunosensor. This point-of-care approach represents a great potential value for use in epidemic situations and can facilitate the early screening of patients in acute phase of dengue virus.

1. Introduction

Dengue is considered a major public health problem in tropical and subtropical regions of the world and is endemically prevalent in approximately 112 countries (Gurugama et al., 2010). It is a self-limiting, non-specific illness characterized by fever, headache, myalgia, and constitutional symptoms. Its severe forms (hemorrhagic fever and shock syndrome) may lead to multisystem involvement and death, mostly amongst children. The incidence of this disease has increased over the last 50 years with 2.5 billion people living in areas where dengue is endemic (Smith et al., 2009). In view of the high mortality rate and to reduce the disease burden, it is desirable to have a rapid and practical diagnostic method for early detection of dengue virus (Singhi et al., 2007). The major laboratorial methods currently available for diagnosis of the disease are viral culture (Samuel and Tiyagi, 2006), viral RNA detection by reverse transcriptase PCR (RT-PCR) (Huhtamo et al., 2010) and serological tests such as an immunoglobulin M (IgM) capture enzyme-linked immunosorbent assay (MAC-ELISA). The first two assays have restricted scope as a routine diagnostic procedure due to its requirement of highly skilled personnel, laborious procedure and time consumption (Huy et al., 2011). The MAC-ELISA, which is a commonly used assay, has a low sensitivity in the first four days of illness (Alcon et al., 2002). Therefore, early dengue diagnosis still remains a problem, as all these mentioned assays have their own pitfalls.

Dengue virus is an enveloped positive-sense RNA virus. The genomic RNA is approximately 11 kb in length and is composed of three structural protein genes that encode for nucleocapsid or core protein, a membrane-associated protein, an envelope protein and seven non-structural protein genes including NS1 protein (Shrivastava et al., 2011). Recently, ELISA assays specific to NS1 protein have been carried out showing that NS1 secretory protein is found at high concentrations during the early clinical phase of the disease, suggesting it as a predictive marker for dengue diagnosis and responsive to four serotypes (Lapphra et al., 2008). By aiming to achieve a practical diagnostic, rapid, immunochromatographic tests (RDTs) to NS1 detection have been proposed; however, they are limited due to their instability to provide qualitative responses and poor sensitivity on admission samples (Blacksell et al., 2006). Compared with RT-PCR analyzers and RDTs, biosensors present numerous advantages such as simpler management, easier miniaturization, faster and quantitative responses and, moreover, they can permit on-site monitoring (Dai et al., 2011). So far, only a few immunosensors have been developed to detect NS1 antigen and non-commercial approaches are available. Oliveira et al. (2011) developed a biosensor based on concanavalin A lectin as a bioreceptor; however, it is limited in the detection of NS1 due to its interaction with carbohydrates and

* Corresponding author. Tel./fax: +55 81 21268200.
E-mail addresses: rosa.dutra@ufpe.br, rfiremandutra@yahoo.com.br (R.F. Dutra).

0956-5663/$ - see front matter © 2012 Elsevier B.V. All rights reserved.
http://dx.doi.org/10.1016/j.bios.2012.12.033

glycoproteins that are present in the acute phase of dengue disease, including the cytokines, IFNα and others. Su et al. (2003) developed a quartz crystal microbalance immunosensor to simultaneously detect NS1 and envelope proteins in 1:10 diluted serum with 500 μg mL^{-1}. Although some progresses have been achieved, new attempts to obtain a practical and selective NS1 biosensor are required for diagnostic of dengue virus in acute phase.

Different types of transduction can be employed in a biosensor, after the analyte recognition through the sensing biomolecules. Although optical and piezoelectric transduction by using surface plasmon resonance (Dutra and Kubota, 2007) and quartz crystal microbalance (Mattos et al., 2012), respectively, have been more commonly employed for immunoassay, electrochemical transduction has received great attention, especially by using the screen printed electrodes (SPEs) (Kumbhat et al., 2010). SPEs have been shown to be more attractive since they combine a good strategy to accomplish disposable, safe and quantitative point-of-care testing (Silva et al., 2010). They are constructed by printing a conductive ink onto a solid support with significant advantages, like the feasibility to obtain printed electrodes in different sizes and designs, as well as the facility to incorporate diverse compounds in order to change their nature and electrochemical properties (Gornall et al., 2009). It is possible to develop SPEs with high performance, low background current and improved electron transfer kinetic, by simply adding conductive modifiers (Mohamed et al., 2010).

Nowadays, the important role that the carbon nanotubes play in the performance of electrochemical biosensors is well-known (Laschi et al., 2008). Due to their extraordinary chemical and physical properties, such as high electrical conductivity and good chemical stability, it is possible to obtain nanostructured electrodes with faster electron transfer reactions (Tam and Hieu, 2011). In addition, the carbon nanotubes can be functionalized with reactive groups to purposely attach biomolecules and other compounds (Li et al., 2010; Leng et al., 2011). Herein, caboxylated carbon nanotubes were incorporated into the carbon ink to produce SPEs with enhanced sensitivity and stability. A thin film containing amine groups was deposited on the caboxylated carbon nanotube-screen printed electrode (CNT-SPE) in order to perform a covalent and oriented immobilization of the anti-NS1 antibodies. This immunosensor showed to be an innovative electrochemical method for diagnosis of early clinical phase of dengue infection.

2. Experimental

2.1. Materials and reagents

Electrodag PF-407 C carbon ink was acquired from Acheson Henkel Corporation (USA). COOH-functionalized multi-walled carbon nanotubes (COOH-MWCNT), 95% purity degree, were obtained from Dropsens (Oviedo, SPA). Mouse monoclonal antibodies against NS1 glycoprotein of dengue virus (Anti-NS1) and Dengue Virus NS1 glycoprotein were purchased from Abcam (Cambridge, UK). Ethylenediamine (EDA) was acquired from Sigma-Aldrich (St. Louis, USA). Dimethylformamide (DMF) and hydrogen peroxide (H_2O_2) (30% w/v) were obtained from F. Maia (Cotia, BRA). Anti-NS1 antibody was labeled with horseradish peroxidase (HRP) according to Avrameas (1969). For the coupling of HRP to the anti-NS1, 12 mg of peroxidase was dissolved in 1 mL of 0.1 M phosphate buffer (pH 6.8) containing 5 mg of anti-NS1 antibody. While the solution was gently stirred, 0.05 mL of a 1% aqueous solution of glutaraldehyde was added. The mixture was allowed to stand at room temperature (approximately 25 °C) for 2 h and then twice dialyzed against 5 L of PBS at 4 °C overnight. The precipitate was removed by centrifugation for 30 min at 20,000 rpm. This stock solution of peroxidase labeled-antibody was kept at +4 °C until used.

The pool of blood samples used in this work consisted of five serum samples from voluntary donors, kindly provided by Oswaldo Cruz Hospital of the Pernambuco University, according to the ethics committee's recommendations. All voluntary donors were found negative for dengue virus. The serum samples were collected from venous blood and immediately centrifuged for 120 s at 3000g and stored at −20 °C. The positive pool was spiked with NS1 fixing with a same volume at concentrations similar to those detected in the viremic dengue patients (Alcon et al., 2002).

Unless indicated, all the antibodies and antigen solutions was prepared in 0.01 mmol L^{-1} phosphate buffer saline (PBS) at pH 7.0. Ultrapure water (18 MΩ cm) used to prepare all solutions was obtained from a Milli-Q water purification system (Millipore Inc., Billerica, USA).

2.2. Apparatus

All the electrochemical experiments were performed in an Ivium Compact Stat potentiostat/galvanostat from Ivium Technologies (Eindhoven, The Netherlands) interfaced with a microcomputer and controlled by Ivium Soft software. A three-electrode system consisting of the CNT-SPE as the working electrode (4 mm diameter), an Ag/AgCl electrode as the reference electrode and a helical platinum wire as the counter electrode was used. The electrodes were set up in a glassy electrochemical cell with 5 mL volume.

The experiments to characterize the assembling of the CNT-SPE were conducted by using cyclic voltammetry in 5 mmol L^{-1} $K_3Fe(CN)_6/K_4Fe(CN)_6$ prepared in 0.1 mol L^{-1} KCl solution, at 0.1 V s^{-1} scan rate and potential ranging from −0.6 to 1.0 V.

The atomic force microscopy (AFM) technique was used for morphological and topographic characterization of the CNT-SPE. The micrographs were obtained using a WITec Alpha 300S AFM microscope (WITec Instruments, Ulm, Germany) operating in contact mode with a silicon tip at 0.2 N/m constant force.

2.3. Preparation of the CNT-SPE

The CNT-SPEs were obtained from a mixture containing carbon ink and COOH-MWCNT. Prior to mixing, 1 mg COOH-MWCNT was dispersed in 1 mL DMF solvent and sonicated in an ultrasonic batch for 2 h. After that, the CNT-SPEs were manufactured by squeezing the mixture over the adhesive plastic mold fixed on the rectangular support of polyethylene terephtalate (Fig. S1, supplementary information). Afterwards, the electrodes were cured at 60 °C for 20 min and finally, the adhesive plastic mold was removed. The circular area of the working electrode (approximately 4 mm of diameter) was delimited using adhesive tape resistant to chemical (electroplating and anodizing vinyl tape 470 supplied from 3M Co., USA). After they were ready, the CNT-SPEs were pretreated by cyclic voltammetry using 30 cycles at a scan rate of 0.1 V s^{-1}, potential ranging from −2.0 to 2.0 V and 2.44 mV step potential in 0.1 mol L^{-1} KCl solution as supporting electrolyte (Alonso-Lomillo et al., 2009).

2.4. Immobilization of the anti-NS1

Anti-NS1 antibodies were immobilized via EDA film deposited on the electrode surface. The pretreated CNT-SPEs were immersed in a 10% (v/v) EDA aqueous solution for 1 h and dried at room temperature (~25 °C) by forming EDA film. Afterwards, 10 μL of anti-NS1 (1 μg mL^{-1}) prepared in PBS was incubated on the

electrode surface for 1 h. Anti-NS1 antibodies non-covalently linked, i.e. simply adsorbed on the electrode surface were removed with 50 mmol L^{-1} NaCl solution. Non-specific bindings were blocked by incubating the electrode surface, with 50 mmol L^{-1} glycine solution for 1 h. For preservation of the anti-NS1, the immobilized CNT-SPEs were stored in a refrigerator (approximately at +4 °C) in a moist chamber.

2.5. Immunosensor performance

The analytical responses of the immunosensor were evaluated by the following procedure: the CNT-SPEs were incubated with 10 µL of NS1 samples for 30 min followed by exhaustive PBS washings. Subsequently, the CNT-SPEs were incubated with 10 µL of anti-NS1–HRP (1 µg mL^{-1}) in PBS for 30 min and then with PBS washings. Electrochemical responses were obtained by catalytic reaction of the H_2O_2 with the peroxidase conjugated to anti-NS1 and measured by chronoamperometry applying a fixed potential of −0.5 V vs. Ag/AgCl for 120 s.

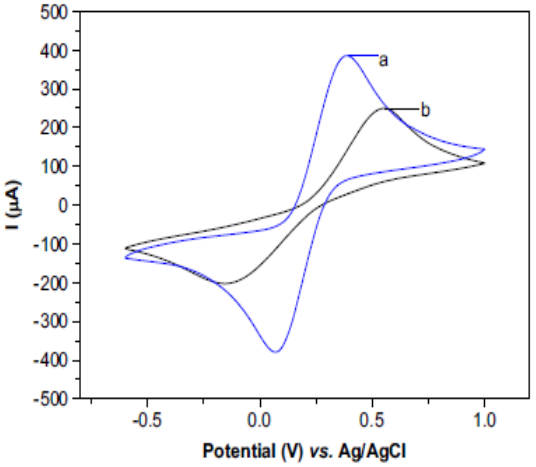

Fig. 1. Cyclic voltammograms profile of the carbon ink-printed electrode with CNT (a) and without CNT (b). Scans performed in 5 mmol L^{-1} $K_3Fe(CN)_6/K_4Fe(CN)_6$, at 0.1 V s^{-1} scan rate.

3. Results and discussion

3.1. Preparation of the CNT-SPE

CNTs have raised considerable interest in electrochemistry due to their ability to increase the electron transfer kinetics, to enlarge the electroactive surface area and to enhance the sensitivity of sensors (Taurino et al., 2012). However the electrocatalytic properties of the CNTs are strongly influenced by many factors. Herein, the incorporation of the CNT in carbon ink resulted in an increase of 190% of the electroactive surface area, as can be seen in the cyclic voltammograms in Fig. 1. Regarding the stability parameter, a synergic effect between CNT and carbon ink was observed. After 20 cycles in the presence of 5 mmol L^{-1} $K_3Fe(CN)_6/K_4Fe(CN)_6$ prepared in 0.1 mol L^{-1} KCl solution, at 0.1 V s^{-1} scan rate and potential ranging from −0.6 to 1.0 V, the voltammograms kept the redox peaks practically constant (3.4% of variation coefficient), i.e. more stable than the electrode without CNT (9.2% of the variation coefficient) (data not shown).

The functionalization of the sensing surface by introducing reactive groups for an oriented immobilization of the antibodies is a crucial step to obtain an immunosensor with a high performance (Cavalcanti et al., 2012). Herein, the EDA film containing amine groups was used to covalently bind the anti-NS1 by its Fc portion. On the other hand, the remaining amine groups of the EDA film were also utilized to form amide bonds with carboxyl groups of the CNT-SPE surface (Fig. 2). The EDA film acted as a bifunctional linker since the amide bonds were formed between the anti-NS1 and the carboxylated electrode surface. This assembly resulted in a stable and oriented matrix of immobilized antibodies.

Optimizing the EDA concentration for a maximal immunosensor response, cyclic voltammograms were obtained using a redox probe. Electrodes with EDA films in different concentrations were analyzed according to the maximal amplitude of the redox peaks (Fig. S2, supplementary information). It was found that the redox peaks increased with the EDA concentration, achieving a plateau at 10% (v/v) EDA. Thus, this concentration was used in all remaining experiments.

3.2. AFM analysis of the CNT-SPE surface

The morphology of the CNT-SPE surfaces was studied in three different steps using the AFM on contact mode. The topographic images of stepwise modification on the electrode surface are

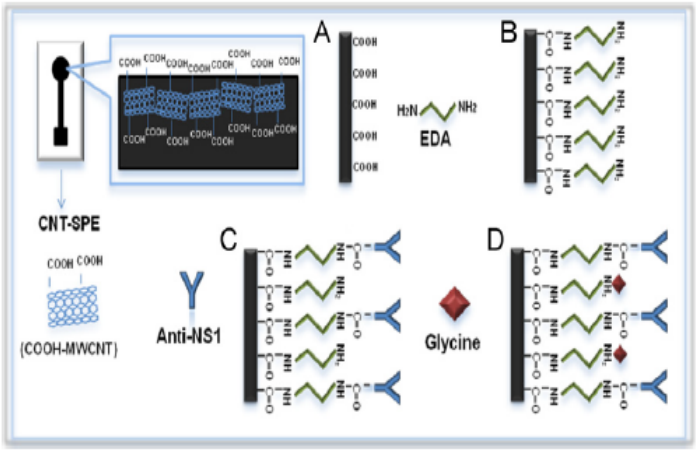

Fig. 2. Schematic illustration of the stepwise preparation of the immunosensor: (a) bare CNT-SPE, (b) EDA film formation, (c) anti-NS1 immobilization, and (d) blocking with glycine.

exhibited in Fig. 3. The CNT-SPE surface became flatter after EDA modification, by decreasing the roughness (R) from approximately 376 nm to 190 nm, probably attributed to filling up of the interstices in the electrode surface. After incubation with the anti-NS1, an agglomerate of globular structures was observed ($R \cong 240$ nm), confirming that the anti-NS1 was attached to the EDA film.

3.3. Electrochemical characterization

Quantitative analysis of the coverage with EDA film can be calculated by cyclic voltammetric investigations (Campuzano et al., 2006). The area of the redox peaks can be used in the characterization of the layers with respect to their degree of coverage and stability. Fig. 1b shows cyclic voltammograms using 5 mmol L^{-1} $K_3Fe(CN)_6/K_4Fe(CN)_6$ prepared in 0.1 mol L^{-1} KCl solution as a redox probe. When the electrode surface was modified by the EDA film, the electron transfer kinetic of $Fe(CN)_6^{3-/4-}$ was enhanced. As shown in Fig. 4, the stepwise assembly of the EDA on the electrode is accompanied by increase in the amplitude of the redox peaks. The current increase can be attributed to formation of the positively charged film on the electrode attracting the hexacyanoferrate that is negatively charged, which is consistent with the enhanced electron transfer. According to the area of the redox peaks, an increase of approximately 16%, with increase of the electroactive area was observed. The electrochemical nature of EDA layer implies in an increase of the catalytic activity, which can be confirmed by the increase in the redox peaks between the bare electrode and EDA modified electrode. Alternatively, a decrease in the current redox peaks was observed after incubation with anti-NS1. This decrease in the area of the redox peaks was expected due to insulating nature of the antibodies (Yun et al., 2007). Similar behavior was also observed after the blocking step of the non-specific bindings with incubation of the electrode in 5 mmol L^{-1} glycine solution.

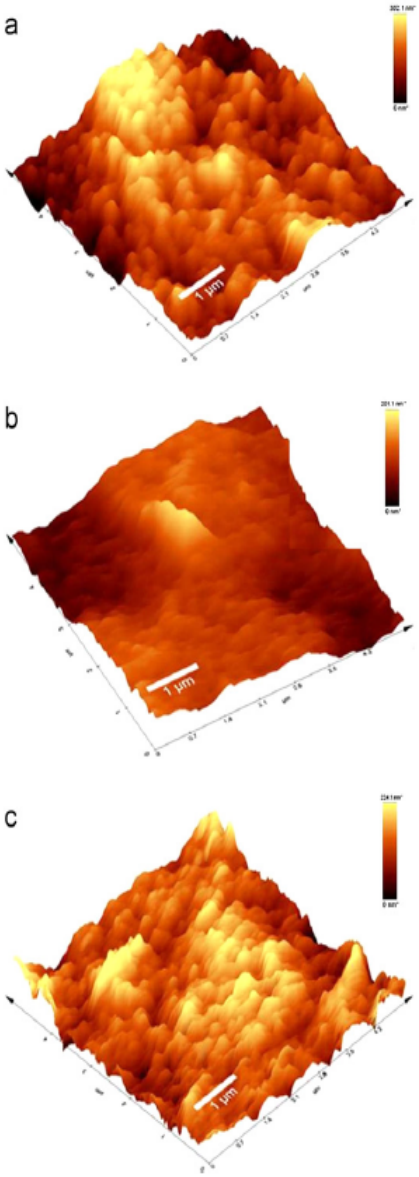

Fig. 3. AFM images: (a) bare CNT-SPE; (b) CNT-SPE modified by EDA and (c) CNT-SPE with immobilized anti-NS1.

3.4. Optimization of the experimental conditions

Since the maximum loading amount directly influences the immunoassay sensitivity, the antibody concentration of the sensing interface must be optimized (Zhang et al., 2008). Different concentrations of anti-NS1 (from 0.1 to 5 µg mL^{-1}) prepared in PBS were immobilized on the electrode surface using the same concentration of the NS1 measured (0.5 µg mL^{-1}). The immunosensor response showed a maximal concentration at 1 µg mL^{-1} anti-NS1, as a result of the antigen–antibody equilibrium required (Fig. S3, supplementary information). Thus, this concentration was chosen for the remaining experiments.

The activity of the enzyme used as electroactive species in the sandwich immunoassay is influenced by the pH of the solution. Most of these enzymes have an optimum activity in a limited range of pH (Liu et al., 2006). It is well known that at relatively high pH, the activity of the enzyme is inhibited (Darain et al., 2003). Thus, a study of the pH effect (from 5.5 to 8.0) on the immunosensor response was carried out in which the optimum catalytic activity of the enzyme was obtained at PBS pH 7.0 (Fig. S4(a), supplementary information). Several studies of immunoreactions exhibit optimal binding at this pH and hence it was adopted in all studies.

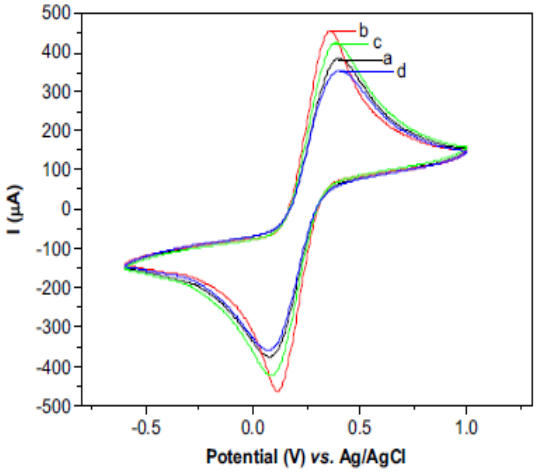

Fig. 4. Cyclic voltammograms of the immunosensor in each step of immobilization: (a) bare CNT-SPE; (b) EDA/CNT-SPE; (c) anti-NS1/EDA/CNT-SPE and (d) glycine/anti-NS1/EDA/CNT-SPE. Scans performed in 5 mmol L^{-1} $K_3Fe(CN)_6/K_4Fe(CN)_6$ at 0.1 V s^{-1} scan rate.

Incubation time exerts an important influence on the analytical performance of the immunosensor (Mao et al., 2010). Studies of the incubation time effect were carried out with the electrode surface incubated in NS1 solution (1 μg mL^{-1} in PBS) for 10, 20, 30, 45 and 60 min. The analytical response of the CNT-SPE increased with the incubation time reaching a plateau at 30 min, which was chosen for subsequent experiments (Fig. S4(b), supplementary information).

3.5. Analytical response of the immunosensor

Calibration curve was obtained by using the chronoamperometry technique. The analytical response of the CNT-SPE incubated in different concentrations of NS1 antigen prepared in PBS was generated by the catalytic reaction between H_2O_2 and HRP conjugated to anti-NS1, at −0.5 V fixed potential. This working potential was chosen based on the potential of the cathodic peaks exhibited in cyclic voltammograms due to anti-NS1–HRP response to the substrate (hydrogen peroxide). The results showed an increase of the current proportional to the NS1 concentrations. A linear range between 40 ng mL^{-1} and 2 μg mL^{-1} NS1 was obtained, indicating a good analytical performance (r=0.996, n=8) with a sensitivity of 85.59 μA mM^{-1} cm^{-2} (Fig. 5). Limit of detection (LOD) calculated according to IUPAC was found to be approximately 12 ng mL^{-1} for the NS1, being much lower than LOD previously described for the validated quartz crystal microbalance immunosensor developed to detect NS1 and envelope protein (LOD approximately 3 μg mL^{-1}) (Su et al., 2003). The linear range and LOD can be compared to sandwich ELISA kit (Dussart et al., 2003). Alcon et al. (2002) reported that the NS1 antigen was found circulating from the first day after the illness onset up to the 9th day. In primary infections, NS1 levels range from 0.04 to 2 μg mL^{-1} in serum samples of patients in the disease acute phase (up to 7 days). These levels match with the detected levels by the CNT-SPE developed in this work. Thus, this immunosensor presents as a real potential for dengue diagnosis, with the advantage to easily become a point-of-care testing.

3.6. Precision and accuracy studies

The reproducibility of the immunosensor response was evaluated by using six different electrodes incubated with a fixed NS1 concentration of 0.5 μg mL^{-1}. An excellent reproducibility was obtained (coefficient of variation CV=3.4%). The proposed immunosensor also showed good repeatability by measuring 10 replicated from the same CNT-SPE with 0.5 μg mL^{-1} NS1 concentration (CV=4%).

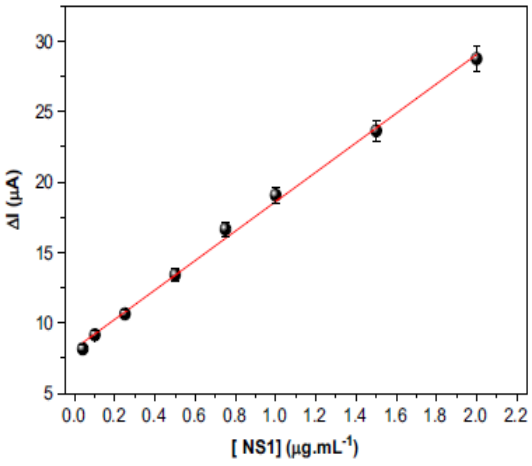

Fig. 5. Calibration curve of the immunosensor for NS1 protein of dengue virus.

Table 1
Recovery values in spiked PBS and serum samples based on the immunosensor. In all cases, n=3.

Concentration (ng mL^{-1})	PBS		Serum	
	Found concentration (ng mL^{-1})	Recovery (%)	Found concentration (ng mL^{-1})	Recovery (%)
0.10	0.104	104.0	0.116	116.0
0.50	0.510	102.0	0.512	102.4
1.00	1.030	103.0	1.010	101.0
1.50	1.480	98.7	1.470	98.0

Attempting to make use of this NS1 immunosensor in blood, recovery studies were done spiking serum samples negative to dengue with different NS1 protein concentrations. Herein, both PBS and serum samples were submitted to the same procedures and measured by the immunosensor. The recovery values are presented in Table 1, showing excellent results for the PBS and serum samples detection methodologies, with average recovery values of 101.9% and 104.4%, respectively.

The analytical accuracy of the immunosensor in PBS was better than in blood serum especially when the NS1 is measured in much lower concentrations. This result is attributed to the complexity of the blood sample that contains substances that alter the measurable concentration of the analyte or the antibody binding capacity. Approximately 40% of the serum samples contain non-analyte antibody binding substances, with 15% interference in non-blocked assays (Tate and Ward, 2004). Based on results obtained from serum sample, the immunosensor also showed effective surface-blocked assays.

4. Conclusions

A screen printed electrode specific to NS1 protein detection based on CNTs was successfully developed. The incorporation of the CNTs into carbon ink to prepare the CNT-SPE promoted an increase of the electroactive area, as well as improved the kinetic electron transfer, besides enhancing stability, reproducibility and sensitivity of the tip sensor. Due to the performance of the immunosensor presented in this work, this strategy can be suitable for the rapid, on-site and screen-out analysis of the NS1 protein. Additionally, this technology is attractive for mass production, with the advantage of being cheaper and more practical than RT-PCR and ELISA test, opening new ways for an early diagnosis of the acute dengue infection.

Acknowledgments

The authors thank the National Council of Scientific and Technological Development—CNPq for financial support and Centre of Strategic Technologies of Northeast for performing AFM imaging. A.C.M.S. Dias thanks FACEPE for its scholarship during this work.

Appendix A. Supporting information

Supplementary data associated with this article can be found in the online version at http://dx.doi.org/10.1016/j.bios.2012.12.033.

References

Alcon, S., Talarmin, A., Debruyne, M., Falconar, A., Deubel, V., Flamand, M.J., 2002. Journal of Clinical Microbiology 40 (2), 376–381.
Alonso-Lomillo, M.A., Domínguez-Renedo, O., Matos, P., Arcos-Martínez, M.J., 2009. Bioelectrochemistry 74, 306–309.
Avrameas, S., 1969. Immunochemistry 6 (1), 43–52.
Blacksell, S.D., Newton, P.N., Bell, D., Kelley, J., Mammen, M.P., Vaughn, D.W., Wuthiekanun, V., Sungkakum, A., Nisalak, A., Day, N.P.J., 2006. Clinical Infectious Diseases 42, 1127–1134.
Campuzano, S., Pedrero, M., Montemayor, C., Fatás, E., Pingarrón, J.M., 2006. Journal of Electroanalytical Chemistry 586, 112–121.
Cavalcanti, I.T., Silva, B.V.M., Peres, N.G., Moura, P., Sotomayor, M.D.P.T., Guedes, M.I.F., Dutra, R.F., 2012. Talanta 91, 41–46.
Dai, Y., Cai, Y., Zhao, Y., Wu, D., Liu, B., Li, R., Yang, M., Wei, Q., Du, B., Li, H., 2011. Biosensors and Bioelectronics 28, 112–116.
Darain, F., Park, S.-U., Shim, Y.-B., 2003. Biosensors and Bioelectronics 18, 773–780.
Dussart, P., Labeau, B., Lagathu, G., Louis, P., Nunes, M.R.T., Rodrigues, D.G., Storck-Herrmann, C., Cesaire, R., Morvan, J., Flamand, M., Baril, L., 2003. Clinical and Vaccine Immunology 13, 1185–1189.
Dutra, R.F., Kubota, L.T., 2007. Clinica Chimica Acta 376, 114–120.
Gornall, D.D., Collyer, S.D., Higson, S.P.J., 2009. Sensors and Actuators B: Chemical. 141, 581–591.
Gurugama, P., Garg, P., Perera, J., Wijewickrama, A., Seneviratne, S.L., 2010. Indian Journal of Dermatology 55, 68–78.
Huhtamo, E., Hasu, E., Uzcátegui, N.Y., Erra, E., Nikkari, S., Kantele, A., Vapalahti, O., Piiparinen, H., 2010. Journal of Clinical Virology 47 (1), 49–53.
Huy, T.Q., Hanh, N.T.H., Thuy, N.T., Chung, P.V., Nga, P.T., Tuan, M.A., 2011. Talanta 86, 271–277.
Kumbhat, S., Sharma, K., Gehlot, R., Solanki, A., Joshi, V., 2010. Journal of Pharmaceutical and Biomedical Analysis 52, 255–259.
Lapphra, K., Sangcharaswichai, A., Chokephaibulkit, K., Tiengrim, S., Piriyakarnsakul, W., Chakorn, T., Yoksan, S., Wattanamongkolsil, L., Thamlikitkul, V., 2008. Diagnostic Microbiology and Infectious Disease 60 (4), 387–391.
Laschi, S., Bulukin, E., Palchetti, I., Cristea, C., Mascini, M., 2008. ITBM-RBM 29, 202–207.
Leng, C., Wu, J., Xu, Q., Lai, G., Ju, H., Yan, F., 2011. Biosensors and Bioelectronics 27, 71–76.
Li, N., Xu, Q., Zhou, M., Xia, W., Chen, X., Bron, M., Schuhmann, W., Muhler, M., 2010. Electrochemistry Communications 12, 939–943.
Liu, Y., Qin, Z., Wu, X., Jiang., H., 2006. Biochemical Engineering Journal 32, 211–217.
Mao, L., Yuan, R., Chai, Y., Zhuo, Y., Yang, X., 2010. Sensors and Actuators B: Chemical 149, 226–232.
Mattos, A.B., Freitas, T.A., Silva, V.L., Dutra, R.F., 2012. Sensors and Actuators B: Chemical 3, 439–446.
Mohamed, G.G., Ali, T.A., El-Shahat, M.F., Al-Sabagh, A.M., Migahed, M.A., Khaled, E., 2010. Analytica Chimica Acta 673, 79–87.
Oliveira, M.D.L., Nogueira, M.L., Correia, M.T.S., Coelho, L.C.B.B., Andrade, C.A.S., 2011. Sensors and Actuators B: Chemical. 155, 789–795.
Samuel, P.P., Tiyagi, B.K., 2006. Indian Journal of Medical Research 123, 615–628.
Shrivastava, A., Dash, P.K., Sahni, A.K., Gopalan, N., Lakshmana Rao, P.V., 2011. Indian Journal of Medical Microbiology 29 (2011), 51–55.
Silva, B.V.M., Cavalcanti, I.T., Mattos, A.B., Moura, P., Sotomayor, M.P.T., Dutra, R.F., 2010. Biosensors and Bioelectronics 26 (3), 1062–1067.
Singhi, S., Kissoon, N., Bansal, A., 2007. Journal of Pediatrics 83, 22–35.
Smith, A.W., Chen, L.H., Massad, E., Wilson, M.E.T., 2009. Emerging Infectious Diseases 15, 8–11.
Su, C.C., Wu, T.Z., Chen, L.K., Yang, H.H., Tai, D.F., 2003. Analytica Chimica Acta 479, 117–123.
Tam, P.D., Hieu, N.V., 2011. Applied Surface Science 257, 9817–9824.
Taurino, I., Carrara, S., Giorcelli, M., Tagliaferro, A., Micheli, G., 2012. Surface Science 606, 156–160.
Tate, J., Ward, G., 2004. ClinicalBiochemist Reviews 25 (2), 105–120.
Yun, Y., Bange, A., Heineman, W.R., Halsall, H.B., Shanov, V.N., Dong, Z., Pixley, S., Behbehani, M., Jazieh, A., Tu, Y., 2007. Sensors and Actuators B: Chemical 123, 177–182.
Zhang, S., Zheng, F., Wu, Z., Shen, G., Yu, R., 2008. Biosensors and Bioelectronics 24, 129–135.

4.2 Manuscrito 2

Manuscrito a ser submetido para publicação no periódico *Colloids and Surfaces B: Biointerfaces,* fator de impacto 4.287:

Electrochemical immunosensor based on amine functionalized gold nanoparticles for NS1 protein detection of dengue virus

Ana Carolina M. S. Dias[a], Jamil Saade[a], Rosa F. Dutra[a]*

[a] *Biomedical Engineering Laboratory, Department of Biomedical Engineering, Federal University of Pernambuco, Av. Prof. Moraes Rego, 1235, 50670-901, Recife, Brazil.*

* Corresponding author:

Rosa Fireman Dutra

E-mail address: rosa.dutra@ufpe.br; rfiremandutra@yahoo.com.br

Tel.: +55 81 21267325

Abstract

Noble metal nanoparticles have gained importance in the field of nanostructured immunosensors for having an excellent chemical stability and electronic conductivity, relatively simple synthesis and ease of chemical modification of the surface. Screen-printed electrodes (SPE) have been widely used in the disposable sensors development for clinical analysis of various diseases. In this work, a label-free electrochemical immunosensor using gold nanoparticles prepared with polyethyleneimine (PEI-AuNPs) was successfully developed for NS1 protein detection of dengue virus. For this purpose, a screen-printed electrode was one-step manufactured depositing a colloidal suspension containing pre-synthetized gold nanoparticles (AuNP) amine modified. PEI-AuNPs were obtained using a modification of the photoinduced method by illuminating the preformed gold seeds reduced by polyethyleneimine (PEI) with light-emitting diodes (LEDs) emitting in the blue region. The use of filters during illumination directly influences the final geometry and size of the nanoparticles. PEI-AuNPs were characterized by UV–Vis spectroscopy and transmission electron microscopy (TEM). AuNPs were functionalized with PEI to provide an oriented immobilization of the anti-NS1 antibodies via amine groups of polymer. The modification of SPE with PEI-AuNPs was confirmed using EDX and FTIR techniques. PEI-AuNPs were used to enhance the sensitivity of the immunosensor and to provide an excellent matrix of antibodies immobilization due to the increase of effective surface area. The sensor electrochemical response was obtained by using square wave voltammetry (SWV) in the concentration range between 0.1 and 2 μg mL^{-1} NS1. The analytical curve showed good linearity with correlation coefficient of 0.995 ($p<0.0001$, $n=7$) and a limit of detection of 0.03 μg mL^{-1}. This work resulted in a simple method of AuNPs synthesis with strategic functional groups for development of an electrochemical immunosensor based on portable and disposable electrodes for application on the detection of NS1 protein of DENV.

Keywords: dengue; immunosensor; screen-printed electrode; functionalized gold nanoparticles.

1. Introduction

New nanomaterials development have excelled for application in diverse areas, such as medicine, biology, chemistry, physics and materials science, due to their attractive electronic, optical, magnetic, thermal and catalytic properties (Wang et el., 2014; Ansari & Husain, 2012; Li et al., 2011). The use of nanomaterials in sensing devices has led to the production of sensitive sensors useful in laboratory and field analysis (Singh et al., 2009). Among the nanomaterials, gold nanoparticles (AuNPs) have attracted enormous interest due to their essential properties which include biocompatibility, chemical stability, ease of synthesis and good electronic conductivity (Brondani et al., 2013; Alkilany & Murphy, 2010). The size and morphology of the nanoparticles can be manipulated, depending on the synthesis employed method.

The chemical modification of AuNPs are attractive for immunosensors development due to their ability to enhance the amount of immobilized biomolecules on the sensor surface with good bioactivity, specificity and accessibility for the antigen (Zhang, Ju & Wang, 2008). AuNPs can be functionalized using a variety of polymers, among them the polyethyleneimine (PEI). PEI is a cationic polymer very stable in aqueous solution, highly branched with high charge density, which contains primary, secondary, and tertiary amine groups (Kadajji and Betageri, 2011). Most applications of PEI are facilitated by its surface activity and its ability to form complexes with both anionic polyelectrolytes and metal ions. PEI have been used both as the shape-directing agent to control the preferential growth of crystal seeds in preparation of several shapes so as stabilizing agent (Brondani et al., 2013). Another advantage of using PEI is to achieve functional groups on the nanoparticles surface in only one stage of the one-pot synthesis. Thereby, sensing devices employing AuNPs and polymers can be developed in order to aid the diagnosis of several diseases, including dengue fever.

Dengue virus (DENV) infection is one of the most neglected tropical diseases and of highest public health importance, with 50 million cases worldwide each year (Linares et al., 2013). This vector-borne disease has rapidly spread affecting mainly poor and urban populations, becoming the leading cause of hospital admissions in several countries (WHO, 2010). Nowadays, the laboratorial diagnostic of the disease can be performed by virus isolation in cell culture (Yamada et al., 2002), viral RNA detection using Polymerase Chain Reaction (PCR) or Reverse Transcription Polymerase

Chain Reaction (RT-PCR) (Najioullah, Viron & Césaire, 2014), serological tests (Rivetz et al., 2009) and detection of viral antigens (Ahmed & Broor, 2014). Virus isolation and PCR or RT-PCR are sensitive and reliable methods, however require specialized laboratory and have a long duration (over a week) (Hunsperger et al., 2014). ELISA kits for IgG and IgM antibodies detection are commonly used for the infection diagnosis in routine laboratories, nevertheless one limitation of these techniques is the variation of the detection threshold during the acute phase of the disease and their vulnerability to cross-reactions caused by antibodies against related flavivirus (Schilling et al., 2004; Huhtamo et al., 2010).

The diagnostic methods based on NS1 antigen detection are able to identify the disease in the acute phase in a fast and reliable way (Zhang et al., 2014). The NS1 antigen is present on all serotypes of DENV, circulates in high concentrations in the blood, both primary and secondary infection and can be detected from first to ninth day after the onset of symptoms (Datta & Wattal, 2010). In this sense, it is necessary the development of new technologies for the DENV infection diagnosis in order to reduce the execution time and test costs without losing the specificity and sensitivity of conventional methods.

In the present work, an innovative label-free electrochemical immunosensor using PEI-coated gold nanoparticles is demonstrated for NS1 protein detection of dengue virus. We describe the preparation and functionalization of the AuNPs with PEI leaving amino terminal groups for anti-NS1 antibodies immobilization. AuNPs were easily synthesized and functionalized in order to enhance the antibodies loading onto surface electrode. The method developed in this paper is a potential candidate for a sensitive and rapid detection of NS1 protein of DENV allowing the diagnostic of the dengue in epidemic situations and facilitating the early screening of patients in acute phase.

2. Experimental

2.1. Materials and reagents

Electrodag PF-407 C carbon ink was acquired from Acheson Henkel Corporation (United States) and graphite powder from Fluka. Polyethyleneimine (PEI, branched, Mw 10,000), chloroauric acid ($HAuCl_4$), N-hydroxysuccinimide (NHS) and

N-ethyl-N′-(3-dimethylaminopropyl) carbodiimide (EDC) were obtained from Sigma-Aldrich (United States). Dengue virus NS1 glycoprotein (>90% purity) and mouse monoclonal antibodies against dengue virus NS1 glycoprotein (anti-NS1) were purchased from Abcam (United Kingdom). All other reagents used for buffer and solution preparation were analytical grade and used without further purification. Ultrapure water (18.2 MΩ cm) was obtained from a Milli-Q water purification system (Millipore Inc., United States).

2.2. Preparation of the SPE

The working electrode was obtained from a carbon ink homogenous mixture containing 10% graphite powder (w/w). The SPEs were manufactured by squeezing the mixture over the adhesive plastic mold fixed on the rectangular support of polyethylene terephthalate. Afterwards, the electrodes were cured at 60ºC for 20 min and finally the adhesive mold was removed. The circular area of the working electrode (approximately 4 mm of diameter) was delimited using an adhesive tape for galvanoplasty (Dias et al., 2013).

Before modifying the SPE, a mechanical cleaning was carried out sanding the working electrode surface by thin grain sandpaper. Then, the SPE surface was pre-treated scanning 40 cyclic voltammograms, at scan rate of 0.1 V s^{-1}, potential ranging from −2.0 to 2.0 V in 0.1 mol L^{-1} KCl solution as supporting electrolyte (Alonso-Lomillo et al., 2009).

2.3. Synthesis of PEI-AuNPs

PEI (1.45 g) was dissolved in 5 mL Milli-Q water and then mixed to 3 mL of $HAuCl_4$ (1.1 mmol L^{-1}) to form a homogeneous solution. Afterwards, the solution was exposed to Light Emission Diode (LED) at 480 nm and 10 watts power. It was observed that the solutions turned into a pale red color after exposure to LED for 6 h. The color of the reaction mixture would gradually deepen with the increase of exposure time. During the reduction of Au (III) metal ions through amine groups of the PEI, it acted as an agent for multiple functions: stabilizer, shape-controller of gold nanoparticles and as a weak reductant.

2.4. Immunosensor preparation

Prior to anti-NS1 immobilization, a solution of PEI-AuNPs (10 μL) was dropped onto the electrode surface and left to react for 1 h. Then, 10 μL of anti-NS1 antibodies solution (10 μg mL^{-1}), prepared in 0.01 mol L^{-1} phosphate buffered saline (PBS) pH 7.4, were incubated on the SPE surface for 1 h. After washing step, the remaining reactive sites of the electrode surface were blocked by incubating the electrode with 0.05 mol L^{-1} glycine solution for 1 h. A schematic design of the PEI-AuNPs/SPE is shown in Figure1.

---- Please insert Figure 1 ---

2.5. Immunosensor performance

The analytical responses of the immunosensor were evaluated by the following procedure: the anti-NS1/PEI-AuNPs/SPEs were incubated with 10 μL of NS1 samples in different concentrations for 30 min, in a moist chamber at room temperature. Afterwards, the electrode was washed with ultrapure water.

Calibration curve was obtained using SWV, ranging concentration from 0.1 to 2 μg mL^{-1} NS1. The current differences were obtained between the blank and the defined concentration and the relative current was calculated for each concentration.

2.6 Technical characterization

AuNPs colloids were characterized by UV–Vis Spectroscopy (Bruker Spectrophotometer UV-vis 3000). The morphology of AuNPs was analyzed by Transmission Electron Microscopy (TEM), using a FEI Tecnai20 transmission electron microscope operating at 200 kV. Chemical composition of PEI-AuNPs nanocomposite was investigated by Energy-Dispersive X-ray spectroscopy (EDX), integrated to a FEI Quanta 200 FEG microscope (Netherlands).

Fourier transform infrared (FTIR) spectroscopy was performed to chemically characterize the SPE. FTIR measurements were performed in attenuated total

reflectance (ATR) mode using a Vertex 70 FTIR (scans=64, energy scanning from 400 cm^{-1} to 4000 cm^{-1}), acquired from Bruker (Germany).

All the electrochemical measurements were performed in an Ivium Compact Stat potentiostat/galvanostat from Ivium Technologies (Netherlands), interfaced with a microcomputer and controlled by Ivium Soft software. A three-electrode system was used consisting of a homemade carbon screen-printed electrode as working electrode, an Ag/AgCl electrode as reference electrode and a helical platinum wire as counter electrode. The experiments to characterize the assembling of the SPE were done using cyclic voltammetry in 0.005 mol L^{-1} $K_3Fe(CN)_6/K_4Fe(CN)_6$ prepared in 0.1 mol L^{-1} KCl solution, at 0.05 V s^{-1} scan rate and potential ranging from −0.6 to 1.0 V, vs. Ag/AgCl (3 mol L^{-1} KCl). Immunosensor performance was monitored by square wave voltammetry (SWV), at potential range from -0.2 to 0.7 V, frequency of 10 Hz and pulse amplitude of 10 mV.

3. Results and discussion

3.1. Characterization of PEI-AuNPs

For the gold nanoparticles in the initial stage of reaction, only one intense adsorption band attributed to the ligand-metal charge-transfer band of the gold salt was observed at ultraviolet, 300 nm in the left band (Pastoriza-Santos & Liz-Marzán, 2002). However, with the increase of exposure time, the extinction spectra showed two additional absorption bands: one placed at 530 nm with a good symmetry, assigned to the in-plane dipole resonance of polyhedral nanoparticles (Wu, Kuo & Huang, 2010; Kim et al., 2009) and a much weaker small band around 370 nm that can be attributed to the interband electronic transitions of the gold in the formed particles (Figure 2).

---- Please insert Figure 2 ---

Size distribution of gold nanoparticles was analyzed by TEM images. The images display that the nanoparticles presented an average diameter of 9.53 ± 0.13 nm (Figure 3).

---- Please insert Figure 3 ---

3.2. Characterization of SPE surface modified by AuNPs-PEI

Different techniques were used to confirm the modification of SPE with PEI-AuNPs. One of them was the EDX analysis, which was carried out to study the elemental composition of the electrode surface before and after modification. Figure 4 shows EDX spectra of the bare SPE (a) and SPE modified with PEI-AuNPs (b). On Figure 4(a), peaks corresponding to C, O and Cl elements were observed on the spectrum. These elements are carbon ink components used in the fabrication of the SPE. On Figure 4(b), it was observed an Au peak, which clearly shows that the Au nanoparticles recovered the SPE surface. The Cr peak is due to thin conductive coating applied to enable SEM investigation.

---- Please insert Figure 4 ---

FTIR spectra were also used to investigate the modification of the SPE with PEI-AuNPs. The FTIR spectra are shown in Figure 5. The fundamental vibrations in the 4000–2500 cm^{-1} region are generally due to O–H, C–H and N–H stretching. O–H stretching produces a broad band that occurs in the range 3700–3600 cm^{-1}. By comparison, N–H stretching is usually observed between 3400 and 3300 cm^{-1} (Stuart, 2004). The curve (a) shows clean SPE spectrum that presents a characteristic band at 3411 cm^{-1} corresponding to O–H molecular stretching. On the other hand, the curve (b), after electrode surface modification with PEI-AuNPs, shows the band of N–H stretching at 3281 cm^{-1} that confirms the presence of PEI on the SPE surface. It is also possible see at the spectrum (b) bands at 1634 cm^{-1} and 1471 cm^{-1} that are associated to N–H asymmetric bending and C–H stretch (Deng et al., 2011).

---- Please insert Figure 5 ---

3.3. Stability of PEI-AuNPs nanocomposite

The stability of the PEI-AuNPs film on the SPE surface was evaluated by 15 successive cyclic voltammograms of the PEI-AuNPs/SPE performed in presence of 0.005 mol L^{-1} of $K_3Fe(CN)_6/K_4Fe(CN)_6$, prepared in 0.1 mol L^{-1} KCl, at 0.05 V s^{-1} scan

rate and at potential ranging from -0.6 to 1.0 V. After 15 cycles, the redox peaks were practically constant. It was obtained a coefficient of variation (CV) of approximately 2%, to anodic peak, and 3%, to cathodic peak (Figure 6), indicating a good stability of the film on the SPE surface (CV < 5%).

---- Please insert Figure 6 ---

3.4. Electrochemical characterization of the immunosensor assembly

Cyclic voltammetry is an effective method to electrochemically characterize the modified electrode surface. This technique clearly shows that the dynamics of charge transfer at the electrochemical interface is strongly influenced by the nature of the electrode surface and also by the structure of the electric double layer (Kulkarni, Mulla & Vijayamohanan, 2006). Each assembly step of the modified electrode was electrochemically characterized using 0.005 mol L^{-1} $K_3Fe(CN)_6/K_4Fe(CN)_6$ as redox probe.

As shown in Figure 7, a couple of well-defined and reversible redox peaks was observed on the bare SPE (curve a). An increase in the amperometric response was noted after modification of the electrode with PEI-AuNPs (curve b), which was attributed to the increase of effective surface area caused by the film formation (Zapp et al., 2014). PEI-AuNPs nanocomposites were incorporated into the sensor platform in order to improve electron transfer and facilitate the electron exchange between the electrode surface and the redox probe due to their high conductivity. The modification of the SPE surface with PEI-AuNPs resulted in an increase of approximately 67% e 77% in the current amplitude of anodic and cathodic peaks, respectively. A consecutive decrease of the amperometric response was observed after the immobilization of the anti-NS1 antibodies and blocking with glycine (curves c and d). This decrease occurred because the anti-NS1 antibodies form an insulating layer on the electrode surface, leading to a higher electron transfer resistance, which was caused by the nonconductive properties of the biomolecules (Zhu et al., 2013).

---- Please insert Figure 7 ---

3.5. Optimization of the experimental conditions

Performance of the immunosensor is highly dependent on the amount of immobilized antibodies and their antigen binding capacity (Pei et al., 2010). In this work, PEI polymer was used to promote a covalent immobilization of the anti-NS1 antibodies via amide bonds. For this, the Fc terminal of the anti-NS1 antibodies was activated by EDC/NHS mixing. The oriented immobilization of antibodies by Fc portion enhances the sensitivity and selectivity of the immunosensor through the exposing of the Fab portions, which have a high affinity for the antigens (Silva et al., 2013). In order to improve the immunoassay sensitivity, the anti-NS1 concentration immobilized on the sensor surface was optimized. Different concentrations of anti-NS1 (from 0.5 to 20 μg mL^{-1}) prepared in PBS were immobilized on the SPE surface. The immunosensor response showed a maximal concentration at 10 μg mL^{-1} anti-NS1 (Figure S1(a)). Therefore, this concentration was chosen for the remaining experiments.

Antigen-antibody reactions have an optimal incubation time that promotes a maximal binding of the antigen to antibody. Short incubation periods may not allow for significant amounts of antibody to be bound as well as prolonged incubation time may result in dissociation of antibody from antigen (Rudmann, 2005). Thereby, the effect of incubation time of NS1 antigen on the response immunosensor was also evaluated. Anti-NS1/PEI-AuNPs/SPE was incubated with NS1 antigen (1 μg/mL) during periods from 10 to 60 min. As shown in Figure S1(b), the incubation time reached the maximum at 30 min and became stable when the time was exceeded, indicating the interaction between NS1 antigen and anti-NS1 antibody. Then, 30 min was chosen as the optimal incubation time in the following experiments.

3.6. Analytical response of the immunosensor

The calibration curve was performed in different NS1 concentrations by using SWV, in a solution of $K_3Fe(CN)_6/K_4Fe(CN)_6$ (0.005 mol L^{-1}) prepared in 0.1 mol L^{-1} KCl, at 0.05 V s^{-1} scan rate. The immunosensor was incubated with successive NS1 samples, under optimized experimental conditions, in the range of concentration of 0.1 to 2.0 μg mL^{-1}, diluted in PBS solution (0.01 mol L^{-1}, pH 7.4). The results showed a decrease of the peak current proportional to the increase of NS1 concentration (Figure 8a). A linear calibration curve was obtained in the concentration range from 0.1 to 2.0

μg mL^{-1} NS1 with a correlation coefficient of 0.99515 ($p < 0.0001$, $n = 7$). The calculated limit of detection (LOD = three times the standard deviation of the intercept/slope) was found to be 0.09 μg mL^{-1}. A report by Alcon et al. (2002) demonstrated that serum levels of NS1 antigen in primary and secondary infections by DENV1 were found in the range from 10 ng mL^{-1} to 2 μg mL^{-1}. Libraty et al. (2002) also detected elevated levels of free secreted NS1 (≥600 ng mL^{-1}) in patients on the illness onset, at risk for developing dengue hemorrhagic fever. This clinical range for NS1 protein is matched with values detected by the developed immunosensor.

The selectivity of immunosensor was evaluated in relation to native antigens from different serotypes of DENV obtained through culture supernatant collected on the 5^{th} day after inoculation in C6/36 cell monolayers, period which the NS1 native protein reach maximal production. The immunosensor showed a positive response to the four serotypes of DENV and slight difference in current for the negative control (Figure 8b).

The reproducibility of the immunosensor was also investigated by performing SWV measurements in $K_3Fe(CN)_6/K_4Fe(CN)_6$ (0.005 mol L^{-1}) prepared in 0.1 mol L^{-1} KCl , at 0.05 V s^{-1} scan rate. The analytical response of 8 different electrodes prepared under the same conditions was evaluated. For this, the electrodes were incubated with 1 μg mL^{-1} NS1 protein during 30 min. Coefficient of variation of 4.3% was achieved, indicating a good reproducibility of the immunosensor.

4. Conclusions

In this work, a promising electrochemical immunosensor approach based on AuNPs-PEI was demonstrated for NS1 detection. The PEI-AuNP nanocomposite had been successfully synthesized and applied to a dengue immunosensor. The one-step synthesis by photoreduction is an efficient, rapid and simple method for producing functionalized gold nanoparticles. Due to the extraordinary performance, the immunosensor presented in this work can be suitable for the rapid and on-site detection of the NS1 protein, opening new ways for an early diagnosis of the acute dengue infection.

Acknowledgements

The authors thank the National Council of Scientific and Technological Development (CNPq) and Foundation of Support to Science and Technology of the State of Pernambuco (FACEPE) for financial support.

References

Ahmed, N.H.; Broor, S., 2014. Journal of Vector Borne Diseases 51, 194-199.

Alcon, S., Talarmin, A., Debruyne, M., Falconar, A., Deubel, V., Flamand, M. J., 2002. Journal of Clinical Microbiology 40 (2), 376–381.

Alkilany, A. M., Murphy, C. J. 2010. J Nanopart Res 12, 2313–2333.

Alonso-Lomillo, M. A., Domínguez-Renedo, O., Matos, P., Arcos-Martínez, M. J., 2009. Bioelectrochemistry 74, 306-309.

Ansari, S.A., Husain, Q. 2012. Biotechnology Advances 30, 512-523.

Brondani, D., Souza, B., Souza, B. S., Neves, A., Vieira, I. C., 2013. Biosensors and Bioelectronics 42, 242-247.

Datta, S., Wattal, C., 2010. Indian Journal of Medical Microbiology 28, 107-110.

Deng, S., Fulghum, T. M., Krueger, G., Patton, D., Park, J. Y., Advincula, R. C., 2011. Chem. Eur. J. 17, 8929-8940.

Dias, A.C.M.S, Gomes-Filho, S.L.R., Silva, M.M.S, Dutra, R.F. 2013. Biosensors and Bioelectronics 44, 216–221.

Huhtamo, E., Hasu, E., Uzcáteguia, N. Y., Erra, E., Nikkari, S., Kantele, A., Vapalahti, O., Piiparinen, H., 2010. Journal of Clinical Virology, 47, 49-53.

Hunsperger, E.A., Yoksan, S., Buchy, P., Nguyen, V. C., Sekaran, S. D., Enria, D. A., Vazquez, S., Cartozian, E., Pelegrino, J. L., Artsob, H., Guzman, M.G., Olliaro, P., Zwang, J., Guillerm, M., Kliks, S., Halstead, S., Peeling, R.W., Margolis, H.S., 2014. Neglected Tropical Diseases 8 (10), e3171.

Kadajji, V. G., Betageri, G. V., 2011. Polymers 3, 1972-2009.

Kim, D., Heo, J., Kim, M., Lee, Y. W., Han, S. W., 2009. Chemical Physics Letters 468, 245-248.

Kulkarni, S. A., Mulla, I. S., Vijayamohanan, K., 2006. Journal of Physics: Conference Series 34, 322-329.

Li, D. X., Jang, Y. J., Lee, J., Lee, J. E., Kochuveedu, S. T., Kim, D. H. J. Mater. Chem. 2011, 21, 16453-16460.

Libraty, D. H., Young, P. R., Pickering, D., Endy, T. P, Kalayanarooj, S., Green, S., Vaughn, D. W., Nisalak, A., Ennis, F. A., Rothman, A. L., 2002. The Journal of Infectious Diseases 186, 1165-1168.

Linares, E. M., Pannuti, C. S., Kubota, L. T., Thalhammer, S., 2013. Biosensors and Bioelectronics 41, 180-185.

Najioullah, F.; Viron, F.; Césaire, R., 2014. Virology Journal 11, 164-168.

Pastoriza-Santos, I., Liz-Marzán, L.M., 2002. Langmuir 18 (7), 2888-2894.

Pei, Z., Anderson, H., Myrskog, A., Dunér, G., Ingemarsson, B., Aastrup, T., 2010. Anal. Biochem. 398, 161-168.

Rivetz, B.; Siman-Tov, D.; Ambal, E.; Jaramillo, A.C.; Ben-Zvi, A.; Tartakovsky, B.; Fish, F., 2009. Clinical Biochemistry 42, 180-184.

Rudmann, S. V. Textbook of Blood banking and transfusion medicine. 2 ed. 2005. Philadelphia: Elsevier Saunders, 686 p.

Schilling, S., Ludolfs, D., Van An, L., Schmitz, H., 2004. Journal of Clinical Virology, 31, 179-184.

Silva, B. V. M., Cavalcanti, I. T., Silva, M. M. S., Dutra, R. F., 2013. Talanta 117, 431-437.

Singh, A. K., Senapati, D., Wang, S., Griffin, J., Neely, A., Candice, P., Naylor, K. M., Varisli, B., Kalluri, J. R., Ray, P. C. 2009. ACS Nano 3, 1906-1912.

Stuart, B. H. Infrared Spectroscopy: Fundamentals and Applications. 2004. Wiley, 244p.

Wang, D., Dou, W., Zhao, G., Chen, Y. 2014. Journal of Microbiological Methods 106, 110-118.

World Health Organization. Working to overcome the global impact of neglected tropical diseases. França, 1-184, 2010.

Wu H-L., Kuo, C-H., Huang, M. H., 2010. Langmuir 26 (14), 12307-12313.

Yamada, K-I.; Takasaki, T.; Nawa, M.; Kurane, I., 2002. Journal of Clinical Virology 24, 203-209.

Young, P. R., Hilditch, P. A., Bletchly, C., Halloran, W., 2000. Journal of Clinical Microbiology, 38 (3), 1053-1057.

Zapp, E., Westphal, E., Gallardo, H., Souza, B., Vieira, I. C., 2014. Biosensors and Bioelectronics 59,127-133.

Zhang, H., Li, W., Wang, J., Peng, H., Che, X., Chen, X., Zhou, Y., 2014. International Journal of Infectious Diseases, 26, 57-66.

Zhang, X.; Ju, H.; Wang, J.. Electrochemical sensors, biosensors and their biomedical applications. Nova York: Elsevier, 2008.

Zhu, Y.; Cao, Y.; Sun, X.; Wang, X. 2013. Sensors 13, 5286-5301.

FIGURE CAPTIONS

Figure 1. Schematic illustration of the stepwise preparation of the immunosensor: (I) modification of SPE surface by PEI-AuNPs film formation, (II) anti-NS1 antibodies immobilization, and (III) blocking with glycine.

Figure 2. Extinction spectrum of Au colloid stabilized with PEI.

Figure 3. TEM micrograph of the PEI-synthesized AuNPs. The inset shows the nanoparticles histogram based on approximately 200 particles.

Figure 4. EDX spectra: (a) bare SPE and (b) SPE modified with PEI-AuNP.

Figure 5. FTIR spectra in ATR mode: (a) bare SPE and (b) PEI-AuNP/SPE.

Figure 6. Cyclic voltammograms of the AuNP-PEI/SPE performed in presence of 0.005 mol L^{-1} of $K_3Fe(CN)_6/K_4Fe(CN)_6$ prepared in 100 mmol L^{-1} KCl, at scan rate of 0.05 V s^{-1}.

Figure 7. Cyclic voltammograms of the immunosensor in each step of immobilization: (a) bare SPE; (b) AuNP-PEI/SPE; (c) anti-NS1/AuNP-PEI/SPE and (d) glycine/anti-NS1/AuNP-PEI/SPE. Scans performed in 0.005 mol L^{-1} $K_3Fe(CN)_6/K_4Fe(CN)_6$, at 0.05V s^{-1} scan rate.

Figure 8. (a) Calibration curve of NS1 immunosensor; (b) Selectivity study of immunosensor to native antigens.

FIGURES

Figure 1

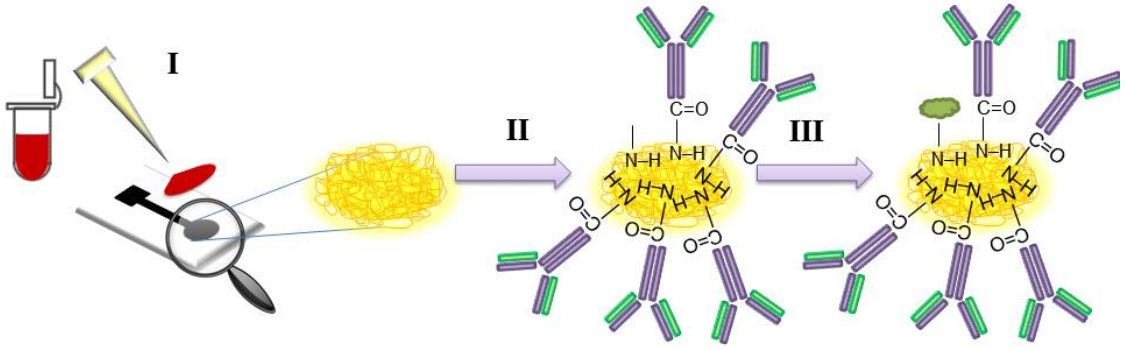

Figure 2

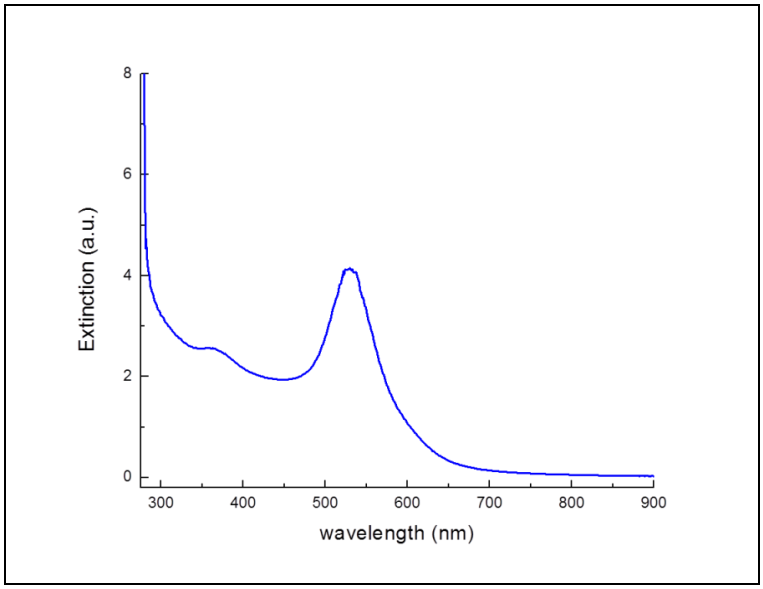
Extinction (a.u.)
0
2
4
6
8
300
400
500
600
700
800
900
wavelength (nm)

Figure 3

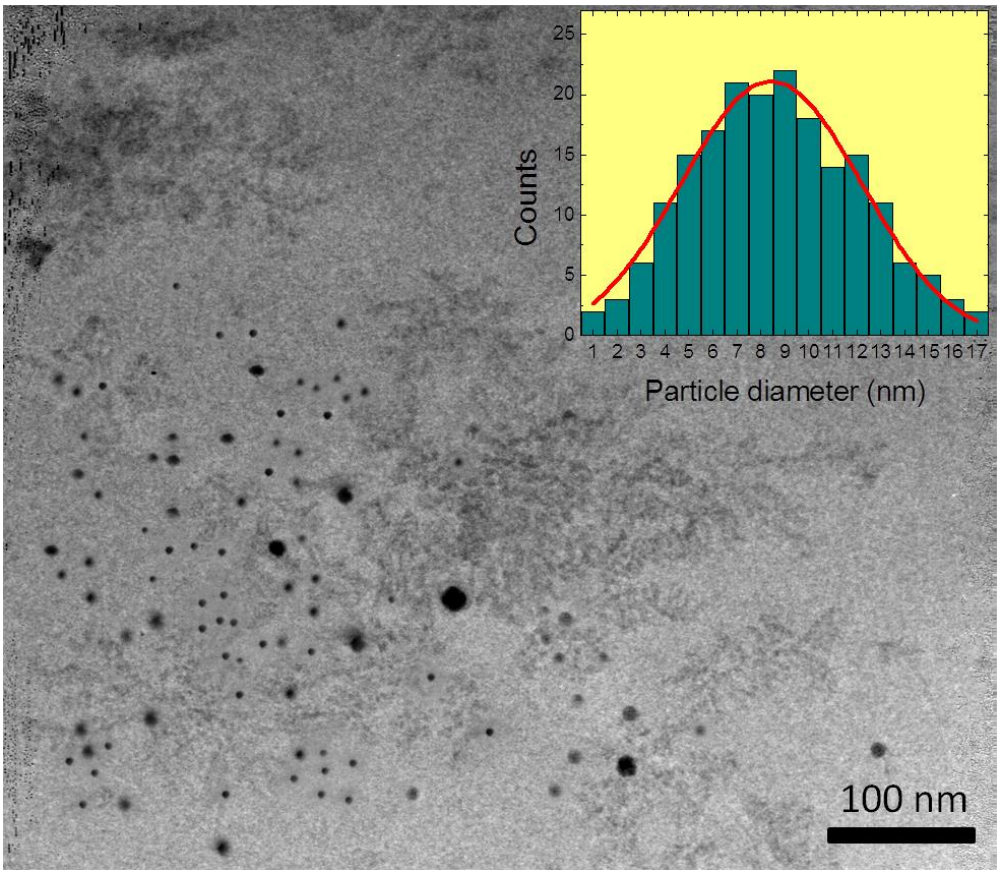
Counts
0
5
10
15
20
25
1 2 3 4 5 6 7 8 9 10 11 12 13 14 15 16 17
Particle diameter (nm)
100 nm

Figure 4

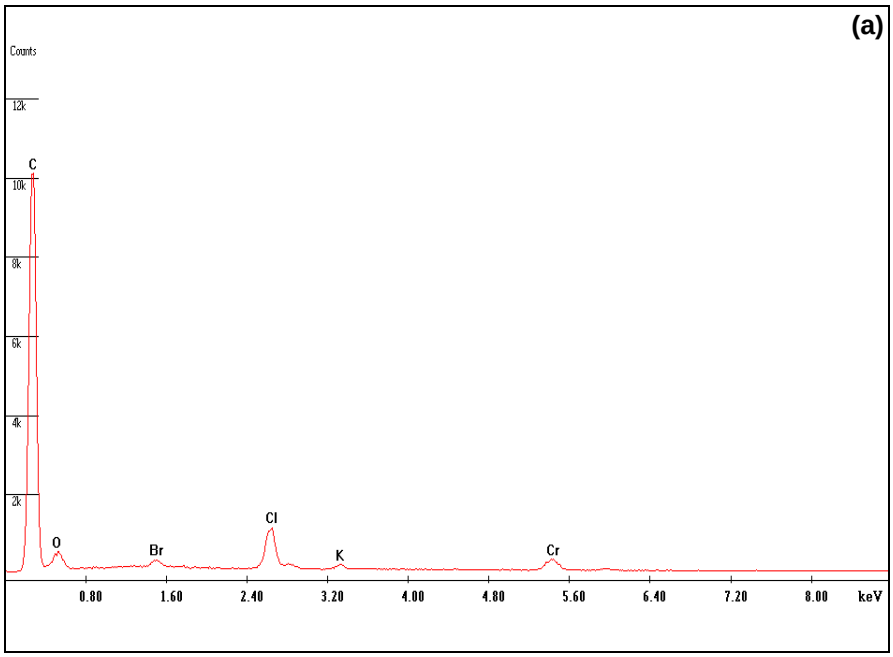
(a)
Counts
12k
10k
8k
6k
4k
2k
C
O
Br
Cl
K
Cr
0.80
1.60
2.40
3.20
4.00
4.80
5.60
6.40
7.20
8.00
keV

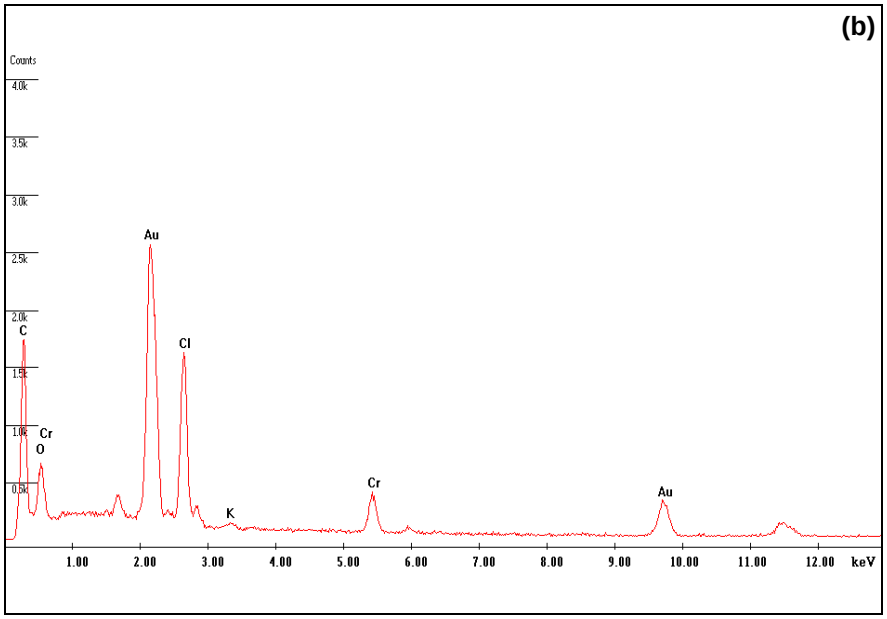
(b)
Counts
4.0k
3.5k
3.0k
2.5k
2.0k
1.5k
1.0k
0.5k
C
Cr
O
Au
Cl
K
Cr
Au
1.00
2.00
3.00
4.00
5.00
6.00
7.00
8.00
9.00
10.00
11.00
12.00
keV

Figure 5

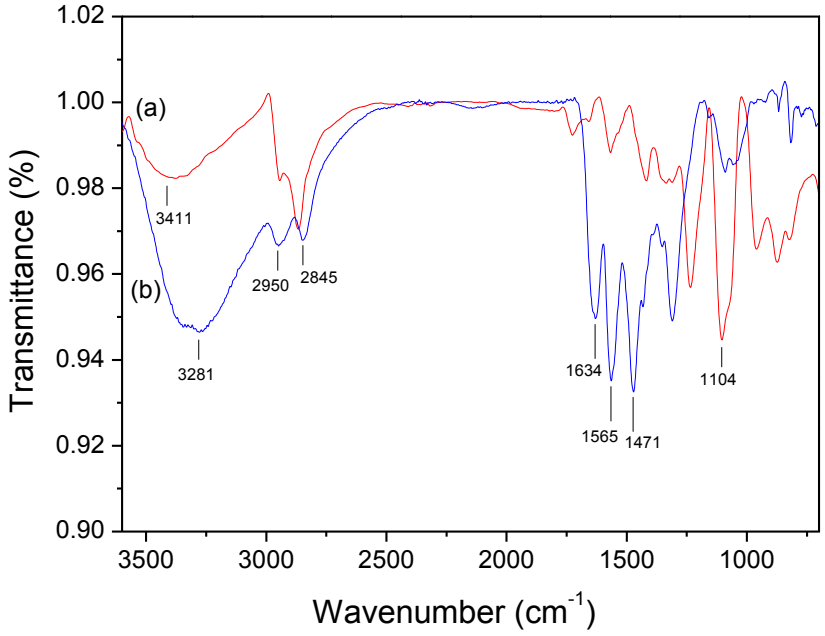
1.02
1.00
0.98
0.96
0.94
0.92
0.90
Transmittance (%)
(a)
(b)
3411
3281
2950
2845
1634
1565
1471
1104
3500
3000
2500
2000
1500
1000
Wavenumber (cm-1)

Figure 6

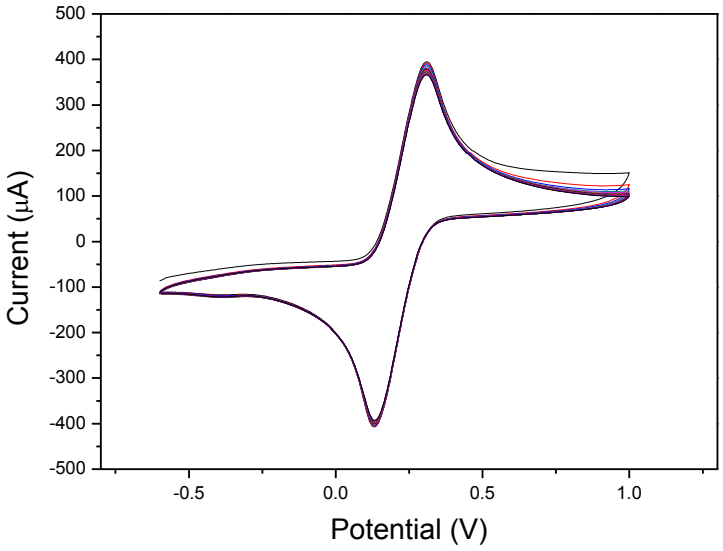
500
400
300
200
100
0
-100
-200
-300
-400
-500
Current (μA)
-0.5
0.0
0.5
1.0
Potential (V)

Figure 7

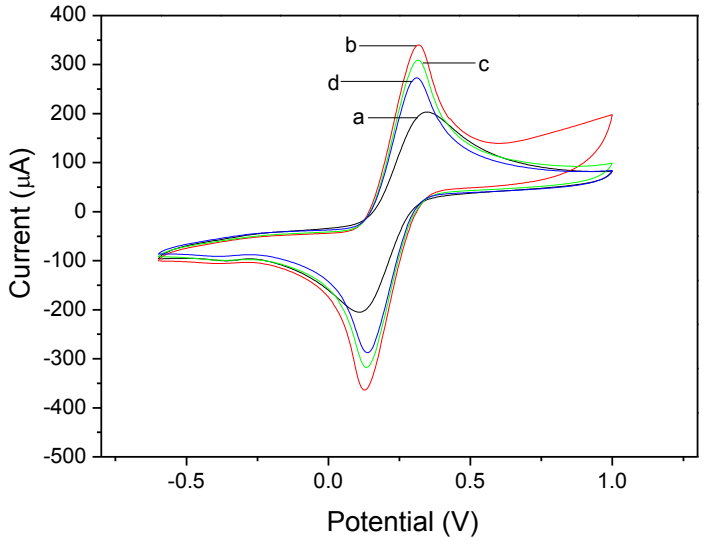
400
300
200
100
0
-100
-200
-300
-400
-500
Current (μA)
-0.5
0.0
0.5
1.0
Potential (V)
b
c
d
a

Figure 8

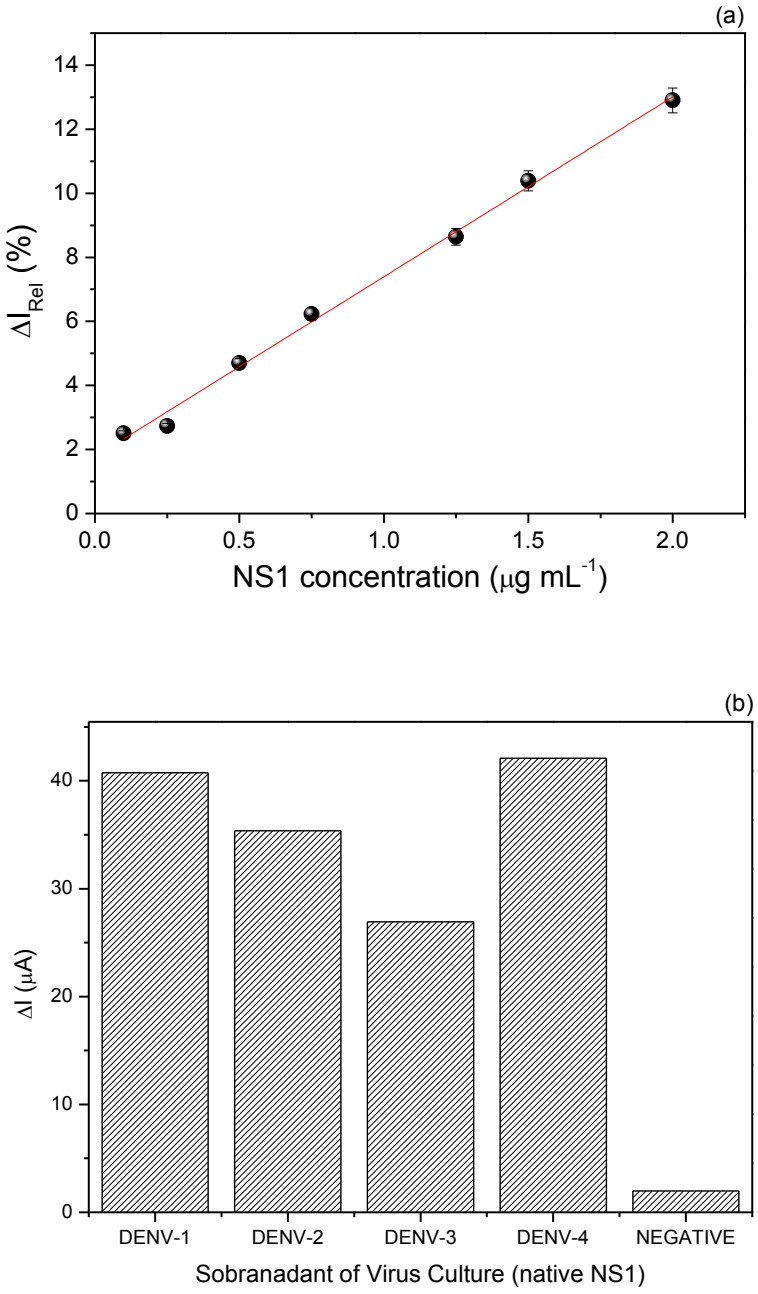
(a)
14
12
10
8
6
4
2
0
0.0
0.5
1.0
1.5
2.0
ΔI_Rel (%)
NS1 concentration (μg mL-1)
(b)
40
30
20
10
0
ΔI (μA)
DENV-1
DENV-2
DENV-3
DENV-4
NEGATIVE
Sobranadant of Virus Culture (native NS1)

SUPPLEMENTARY INFORMATION

Figure S1. Optimization of experimental parameters: (a) Effect of Anti-NS1 concentration on the immunosensor response; (b) Effect of incubation time on the immunosensor response.

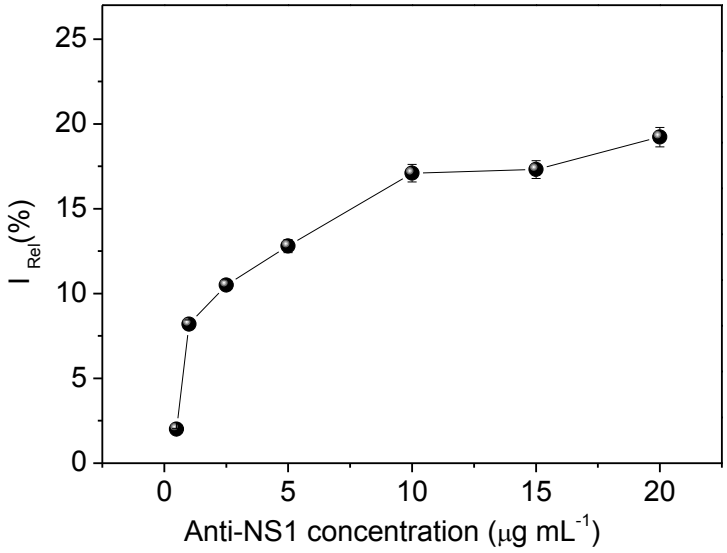

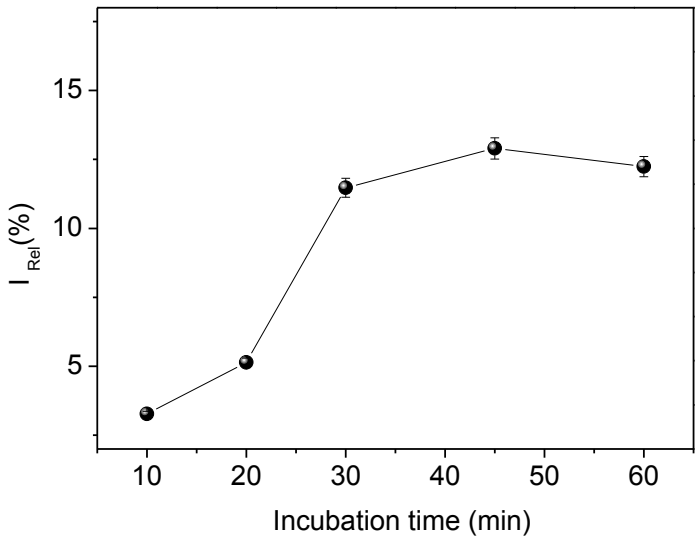

5 CONCLUSÕES

Nesta tese, foram desenvolvidos dois imunossensores eletroquímicos para detecção do antígeno NS1 do DENV. Os dois trabalhos apresentaram *tips* sensores descartáveis empregando uso de diferentes nanomateriais. O primeiro imunossensor teve como ponto forte a confecção de eletrodos impressos já modificados com nanotubos de carbono para imobilização de anticorpos anti-NS1, porém, a resposta foi obtida através de ensaio tipo sanduíche, sendo, portanto, mais demorada. O segundo imunossensor baseou-se na detecção *label-free* da proteína NS1 e utilizou NPsAu modificadas com PEI recobrindo a superfície do eletrodo impresso depois de confeccionado. Ambos foram capazes de identificar concentrações da proteína NS1 em níveis detectáveis para o diagnóstico clínico da dengue, demonstrando grande potencial e boa confiabilidade para serem usados no desenvolvimento de dispositivos sensores.

6 REFERÊNCIAS

AHMED, N.H.; BROOR, S. Comparison of NS1 antigen detection ELISA, real time RT-PCR and virus isolation for rapid diagnosis of dengue infection in acute phase. **Journal of Vector Borne Diseases**, 51, 194-199, 2014.

AHMET, K.; AHLATCIOĞLU, E.; İPEK, Y. K. (2012). **Biosensors and their principles.** In A roadmap of biomedical engineers and milestones, Prof. Sadik Kara (Ed.), ISBN: 978-953-51-0609-8, InTech, DOI: 10.5772/48824. Disponível em: http://www.intechopen.com/books/a-roadmap-of-biomedical-engineers-and-milestones/biosensors-and-their-principles

ALBERT, S.; ALBERT, K.K.; QUACK, M. **High-resolution Fourier Transform Infrared Spectroscopy.** Handbook of high-resolution spectroscopy. New York: John Wiley & Sons, 2011.

ALCON, S.; TALARMIN, A.; DEBRUYNE, M.; FALCONAR, A.; DEUBEL, V.; FLAMAND, M. Enzyme-linked immunosorbent assay specific to dengue virus type 1 nonstructural protein NS1 reveals circulation of the antigen in the blood during the acute phase of disease in patients experiencing primary or secondary infections. **Journal of Clinical Microbiology**, 40, 376-81, 2002.

ALONSO-LOMILLO, M. A.; DOMÍNGUEZ-RENEDO, O.; MATOS, P.; ARCOS-MARTÍNEZ, M. J.. Electrochemical determination of levetiracetam by screen-printed based biosensors. **Bioelectrochemistry**, 74, 306-309, 2009.

ARYA, S.K.; DATTA, M.; MALHOTRA, B.D. Recent advances in cholesterol biosensor. **Biosensors and Bioelectronics**, 23, 1083-1100, 2008.

BACKMANN, N.; ZAHND, C.; HUBER, F.; BIETSCH, A.; PLÜCKTHUN, A.; LANG, H.-P.; GÜNTHERODT, H.-J.; HEGNER, M.; GERBER, C. A label-free immunosensor array using single-chain antibody fragments. **Proceedings of the National Academy of Sciences**, 102, 14587-14592, 2005.

BARBOSA, P. R. M.; RODRIGUES, W. C.; CABRAL, M. M. O. Incidência das formas imaturas de *Aedes albopictus* (Skuse) e *Aedes aegypti* (Linnaeus) no município de Miguel Pereira, RJ, Brasil. EntomoBrasilis 3 (2), 55-58, 2010.

BARD, A.J.; FAULKNER, L.R. **Electrochemical Methods: Fundamentals and Applications**. 2 ed. New York: John Wiley & Sons, 2001. 827 p.

BARKER, G.C.; GARDNER, A.W.; Pulse Polarography. Z. **Analytical Chemistry**, 173, 79-83, 1960.

BARKER, G.C.; JENKINS, I.L.; Square-Wave Polarography. **Analyst**, 77, 685-696, 1952.

BELARMINO, G. O. Alteração no perfil etário dos casos de dengue no Ceará de 2001 a 2011. 2013. **Dissertação** (Mestrado em Patologia) – Faculdade de Medicina, Universidade Federal do Ceará, Fortaleza.

BERGAMINI, M. F.; OLIVEIRA, F. C. M.; ZANONI, M. V. B. Análise voltamétrica do corante têxtil do tipo antraquinona empregando eletrodos de carbono impresso. **Eclética Química**, 30 (2), 53-59, 2005.

BRETT, C.M.A.; BRETT, A.M.O. **Electrochemistry: Principles, Methods, and Applications**. New York: Oxford University Press, 1993. 464 p.

BRONDANI, D.; SOUZA, B.; SOUZA, B. S.; NEVES, A.; VIEIRA, I. C. PEI-coated gold nanoparticles decorated with laccase: A new platform for direct electrochemistry of enzymes and biosensing applications. **Biosensors and Bioelectronics**, 42, 242-247, 2013.

BUCHY, P.; YOKSAN, S.; PEELING, R.W.; HUNSPERGER, E. Laboratory tests for the diagnosis of dengue virus infection. **Special Programme for Research and Training in Tropical Diseases**, Geneva, 2007.

CAMARA, A.R.; GOUVÊA, P.M.P.; DIAS, A.C.M.S.; BRAGA, A.M.B.; DUTRA, R.F.; ARAÚJO, R.E.; CARVALHO, I.C.S. Dengue immunoassay with an LSPR fiber optic sensor. **Optics Express**, 21 (22), 27023-27031, 2013.

CARIDADE, C. I. M. G.. Eléctrodos de filme de carbono: Caracterização e aplicação em sensores e biossensores electroquímicos. 2008. **Tese** (Doutorado em Química) – Faculdade de Ciências e Tecnologia, Universidade de Coimbra, Coimbra.

CAVALCANTI, I. T.; GUEDES, M. I. F.; SOTOMAYOR, M. D. P. T.; YAMANAKA, H.; DUTRA, R. F. A label-free immunosensor based on recordable compact disk chip for early diagnostic of the dengue virus infection. **Biochemical Engineering Journal,** 67, 225-230, 2012.

CHANG, C. M.; LIU, Y. L.. Functionalization of multi-walled carbon nanotubes with non-reactive polymers through an ozone-mediated process for the preparation of a wide range of high performance polymer/carbon nanotube composites. **Carbon**, 48, 1289-1297, 2010.

CHEN, X.; DONG, S. J. Sol–gel-derived titanium oxide/copolymer composite based glucose biosensor. **Biosensors and Bioelectronics**, 18, 999-1004, 2003.

CLARK, R.J.; LYONS, C. Electrode systems for continuous monitoring in cardiovascular surgery. **Annals of the New York Academy of Sciences**, 334, 29-45, 1962.

COSTA, P. R.. Síntese e caracterização de nanopartículas de ouro como ferramenta terapêutica e diagnóstica. 2012. **Dissertação** (Mestrado em Ciência e Tecnologia das Radiações, Minerais e Materais) – Centro de Desenvolvimento da Tecnologia Nuclear, Comissão Nacional de Energia Nuclear, Belo Horizonte.

CUI, G.; YOO, J.H.;LEE, J.S.; YOO, J.; UHM, J.H.; CHA, G.S.; NAM, H. Effect of pretreatment on the surface and electrochemical properties of screen-printed carbon paste electrodes. **Analyst**, 126, 1399–1403, 2001.

DEDAVID, B. A.; GOMES, C. I.; MACHADO, G. **Microscopia eletrônica de varredura: aplicações e preparação de amostras**. Porto Alegre: EDIPUCRS, 2007, 60 p.

FANJUL-BOLADO, P.; HERNÁNDEZ-SANTOS, D.; LAMAS-ARDISANA, P. J.; MARTÍN-PERNÍA, A.; COSTA-GARCÍA, A. Electrochemical characterization of screen-printed and conventional carbon paste electrodes. **Electrochimica Acta**, 53, 3635-3642, 2008.

FANJUL-BOLADO, P.; QUEIPO, P.; LAMAS-ARDISANA, P. J.; COSTA-GARCÍA, A.. Manufacture and evaluation of carbon nanotube modified screen-printed electrodes as electrochemical tools. **Talanta**, 74, 427-433, 2007.

FELIX, F. S.. Novos materiais para aplicações analíticas nas determinações de compostos orgânicos de interesse farmacêutico e ambiental. 2009. **Tese** (Doutorado em Química) – Instituto de Química, Universidade de São Paulo, São Paulo.

FERREIRA, A. A. P.; ULIANA, C. V.; CASTILHO, M. S.; PESQUERO, N. C.; FOGUEL, M. V.; SANTOS, G. P.; FUGIVARA, C. P.; BENEDETTI, A. V.; YAMANAKA, H. **Amperometric biosensor for diagnosis of disease, State of the Art in Biosensors - Environmental and Medical Applications**, Dr. Toonika Rinken (Ed.), 2013. ISBN: 978-953-51-1035-4, InTech, DOI: 10.5772/53656. Disponível em: http://www.intechopen.com/books/state-of-the-art-in-biosensors-environmental-and-medical-applications/amperometric-biosensor-for-diagnosis-of-disease.

FIGUEIREDO, R. M. P.; NAVECA, F. G.; BASTOS, M. S.; MELO, M. N.; VIANA, S. S.; MOURÃO, M. P. G.; COSTA, C. A.; FARIAS, I. P. Dengue Virus Type 4, Manaus, Brazil. **Emerging Infectious Diseases Journal**, 14 (4), 667-669, 2008.

FOSCHINI, M. Eletrossíntese e caracterização de filmes de polipirrol-2-ácido carboxílico para uso em biossensores amperométricos construídos em eletrodos miniaturizados. 2009. **Tese** (Doutorado em Ciências) – Instituto de Física de São Carlos, Universidade de São Paulo, São Carlos.

FOWLER, J. M.; WONG, D. K. Y.; HALSALL, H. B.; HEINEMAN, W. R.. Recent developments in electrochemical immunoassays and immunosensors. **Electrochemical Sensors, Biosensors and their Biomedical Applications**, 115-143, 2008.

FRASCA, S.; ROJAS, O.; SALEWSKI, J.; NEUMANN, B.; STIBA, K.; WEIDINGER, I. M.; TIERSCH, B.; LEIMKÜHLER, S.; KOETZ, J.; WOLLENBERGER, U. Human sulfite oxidase electrochemistry on gold nanoparticles modified electrode. **Bioelectrochemistry**, 87, 33-41, 2012.

FRENS, G. Controlled nucleation for the regulation of the particle size in monodisperse gold suspensions. **Nature Physical Science**, 241, 20-22, 1971.

GALLI, A.; SOUZA, D.; GARBELLINI, G. S.; COUTINHO, C. F. B.; MAZO, L. H.; AVACA, L. A.; MACHADO, S. A. S.. Utilização de técnicas eletroanalíticas na determinação de pesticidas em alimentos. **Química Nova**, 29, 105-112, 2006.

GANDRA, P. G.; ALVES, A. A.; MACEDO, D. V.; KUBOTA, L. T.. Electrochemical determination of antioxidant capacity for physical exercise evaluation. **Química Nova**, 27, 980-985, 2004.

GORNALL, D.D.; COLLYER, S.D.; HIGSON, S.P.J. Investigations into the use of screen-printed carbon electrodes as templates for electrochemical sensors and sonochemically fabricated microelectrode arrays. **Sensors and Actuators B: Chemical**, 141, 581-591, 2009.

GORUP, L. F. Nanopartículas coloidais de ouro e prata e sua funcionalização com dibutil-dicalcogenetos. 2010. **Dissertação** (Mestrado em Química) – Universidade Federal de São Carlos, São Carlos.

GRIESHABER, D.; MACKENZIE, R.; VÖROS, J.; REIMHULT, E. Electrochemical Biosensors - Sensor Principles and Architectures. **Sensors**, 8, 1400-1458, 2008.

GRIFFITHS, P.; HASETH, J.A.D. **Fourier Transform Infrared Spectrometry**. 2 ed. New York: John Wiley & Sons, 2007. 560 p.

GUZMAN, M. G.; HALSTEAD, S. B.; ARTSOB, H.; BUCHY, P.; FARRAR, J.; GUBLER, D. J.; HUNSPERGER, E.; KROEGER, A.; MARGOLIS, H. S.; MARTÍNEZ, E.; NATHAN, M. B.; PELEGRINO, J. L.; SIMMONS, C.; YOKSAN, S.; PEELING, R. W. Dengue: a continuing global threat. **Nature Reviews Microbiology,** S7-S16, 2010.

HALSTEAD, S. B. Dengue. **The Lancet**, 370, 1644-1652, 2007.

HAO, W.; YANG, W.; HUANG, W.; ZHANG, G.; WU, Q.. Time evolution of gold nanoparticles in HPC solution after UV irradiation. **Materials Letters**, 62, 3106-3109, 2008.

HART, J. P.; CREW, A.; CROUCH E.; HONEYCHURCH, K. C.; PEMBERTON, R. M. Some recent designs and developments of screen-printed carbon electrochemical sensors/biosensors for biomedical, environmental, and industrial analyses. **Analytical Letters**, 37, 789-830, 2004.

HASAN, A.; NURUNNABI, M.; MORSHED, M.; PAUL, A.; POLINI, A.; KUILA, T.; AL HARIRI, M.; LEE, Y., JAFFA, A. A. Recent advances in application of biosensors in tissue engineering. **BioMed Research International**, 307519, 2014.

HAYAT, A.; MARTY, J. L. Disposable screen printed electrochemical sensors: tools for environmental monitoring. **Sensors**, 14, 10432-10453 2014.

HUHTAMO, E.; HASU, E.; UZCÁTEGUIA, N.Y.; ERRA, E.; NIKKARI, S.; KANTELE, A.; VAPALAHTI, O.; PIIPARINEN, H. Early diagnosis of dengue in travelers: Comparison of a novel real-time RT-PCR, NS1 antigen detection and serology. **Journal of Clinical Virology**, 47, 49-53, 2010.

HUNSPERGER, E.A.; YOKSAN, S.; BUCHY, P.; NGUYEN, V.C.; SEKARAN, S.D.; ENRIA, D.A.; VAZQUEZ, S.; CARTOZIAN, E.; PELEGRINO, J.L.; ARTSOB, H.; GUZMAN, M.G.; OLLIARO, P.; ZWANG, J.; GUILLERM, M.; KLIKS, S.; HALSTEAD, S.; PEELING, R.W.; MARGOLIS, H.S. Evaluation of commercially

available diagnostic tests for the detection of dengue virus NS1 antigen and anti-dengue virus IgM antibody. **Neglected Tropical Diseases**, 8(10), 2014.

IIJIMA, S. Helical microtubules of graphitic carbon. **Nature**, 354, 56-58, 1991.

IIJIMA, S. Carbon nanotubes: past, present, and future. **Physica B**, 323, 1-5, 2002.

JAHAN, S.; MANSOOR, F.; KANWAL, S. Polymers effects on synthesis of AuNPs, and Au/Ag nanoalloys: Indirectly generated AuNPs and versatile sensing applications including anti-leukemic agent. **Biosensors and Bioelectronics**, 53, 51-57, 2014.

JAHANSHAHI, P.; ZALNEZHAD, E.; SEKARAN, S. D.; ADIKAN, F. R. M. Rapid immunoglobulin M-based dengue diagnostic test using surface plasmon resonance biosensor. **Scientific Reports**, 4, 3851, 2014.

JEYKUMARI, D. R.; NARAYANAN, S. S.. Functionalized carbon nanotube-bienzyme biocomposite for amperometric sensing. **Carbon**, 47, 957-966, 2009.

JUBETE, E.; LOAIZA, O. A.; OCHOTECO, E.; POMPOSO, J. A.; GRANDE, H.; RODRÍGUEZ, J. Nanotechnology: A Tool for Improved Performance on Electrochemical Screen-Printed (Bio)Sensors. **Journal of Sensors**, 1-13, 2009.

KERMAN, K.; SAITO, M.; TAMIYA, E.; YAMAMURA, S.; TAKAMURA, Y.. Nanomaterial-based electrochemical biosensors for medical applications. **Trends in Analytical Chemistry**, 27, 7, 585-592, 2008.

KIM, J. H.; NAM, K.; MA, S. B.; KIM, K. B.. Fabrication and electrochemical properties of carbon nanotube film electrodes. **Carbon**, v. 44, p. 1963-1968, 2006.

KOZAN, J. V. B.. Microssensor para glicose integrado a catéter. 2007. **Dissertação** (Mestrado em Química) – Instituto de Química, Universidade de São Paulo, São Paulo.

KUMARASAMY, V.; ABDUL WAHAB, A. H.; CHUA, S. K.; HASSAN, Z.; CHEM, Y. K.; MOHAMAD, M.; CHUA, K. B.. Evaluation of a commercial dengue NS1

antigen-capture ELISA for laboratory diagnosis of acute dengue virus infection. **Journal of Virological Methods**, 75-79, 2007.

LAPPHRA, K.; SANGCHARASWICHAI, A.; CHOKEPHAIBULKIT, K.; TIENGRIM, S.; PIRIYAKARNSAKUL, W.; CHAKORN, T.; YOKSAN, S.; WATTANAMONGKOLSIL, L.; THAMLIKITKUL, V.. Evaluation of an NS1 antigen detection for diagnosis of acute dengue infection in patients with acute febrile illness. **Diagnostic Microbiology and Infectious Disease**, 60, 387-391, 2008.

LINARES, E. M., PANNUTI, C. S., KUBOTA, L. T., THALHAMMER, S., Immunospot assay based on fluorescente nanoparticles for dengue fever detection. **Biosensors and Bioelectronics** 41, 180-185, 2013.

LINDENBACH, B.D.; RICE, C. M. Molecular biology of flaviviruses. **Advances in Virus Research**, 59, 23-61, 2003.

LIU, G.; LIN, Y. Nanomaterial labels in electrochemical immunosensors and immunoassays. **Talanta**, v. 74, p. 308-317, 2007.

MARTINS, L. D. M. Desenvolvimento de biossensores eletroquímicos como ferramenta para avaliação da capacidade antioxidante de extratos vegetais. 2005. **Tese** (Doutorado em Ciências) - Instituto de Química, Universidade Estadual de Campinas, Campinas.

MCBRIDE, W. J. H.. Evaluation of dengue NS1 test kits for the diagnosis of dengue fever. **Diagnostic Microbiology and Infectious Disease**, 64, 1, 31-36, 2009.

MINISTÉRIO DA SAÚDE$_a$. Secretaria de Vigilância em Saúde. **Guia de vigilância epidemiológica.** (Série A. Normas e Manuais Técnicos). 6. ed. Brasília: Ministério da Saúde, 2005.

MINISTÉRIO DA SAÚDE$_b$. Secretaria de Vigilância em Saúde. Diretoria Técnica de Gestão. **Dengue: diagnóstico e manejo clínico**. (Série A Normas e Manuais Técnicos). 2 ed. Brasília: Ministério da Saúde, 2005.

MINISTÉRIO DA SAÚDE$_a$. Programa Nacional de Controle da Dengue. Disponível em: <http://portal.saude.gov.br/portal/saude/default.cfm>. Acesso em: 24 de março de 2014.

MINISTÉRIO DA SAÚDE$_b$. Sistema de Informação de Agravos de Notificação. Disponível em: http://dtr2004.saude.gov.br/sinanweb/. Acesso em 23 de outubro de 2014.

MORITA, S.; WIESENDANGER, R.; MEYER, E. **Noncontact atomic force microscopy**. Berlin: Springer, 2002. 439 p.

NAJIOULLAH, F.; VIRON, F.; CÉSAIRE, R. Evaluation of four commercial real-time RT-PCR kits for the detection of dengue viruses in clinical samples. **Virology Journal**, 11, 164-168, 2014.

NEWMAN, J. D.; SETFORD, S. J. Enzymatic biosensors. **Molecular Biotechnology**, 32, 249-268, 2006.

NOGUEIRA, R. M.; ARAÚJO, J. M.; SCHATZMAYR, H.G. Dengue viruses in Brazil, 1986-2006. **Revista Panamericana de Salud Pública**, 22 (5), 358-363, 2007.

NOSSER, A. J. The characterization of AuNP-PEI conjugates for siRNA delivery to cancer cells. 2013. **Tese** de Honra. Paper 179. The University of Southern Mississippi.

NUNES, J. S. Dengue: Etiologia, patogênese e suas implicações a nível global. 2011. **Dissertação** (Mestrado em Medicina) – Universidade da Beira Interior, Covilhã.

OLIVEIRA, B. L. Síntese de nanotubos de carbono (NTC) por deposição química de vapor empregando Fe/$CaCO_3$ e Fe/NTC como catalisador. 2009. **Dissertação** (Mestrado em Engenharia Química) – Universidade Federal do Rio de Janeiro, Rio de Janeiro.

OLIVEIRA, M. B. Extração, caracterização e avaliação da atividade larvicida do óleo essencial do *Citrus limon* Linneo (limão) frente ao mosquito *Aedes aegypti*. 2012. **Dissertação** (Mestrado em Química) – Universidade Federal do Maranhão, São Luís.

OLTEANU, N.L.; MEGHEA, A.; ENACHESCU, M.; MIHALY, M. Tunning gold nanoparticles size and surface charge by oil-in-water microemulsion template. **Digest Journal of Nanomaterials and Biostructures,** 8, 4, 1687-1697, 2013.

ORGANIZAÇÃO MUNDIAL DE SAÚDE (OMS) / WORLD HEALTH ORGANIZATION (WHO). **Dengue: Guidelines for Diagnosis, Treatment, Prevention and Control: New Edition.** Geneva, 1-16, 2009.

ORGANIZAÇÃO MUNDIAL DE SAÚDE (OMS) / WORLD HEALTH ORGANIZATION (WHO). **Global strategy for dengue prevention and control 2012-2020**. World Health Organization. França, 1-43, 2012.

OSMA, J. F.; STOYTCHEVA, M. **Biosensors: recent advances and mathematical challenges**. 1 ed. Omnia Science, 2014.

PACHECO, W. F.; SEMAAN, F. S.; ALMEIDA, V. G. K.; RITTA, A. G. S. L.; AUCÉLIO, R. Q. Voltametrias: Uma Breve Revisão Sobre os Conceitos. **Revista Virtual de Química**, 5 (4), 516-537, 2013.

PATACAS, R. C.. Desenvolvimento, caracterização e optimização de um biossensor amperométrico para a determinação de nitrato baseado em microinterfaces geleificadas. 2007. **Dissertação** (Mestrado em Química) – Faculdade de Ciências, Universidade do Porto, Porto.

PEI, Z.; ANDERSON, H.; MYRSKOG, A.; DUNÉR, G.; INGEMARSSON, B.; AASTRUP, T.. Optimizing immobilization on two-dimensional carboxyl surface: pH dependence of antibody orientation and antigen binding capacity. **Analytical Biochemistry**, 398, 161-168, 2010.

PHUONG, H. L.; THAI, K. T. D.; NGA, T. T. T.; GIAO, P. T.; HUNG, L. Q.; BINH, T. Q.; NAM, N. V.; GROEN, J.; VRIES, P. J.. Detection of dengue nonstructural 1 (NS1) protein in Vietnamese patients with fever. **Diagnostic Microbiology and Infectious Disease**, 63, 372-378, 2009.

POPIOLSKI, T. M. Avaliação da incorporação de nanopartículas de ouro em filmes automontados de polieletrólitos fracos. 2011. **Dissertação** (Mestrado em Materiais) – Universidade de Caxias do Sul, Caxias do Sul.

RAPP, B.E.; GRUHL, F.J.; LÄNGE, K. Biosensors with label-free detection designed for diagnostic applications. **Analytical and Bioanalytical Chemistry**, 398, 2403-2412, 2010.

REDDY, V. R. Gold nanoparticles: synthesis and applications. **Synlett**, 11, 1791-1792, 2006.

REIMER, L. **Transmission Electron Microscopy**. 4th Edition, Springer Verlag, Berlin, 1997.

RICCARDI, C. S.; COSTA, P. I.; YAMANAKA, H. Imunossensor amperométrico. **Química Nova**, 25 (2), 316-320, 2002.

RICCI, F.; PALLESCHI, G. Sensor and biosensor preparation, optimisation and applications of prussian blue modified electrodes. **Biosensors and Bioelectronics**, 21, 389-407, 2005.

RIVETZ, B.; SIMAN-TOV, D.; AMBAL, E.; JARAMILLO, A.C.; BEN-ZVI, A.; TARTAKOVSKY, B.; FISH, F. New dengue antibody assay with unique differential detection of IgG and IgM antibodies. **Clinical Biochemistry**, 42, 180-184, 2009.

ROTHMAN, A. L. Immunity to dengue virus: a tale of original antigenic sin and tropical cytokine storms. **Nature Reviews Immunology**, 11(8), 532-543, 2011.

SCHILLING, S.; LUDOLFS, D.; VAN AN, L.; SCHMITZ, H.. Laboratory diagnosis of primary and secondary dengue infection. **Journal of Clinical Virology**, 31, 179-184, 2004.

SHU, P. Y.; HUANG, J. H.. Current advances in dengue diagnosis. **Clinical and Diagnostic Laboratory Immunology**, 11, 642-650, 2004.

SILVA, B. V. M. Emprego de nanomateriais em imunossensores eletroquímicos para detecção da troponina T cardíaca humana. 2012. **Dissertação** (Mestrado em Biologia Celular e Molecular Aplicada) – Universidade de Pernambuco, Recife.

SILVA, B. V. M.; CAVALCANTI, I. T.; MATTOS, A. B.; MOURA, P.; SOTOMAYOR, M. P. T.; DUTRA, R. F.. Disposable immunosensor for human cardiac troponin T based on streptavidin-microsphere modified screen-printed electrode. **Biosensors and Bioelectronics**, 26, 1062-1067, 2010.

SILVA, B. V. M.; CAVALCANTI, I. T.; SILVA, M. M. S.; DUTRA, R. F. A carbon nanotube screen-printed electrode for label-free detection of the human cardiac troponin T. **Talanta**, 117, 431-437, 2013.

SILVA$_a$, M. M. S.; DIAS, A. C. M. S.; SILVA, B. V. M.; GOMES-FILHO, S. L. R.; KUBOTA, L. T.; GOULART, M. O. F.; DUTRA, R. F. Electrochemical detection of dengue virus NS1 protein with a poly(allylamine)/carbon nanotube layered immunoelectrode. **Journal of Chemical Technology and Biotechnology**, 90, 194-200, 2014.

SILVA$_b$, M. M. S.; DIAS, A. C. M. S.; CORDEIRO, M. T.; MARQUES JR., E.; GOULART, M. O. F.; DUTRA, R. F.. A thiophene-modified screen printed electrode for detection of dengue virus NS1 protein. **Talanta**, 128, 505-510, 2014.

SINGHI, S.; KISSOON, N.; BANSAL, A.. Dengue e dengue hemorrágico: aspectos do manejo na unidade de terapia intensiva. **Jornal de Pediatria,** 83, 2, 22-35, 2007.

SMITH, B.C. **Infrared spectral interpretation: a systematic approach.** New York: CRC Press, 1998. 256 p.

SONG, S.; XU, H.; FAN, C. Potential diagnostic applications of biosensors: current and future directions. **International Journal of Nanomedicine**, 1 (4), 433-440, 2006.

SOUZA, D.; CODOGNOTO, L.; MALAGUTTI, A.R.; TOLEDO, R.A.; PEDROSA, V.A.; OLIVEIRA, R.T.S.; MAZO, L.H.; AVACA, L.A.; MACHADO, S.A.S. Voltametria de onda quadrada. Segunda parte: aplicações. **Quimíca Nova**, 27, 5, 790-797, 2004.

SOUZA, D.; MACHADO, S.A.S.; AVACA, L.A. Voltametria de onda quadrada. Aspectos teóricos. **Química Nova**, 1, 81–89, 2003.

SOUZA FILHO, A. G.; FAGAN, S. B.. Funcionalização de nanotubos de carbono. **Química Nova**, 30, 7, 1695-1703, 2007.

SOUZA, L. J.. **Dengue - Diagnóstico, Tratamento e Prevenção**. 2 ed. Rio de Janeiro: Rubio, 2008.

SRIVASTAVA, A.; O'CONNOR, I. B.; PANDIT, A.; WALL, J. G. Polymer-antibody fragment conjugates for biomedical applications. **Progress in Polymer Science**, 39, 308-329, 2014.

TAUIL, P. L. Aspectos críticos do controle do dengue no Brasil. **Caderno de Saúde Pública**, 18 (3), 867-871, 2002.

TEIXEIRA, M. G.; COSTA, M. C.; BARRETO, F.; BARRETO, M. L. Dengue: twenty-five years since reemergence in Brazil. **Cadernos de Saúde Pública**, 1, S7-18, 2009.

TUNCAGIL, S.; ODACI, D.; VARIS, S.; TIMUR, S.; TOPPARE, L. Electrochemical polymerization of 1-(4-nitrophenyl)-2,5-di(2-thienyl)-1 H-pyrrole as a novel

immobilization platform for microbial sensing. **Bioelectrochemistry**, 76, 169–174, 2009.

TURKEVICH, J.; STEVENSON, P. C.; HILLIER, J. A study of the nucleation and growth processes in the synthesis of colloidal gold. **Discussions of the Faraday Society**, 11, 55-75, 1951.

USLU, B.; OZKAN, S. A. Electroanalytical Application of Carbon Based Electrodes to the Pharmaceutical. **Analytical Letters**, 40, 817-853, 2007.

VASQUEZ, S.; RUIZ, D.; BARRERO, R.; RAMIREZ, R.; CALZADA, N.; PEÑA, B. R.; REYES, S.; GUZMAN, M. G.. Kinetics of dengue virus NS1 protein in dengue 4-confirmed adult patients. **Diagnostic Microbiology and Infectious Disease**, 68, 46-49, 2010.

VERHAGEN, L.M.; GROOT, R. Dengue in children. **Journal of Infection**, 69 (S1), S77–S86, 2014.

VETCHINKINA, E. P.; BUROV, A. M.; AGEEVA, M. V.; DYKMAN, L. A.; NIKYTINA, V. E. Biological synthesis of gold nanoparticles by the xylotrophic basidiomycete *Lentinula edodes*. **Applied Biochemistry and Microbiology**, 49, 406-411, 2013.

VIEIRA, S. N. Contribuição para o desenvolvimento de biossensores eletroquímicos para detecção de hepatopatias. 2007. **Dissertação** (Mestrado em Química) – Instituto de Química, Universidade Federal de Uberlândia, Minas Gerais.

WANG, D.; DOU, W.; ZHAO, G.; CHEN, Y.. Immunosensor based on electrodeposition of gold-nanoparticles and ionic liquid composite for detection of *Salmonella pullorum*. **Journal of Microbiological Methods**, 106, 110-118, 2014.

WANG, J.; TIAN, B.; NASCIMENTO, V.B.; ANGNES, L. Performance of screen-printed carbon electrodes fabricated from different carbon inks. **Electrochimica Acta**, 43, 3459-3465, 1998.

WANG, Y.; XU, H.; ZHANG, J.; LI, G. Electrochemical Sensors for Clinic Analysis. **Sensors**, 8, 2043-2081, 2008.

WEI, H.; SUN, J. J.; XIE, Y.; LIN, C. G.; WANG, Y. M.; YIN, W. H.; CHEN, G. N. Enhanced electrochemical performance at screen-printed carbon electrodes by a new pretreating procedure**. Analytica Chimica Acta**, 588, 297-303, 2007.

YAMADA, K-I.; TAKASAKI, T.; NAWA, M.; KURANE, I. Virus isolation as one of the diagnostic methods for dengue virus infection. **Journal of Clinical Virology**, 24, 203-209, 2002.

YÁÑEZ-SEDEÑO, P.; PINGARRÓN, J. M.; RIU, J.; RIUS, F. X.. Electrochemical sensing based on carbon nanotubes. **Trends in Analytical Chemistry**, 29 (9), 939-953, 2010.

YANG, S.; QU, L.; LI, G.; YANG, R.; LIU, C.. Gold nanoparticles/ethylenediamine/carbon nanotube modified glassy carbon electrode as the voltammetric sensor for selective determination of rutin in the presence of ascorbic acid. **Journal of Electroanalytical Chemistry**, 645, 115-122, 2010.

YANG, Y. C.; DONG, S. W.; SHEN, T.; JIAN, C. X.; CHANG, H. J.; LI, Y.; ZHOU, J. X.. Amplified immunosensing based on ionic liquid-doped chitosan film as a matrix and Au nanoparticle decorated graphene nanosheets as labels. **Electrochimica Acta**, 56, 6021-6025, 2011.

YELLOW SPRINGS INSTRUMENT COMPANY. Tecnology and environmental monitoring. Disponível em: <https://www.ysi.com/>. Acesso em: 19 de setembro de 2014.

YOUNG, P. R.; HILDITCH, P. A.; BLETCHLY, C.; HALLORAN, W.. An antigen capture enzyme-linked immunosorbent assay reveals high levels of the dengue virus protein NS1 in the sera of infected patients. **Journal of Clinical Virology**, 38, 3, 1053-1057, 2000.

YUAN, O. C.; CHAI, R.; TANG, Y. A novel amperometric immunosensor based on layer-by-layer assembly of gold nanoparticles-multi-walled carbon nanotubes-thionine multilayer films on polyelectrolyte surface. **Analytica Chimica Acta**, 603, 205-213, 2007.

ZARA, A. L. S. A. Avaliação do valor preditivo positivo da suspeita clínica de dengue em períodos epidêmicos no Brasil, 2000 a 2010. 2012. **Dissertação** (Mestrado em Medicina Tropical e Saúde Pública) – Universidade Federal de Goiás, Goiânia.

ZHANG, H.; LI, W.; WANG, J.; PENG, H.; CHE, X.; CHEN, X.; ZHOU, Y. NS1-based tests with diagnostic utility for confirming dengue infection: a meta-analysis. **International Journal of Infectious Diseases**, 26, 57-66, 2014.

ZHANG, X.; CUI, Y.; LV, Z.; LI, M.; MA, S.; CUI, Z.; KONG, Q. Carbon nanotubes, Conductive Carbon Black and Graphite Powder Based Paste Electrodes. **International Journal of Electrochemical Science**, 6, 6063-6073, 2011.

ZHANG, X.; JU, H.; WANG, J.. **Electrochemical sensors, biosensors and their biomedical applications.** Nova York: Elsevier, 2008.

ZHAO, X.; MAI, Z; KANG, X.; DAI, Z.; ZOU, X. Clay–chitosan–gold nanoparticle nanohybrid: Preparation and application for assembly and direct electrochemistry of myoglobin. **Electrochimica Acta**, 53, 4732-4739, 2008.

ZHU, Y.; CAO, Y.; SUN, X.; WANG, X. Amperometric immunosensor for carbofuran detection based on MWCNTs/GS-PEI-Au and AuNPs-Antibody conjugate. **Sensors**, 13, 5286-5301, 2013.

7 APÊNDICES

7.1 Apêndice A – Artigo publicado, ao longo do Doutorado, no periódico *Optics Express*, com fator de impacto de 3,525.

Dengue immunoassay with an LSPR fiber optic sensor

Alexandre R. Camara,[1,5] Paula M. P. Gouvêa,[2,*] Ana Carolina M. S. Dias,[3] Arthur M. B. Braga,[2] Rosa F. Dutra,[3] Renato E. de Araujo,[4] and Isabel C. S. Carvalho[1]

[1]Dept. of Physics, Pontificia Universidade Católica do Rio de Janeiro (PUC-Rio), Rio de Janeiro, Brazil
[2]Dept. of Mechanical Eng., Pontificia Universidade Católica do Rio de Janeiro (PUC-Rio), Rio de Janeiro, Brazil
[3]Biomedical Engineering Laboratory, Universidade Federal de Pernambuco (UFPE), Recife, Brazil
[4]Laboratoratory of Biomedical Optics and Imaging, Universidade Federal de Pernambuco (UFPE), Recife, Brazil
[5]alexandre.camara@fis.puc-rio.br
**pgouvea@puc-rio.br*

Abstract: Dengue fever is a viral disease that affects millions of people worldwide. Specific tests for dengue are not usually performed due to high costs, complicated procedures and, in some cases, long time to yield a result. For widespread use of specific tests to be possible, fast, reliable and fairly simple methods are needed. In this paper, we present a new dengue diagnostic method for the acute phase of the infection. The method proposed uses an all-optical fiber sensor based on Localized Surface Plasmon Resonance (LSPR) and specular reflection from gold nanoparticles (AuNPs). Dengue anti-NS1 antibody was immobilized on AuNPs deposited on the endface of a standard multimode fiber (62.5μm/125μm). The sensor is able to detect NS1 antigen at different concentrations, with limit of quantification estimated to be 0.074 μg/ml = 1.54 nM. These results indicate that the sensor could potentially be used for dengue diagnosis in the acute phase of the infection.

OCIS codes: (280.1415) Biological sensing and sensors; (060.2370) Fiber optics sensors; (240.6680) Surface plasmons.

References and links

1. S. B. Halstead, "Dengue," Lancet **370**(9599), 1644–1652 (2007).
2. World Health Organization (WHO), "Dengue and severe dengue," Fact sheet **117**, (2012). *www.who.int/mediacentre/factsheets/fs117/en/*
3. S. Bhatt, P. W. Gething, O. J. Brady, J. P. Messina, A. W. Farlow, C. L. Moyes, J. M. Drake, J. S. Brownstein, A. G. Hoen, O. Sankoh, M. F. Myers, D. B. George, T. Jaenisch, G. R. Wint, C. P. Simmons, T. W. Scott, J. J. Farrar, and S. I. Hay, "The global distribution and burden of dengue," Nature **496**(7446), 504–507 (2013), doi:10.1038/nature12060.
4. V. E. P. Martins, C. H. Alencar, M. T. Kamimura, F. M. de, C. Araújo, S. G. De Simone, R. F. Dutra, and M. I. F. Guedes, "Occurrence of natural vertical transmission of dengue-2 and dengue-3 viruses in aedes aegypti and aedes albopictus in Fortaleza, Ceará, Brazil," PLoS ONE **7**, 1–9, e41386 (2012), doi:10.1371/journal.pone.0041386.
5. S. D. Blacksell, "Commercial dengue rapid diagnostic tests for point-of-care application: recent evaluations and future needs?" J. Biomed. Biotechnol. **2012**, 151967 (2012), doi:10.1155/2012/151967.
6. R. W. Peeling, H. Artsob, J. L. Pelegrino, P. Buchy, M. J. Cardosa, S. Devi, D. A. Enria, J. Farrar, D. J. Gubler, M. G. Guzman, S. B. Halstead, E. Hunsperger, S. Kliks, H. S. Margolis, C. M. Nathanson, V. C. Nguyen, N. Rizzo, S. Vázquez, and S. Yoksan, "Evaluation of diagnostic tests: dengue," Nat. Rev. Microbiol. **8**(12 Suppl), S30–S37 (2010), doi:10.1038/nrmicro2459.
7. P. Philip Samuel and B. K. Tyagi, "Diagnostic methods for detection & isolation of dengue viruses from vector mosquitoes," Indian J. Med. Res. **123**(5), 615–628 (2006).
8. E. Huhtamo, E. Hasu, N. Y. Uzcátegui, E. Erra, S. Nikkari, A. Kantele, O. Vapalahti, and H. Piiparinen, "Early diagnosis of dengue in travelers: comparison of a novel real-time RT-PCR, NS1 antigen detection and serology," J. Clin. Virol. **47**(1), 49–53 (2010).
9. T. Q. Huy, N. T. H. Hanh, N. T. Thuy, P. V. Chung, P. T. Nga, and M. A. Tuan, "A novel biosensor based on serum antibody immobilization for rapid detection of viral antigens," Talanta **86**, 271–277 (2011).

#196103 - $15.00 USD Received 20 Aug 2013; revised 2 Oct 2013; accepted 7 Oct 2013; published 31 Oct 2013

4 November 2013 | Vol. 21, No. 22 | DOI:10.1364/OE.21.027023 | OPTICS EXPRESS 27023

10. S. Alcon, A. Talarmin, M. Debruyne, A. Falconar, V. Deubel, and M. Flamand, "Enzyme-linked immunosorbent assay specific to dengue virus type 1 nonstructural protein NS1 reveals circulation of the antigen in the blood during the acute phase of disease in patients experiencing primary or secondary infections," J. Clin. Microbiol. **40**(2), 376–381 (2002).
11. Centers for Disease Control and Prevention (CDC), Dengue Homepage, "Laboratory guidance and diagnostic testing," (2010). www.cdc.gov/dengue/clinicalLab/laboratory.html.
12. A. C. M. S. Dias, S. L. R. Gomes-Filho, M. M. S. Silva, and R. F. Dutra, "A sensor tip based on carbon nanotube-ink printed electrode for the dengue virus NS1 protein," Biosens. Bioelectron. **44**, 216–221 (2013).
13. M. D. L. Oliveira, M. L. Nogueira, M. T. S. Correia, L. C. B. B. Coelho, and C. A. S. Andrade, "Detection of dengue virus serotypes on the surface of gold electrode based on cratylia mollis lectin affinity," Sens. Actuators B. **155**, 789–795 (2011), doi:10.1016/j.snb.2011.01.049.
14. C. C. Su, T. Z. Wu, L. K. Chen, H. H. Yang, and D. F. Tai, "Development of immunochips for the detection of dengue viral antigens," Anal. Chim. Acta **479**(2), 117–123 (2003), doi:10.1016/S0003-2670(02)01529-5.
15. D. Atias, Y. Liebes, V. Chalifa-Caspi, L. Bremand, L. Lobel, R. S. Marks, and P. Dussart, "Chemiluminescent optical fiber immunosensor for the detection of IgM antibody to dengue virus in humans," Sens. Actuators B. **140**, 206–215 (2009), doi:10.1016/j.snb.2009.03.044.
16. K. Chan, C. Tan, W. Teng, F. A. Rahman, S. Soon, and Z. R. Zulkifly, "Feasibility study of long period grating as an optical biosensor for dengue virus detection - an alternative approach to dengue virus screening," in *Proceedings of 2010 IEEE EMBS Conference on Biomedical Engineering & Sciences* (IECBES 2010, Kuala Lumpur, Malaysia, 2010), pp. 38–42.
17. L. H. Chen, C. C. Chan, K. Ni, P. B. Hu, T. Li, W. C. Wong, P. Balamurali, R. Menon, M. Shaillender, B. Neu, C. L. Poh, X. Y. Dong, X. M. Ang, P. Zu, Z. Q. Tou, and K. C. Leong, "Label-free fiber-optic interferometric immunosensors based on waist-enlarged fusion taper," Sens. Actuators B Chem. **178**, 176–184 (2013), doi:10.1016/j.snb.2012.12.071.
18. A. J. Haes and R. P. Van Duyne, "A unified view of propagating and localized surface plasmon resonance biosensors," Anal. Bioanal. Chem. **379**(7-8), 920–930 (2004).
19. P. M. P. Gouvêa, H. Jang, I. C. S. Carvalho, M. Cremona, A. M. B. Braga, and M. Fokine, "Internal specular reflection from nanoparticle layers on the end face of optical fibers," J. Appl. Phys. 109, 103114 (2011), doi:10.1063/1.3583582.
20. D. G. Kinniburgh, "General purpose adsorption isotherms," Environ. Sci. Technol. **20**(9), 895–904 (1986).
21. A. J. Haes and R. P. Van Duyne, "A nanoscale optical biosensor: sensitivity and selectivity of an approach based on the localized surface plasmon resonance spectroscopy of triangular silver nanoparticles," J. Am. Chem. Soc. **124**(35), 10596–10604 (2002).
22. C. A. Barrios, M. J. Bañuls, V. González-Pedro, K. B. Gylfason, B. Sánchez, A. Griol, A. Maquieira, H. Sohlström, M. Holgado, and R. Casquel, "Label-free optical biosensing with slot-waveguides," Opt. Lett. **33**(7), 708–710 (2008), doi:10.1364/OL.33.000708.
23. S. Vazquez, D. Ruiz, R. Barrero, R. Ramirez, N. Calzada, B. del Rosario Peña, S. Reyes, and M. G. Guzman, "Kinetics of dengue virus NS1 protein in dengue 4-confirmed adult patients," Diagn. Microbiol. Infect. Dis. **68**(1), 46–49 (2010), doi:10.1016/journal.pntd.0001309.
24. N. J. Geddes, A. S. Martin, F. Caruso, R. S. Urquhart, D. N. Furlong, J. R. Sambles, K. A. Than, and J. A. Edgar, "Immobilisation of IgG onto gold surfaces and its interaction with anti-IgG studied by surface plasmon resonance," J. Immunol. Methods **175**(2), 149–160 (1994).
25. S. Maguis, G. Laffont, P. Ferdinand, B. Carbonnier, K. Kham, T. Mekhalif, and M. C. Millot, "Biofunctionalized tilted fiber Bragg gratings for label-free immunosensing," Opt. Express **16**(23), 19049–19062 (2008), doi:10.1364/OE.16.019049.

1. Introduction

Dengue fever is a tropical disease caused by the dengue virus, transmitted mainly by the female *Aedes aegypti* mosquito [1]. The World Health Organization (WHO) estimates that there are over 2.5 billion people at risk of dengue infection and that there are about 50 - 100 million new cases per year. Of these, over 500,000 would be cases of dengue hemorrhagic fever (severe dengue) [2]. Samir Bhatt et al [3], however, estimate that there are actually about 390 million dengue infections per year. In Brazil, for example, dengue is a major public health problem affecting thousands of people every year [4].

Dengue fever may be fatal if it evolves into hemorrhagic fever (severe dengue) or dengue shock syndrome, which occur in 5% of the cases. In fact, even non-severe dengue fever may be fatal, if untreated. In some Asian and Latin American countries, dengue is a leading cause of death among children [2]. Early detection and appropriate therapy increase the chance of survival; severe dengue mortality rates can be decreased from 20% down to 1% with proper support therapy from experienced healthcare providers [2]. Unfortunately, in some cases, the

#196103 - $15.00 USD Received 20 Aug 2013; revised 2 Oct 2013; accepted 7 Oct 2013; published 31 Oct 2013

patient does not get the necessary support therapy in time to save his/her life, because the illness is initially misdiagnosed. One reason for this is that dengue symptoms can be easily mistaken with those of other illnesses, for example, flu, gastroenteritis or other viral infections. In many locations patients with suspicious symptoms are not routinely checked for dengue infection.

Usually, when a patient arrives at a hospital or clinic with dengue-like symptoms, the initial diagnosis performed is based mainly on observed and reported symptoms. The patient may be submitted to laboratory tests, but most of the times the only type of analyses used are white blood cell and platelet counts. While it is true that patients with dengue infection have low white blood cell and platelet counts, these are not specific to dengue infection. Despite that, specific tests for detection of dengue anti-NS1 antibody, dengue NS1 antigen, dengue viral RNA or dengue virus are rarely performed. In fact, even on the rare occasions when commercial specific tests are available at hospitals and clinics, these have several limitations. As reported by Blacksell [5], there are many challenges that still need to be addressed by researchers, manufacturers and legislators, including lack of regulations, geographical variation, differences between primary and secondary infections, sample type, etc. To make matters worse, the performance of many commercial tests has not been adequately evaluated [6].

The major laboratorial methods currently available for diagnosis of the disease are viral culture [7] and viral RNA detection by reverse transcriptase PCR (RT-PCR) [8], which require highly skilled personnel, laborious procedure and are time consuming [9]. Serological tests such as the frequently used immunoglobulin M (IgM) capture enzyme-linked immunosorbent assay (MAC-ELISA) have low sensitivity during the first four days of illness [10]. In fact, patients with dengue infection for the first time will not have anti-NS1 antibody until about day 5 after the onset of the infection [6, 11], which in some cases may be too late to administer the necessary care. Dengue virus and dengue antigen NS1 are present since day 1 of infection, but dengue virus testing is expensive and may take more than 1 week to yield a result, in addition to requiring expertise from the operator and expensive equipment/appropriate facilities [6]. On the other hand, dengue NS1 antigen detection methods are in general faster, cheaper and, therefore, ideal for early detection. In terms of early diagnosis and management, supplying tests based on NS1 antigen detection to healthcare providers in regions with high dengue incidence or during epidemics could save lives and help manage the disease as a public health problem [6]. Nonetheless, since NS1 antigen levels fall to undetectable levels after 5-6 days (secondary infection) or 8-9 days (primary infection) after the onset of the disease, these can only give a correct positive result during the first few days of infection [5].

Dengue diagnosis is thus complex and requires different solutions for different scenarios. Because current commercial solutions are not completely satisfactory, new diagnostic tools have been proposed in literature recently [12–14]. Among fast, reliable and fairly simple methods developed are solutions based on optical fiber sensors [15–17]. Depending on the method and setup used, optical fiber sensors offer several characteristics that could be advantageous if applied for dengue sensing: cheap sensing elements (optical fiber), portability, robustness, ease of handling and possibility of using a sample as small as a drop.

Localized Surface Plasmon Resonance (LSPR) is a viable phenomenon that can be used with optical fiber sensing in order to obtain a cheap, straightforward, fast and accurate diagnosis via NS1 antigen sensing. LSPR occurs when light impinges upon metal nanoparticles (NPs) surrounded by dielectric material. Due to LSPR, spectral changes in the resonant absorption of the NPs will occur with changes in the surrounding refractive index. This phenomenon can be employed in biosensing and sensing of liquids and gases [18]. In order to impart selectivity to a sensor based on LSPR, a material with affinity to the desired target-substance can be attached to the NPs.

#196103 - $15.00 USD Received 20 Aug 2013; revised 2 Oct 2013; accepted 7 Oct 2013; published 31 Oct 2013

In this paper, we present a sensor for dengue NS1 antigen obtained by immobilizing anti-NS1 antibody on the gold nanoparticles (AuNPs) of an all-optical fiber sensor based on LSPR [19]. The sensor was shown to have a good correlation between wavelength shifts and NS1 antigen concentration, as well as negligible wavelength shift for zero concentration of NS1 antigen. The results discussed in this paper indicate that our sensor can be a powerful tool for sensing of dengue NS1 antigen in samples from patients who exhibit symptoms that fit the clinical presentation of dengue.

2. Materials and methods

2.1. Preparation of the sensing element

The sensing element is located at the tip of each fiber sample. It was prepared by following the first five steps described below, which involve forming and cleaning nanoparticles (NPs) on the fiber endface (Steps 1-2) and immobilizing anti-NS1 antibody on these NPs (Steps 3-5).

Step 1 (AuNPs preparation): Au nanoparticles were created on top of the endface of an optical fiber by sputter deposition of a 6 nm-thick gold thin film followed by a 4 minute-long annealing at 600°C. Figure 1(a) shows a Scanning Electron Microscope (SEM) image of the NPs on top of the fiber endface after the annealing. In the schematics in Fig. 1(b) the NPs are represented by pink spheres. The fibers used in this work were standard multimode fibers with core and cladding diameters equal to 62.5µm and 125µm, respectively.

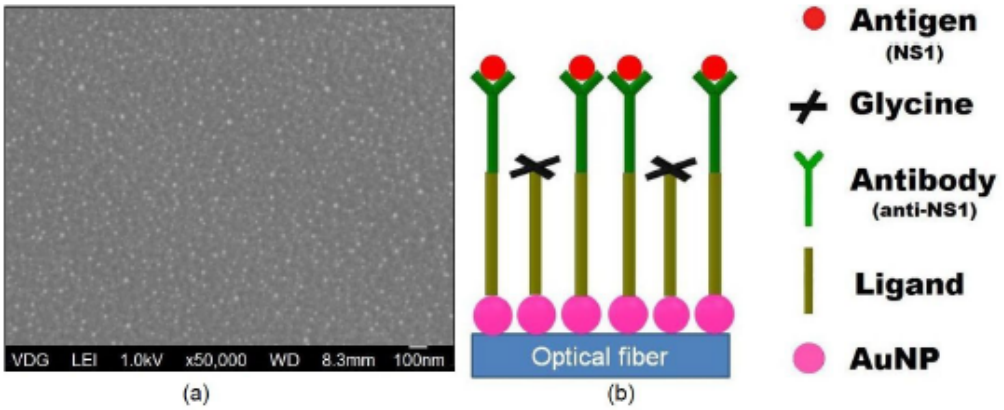

Fig. 1. (a) SEM image of AuNPs (white spots) on the endface of an optical fiber [courtesy of Van der Graaff Lab/PUC-Rio]. (b) Schematic diagram of the fiber endface with AuNPs, ligand, anti-NS1 antibody, Glycine and adsorbed dengue NS1 antigen.

Step 2 (AuNPs cleaning): The fiber tip was immersed in a 0.5 M solution of nitric acid (HNO_3) in water to treat/clean the NPs so that microorganisms would not affect the chemical reactions in the next steps.

Step 3 (ligand deposition/amine-fuctionalization): The fiber tip was immersed for at least 2 hours in a solution of ligand (cysteamine) in ethanol. The ligand allowed the adsorption of dengue anti-NS1 antibody to the NPs, and was represented by the dark yellow/olive lines in Fig. 1(b). Initially, two ligand solutions were tested: a 100mM solution of Mercaptopropionicacid (MPA) in ethanol and a 50 mM solution of Cysteamine (2-aminoethanethiol) in ethanol. Since the fibers with Cysteamine presented larger wavelength shifts and higher reproducibility, all fibers used in the experiments in this paper were prepared with Cysteamine.

Step 4 (anti-NS1 antibody immobilization): The fiber tip was immersed for 1 hour in a solution of anti-NS1 antibody in phosphate buffered saline (PBS) solution. The anti-NS1 antibody is represented by green Ys in Fig. 1(b). The PBS solution (pH7.4, 10 mM) was prepared by dissolving 0.2g KCl, 8.0g NaCl, 0.24g KH_2PO_4 and 1.44g Na_2HPO_4 in 1000mL

#196103 - $15.00 USD Received 20 Aug 2013; revised 2 Oct 2013; accepted 7 Oct 2013; published 31 Oct 2013

of ultra-pure water. Anti-NS1 antibody binds to Cysteamine via amide bond; amine groups of Cysteamine form amide bonds with the carboxyl groups in the anti-NS1 antibody.

Step 5 (blocking with Glycine): The fiber tip was immersed for 1 hour in a 50mM aqueous solution of Glycine (represented by black crosses in Fig. 1(b)) to prevent NS1 antigen from binding free-amine groups of Cysteamine. By blocking, one ensures that NS1 antigen will interact only with anti-NS1 antibody.

The NS1 antigen used was dengue antigen nonstructural protein 1 (1 mg/mL, >90% purity) from *AbCAM*. All the other reagents used in this work were purchased from *Sigma-Aldrich Chemical*.

Step 5 is the last step involved in preparing the sensing element of the sensor, which is now ready for testing.

2.2. Sensor testing (NS1 antigen detection)

After the immobilization of anti-NS1 antibody and isolation of unbound ligand groups, the sensing element was ready to be used for sensing dengue NS1 antigen. In order to test if the sensor could detect the presence of NS1 antigen, the fiber tip was incubated by dipping it for 1 hour in a solution of NS1 antigen (red spheres in Fig. 1(b)) in PBS. Tests were also performed with shorter immersion times (approximately 30 min), yielding similar results.

The anti-NS1 antibody used was IgG.

2.3. Experimental setup

The fiber sample was spliced to the setup in Fig. 2, the all-optical fiber sensor based on LSPR [19].

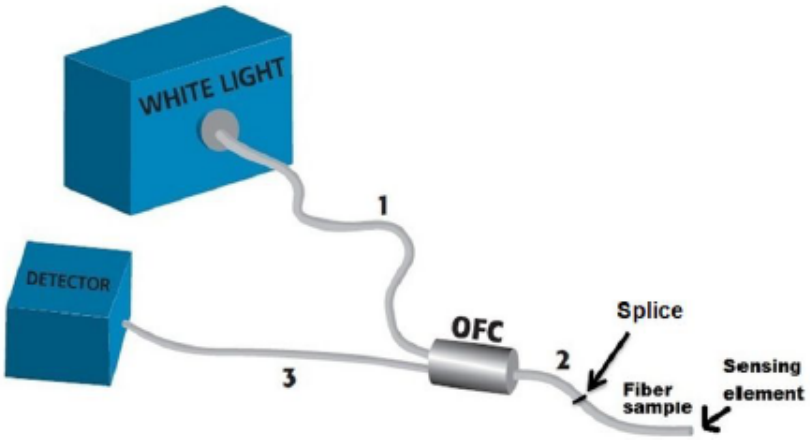

Fig. 2. LSPR-based all-optical fiber sensor: white light source, optical fiber coupler (OFC) and spectrum analyzer (detector). The fiber sample, with the sensing element on its tip, is spliced to Fiber 2.

The system consists of a white light source (*Ando AQ-4303B*), a detector (spectrum analyzer *OceanOptics®USB 2000*) and a 2x1 optical fiber coupler (OFC) with standard multimode fiber (62.5μm/125μm), custom made by *OptoLink Ind e Com Ltda*. The fiber sample was spliced to Fiber 2 of the OFC such that the sensing element was located on the free end (not spliced). Light coupled into Fiber 1 propagated through the coupler and Fiber 2, and into the fiber sample. The light back-reflected from its endface, where the sensing element is located, propagated back though the optical fiber coupler and into Fiber 3, which was connected to the detector/spectrum analyzer. The detected light contained the LSPR signal with information from the sensing element.

#196103 - $15.00 USD Received 20 Aug 2013; revised 2 Oct 2013; accepted 7 Oct 2013; published 31 Oct 2013

3. Results and discussions

3.1 Dengue NS1 antigen sensing: detection

In order to test if our sensor was capable of detecting NS1 antigen, fifteen fiber samples were prepared. After each of the 5 steps described in section 2.1, the fiber sample was removed from the solution and spliced to the setup (Fig. 2) by the other side, i.e. the side that did not contain the sensing element. The reflected signal was then acquired with the sensing element in air. Figure 3(a) shows the reflected signals obtained for a typical fiber throughout the preparation of the sensing element.

Likewise, in order to test the sensor for NS1 antigen detection, the reflected signal was acquired with the fiber sample spliced to the setup after the procedure described in section 2.2. Figure 3(b) shows the reflected signal acquired and for comparison it also shows the reflected signal after the previous step (Step 5).

Note that all curves have a dip at lower wavelengths. This dip is present in reflection curves obtained with the optical fiber LSPR sensor when the medium surrounding the NPs has refractive index in the range from 1 to approximately 1.4, and exhibits a blue-shift as the refractive index increases [19].

In Figs. 3(a) and 3(b), the wavelength shifts between steps occur because the new component added at each step changed the medium surrounding the NPs, therefore changing its effective refractive index. Note that the wavelength shifts along the steps are not all in the same direction. This occurs because adding each new layer in the procedure will increase (blue-shift) or decrease (red-shift) the effective refractive index. No attempt was made to quantify the effective refractive index surrounding the NPs because this was not the focus of the experiment, however, in principle the model introduced in [19] could be used for this.

All curves in Fig. 3 have been smoothed and shifted vertically for clarity.

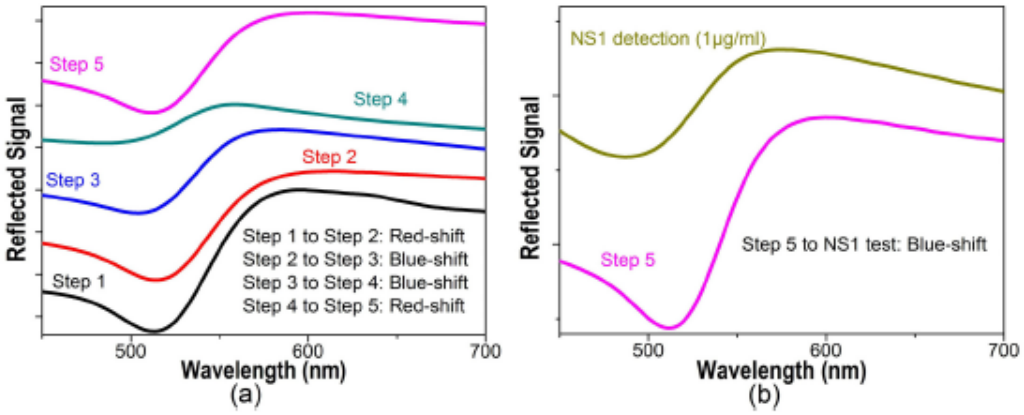

Fig. 3. Reflected signals for a typical fiber sample after (a) Steps 1 to 5 at ligand Cysteamine concentration of 1µg/ml (Step 3) and anti-NS1 antibody concentration of 1µg/ml (Step 4), and (b) when testing the sensor with NS1 antigen with concentration of 1µg/ml.

During the preparation of the sensing element, eleven of the fifteen fiber samples presented the wavelength shift pattern shown in Fig. 3(a): red-shift after the AuNPs cleaning (from Step 1 to Step 2); blue-shift after the ligand deposition/amine-functionalization (from Step 2 to Step 3); another blue-shift after the immobilization of anti-NS1 antibody (from Step 3 to Step 4); and red-shift after the blocking with Glycine (from Step 4 to Step 5). Since the other four fibers presented random wavelength shifts throughout the preparation of the sensing element, they were discarded.

All eleven fiber samples that followed the red-blue-blue-red wavelength shift pattern during the preparation of the sensing element presented a blue-shift when tested with NS1 antigen, as in Fig. 3(b). This result shows that our sensor is reliable for detecting the presence

#196103 - $15.00 USD Received 20 Aug 2013; revised 2 Oct 2013; accepted 7 Oct 2013; published 31 Oct 2013

of dengue NS1 antigen, as long as the wavelength shifts during the preparation of the sensing element follow the red-blue-blue-red pattern.

3.2 Dengue NS1 antigen sensing: concentration

To investigate if the sensor could be used to assess the concentration of dengue NS1 antigen, solutions with different concentrations of NS1 antigen in PBS were prepared and used in the procedure described in section 2.2. A graph similar to the one shown in Fig. 3(b) was obtained for each measurement and the center of the LSPR dip was located for the reflected signals. The wavelength shift was then calculated as the difference ($\lambda_{NS1detection} - \lambda_{Step5}$).

The black squares in Fig. 4 represent the data of the wavelength shift ($\Delta\lambda$) as a function of NS1 antigen concentration (C_{NS1}) for three different fiber samples. It was possible to use each sample for more than one concentration because the measurements were performed from low concentration to high concentration.

Concentrations of NS1 antigen equal to 0.05µg/ml, 0.1µg/ml, 0.3µg/ml, 0.5µg/ml, 0.7µg/ml and 1.0µg/ml were used. The point (0,0) was added for fitting purposes, and is consistent with the result discussed in section 3.3. Note that $\Delta\lambda$ is negative because the wavelength shifts are blue-shifts, as discussed in the section 3.1.

The uncertainty of measurement ($U_\lambda = \pm 0.5$nm) is represented by black lines at each data point and was estimated using uncertainty Type B methods by taking into account the uncertainty of the detector and the uncertainty in determining the central wavelength. The uncertainty for concentration was not considered, since it was estimated to be small.

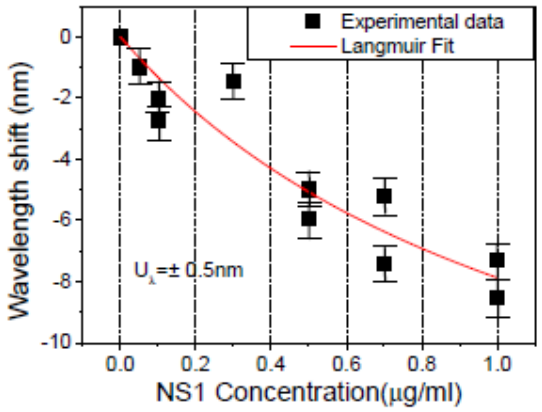

Fig. 4. LSPR wavelength shift ($\Delta\lambda$) at different concentrations of NS1 antigen (C_{NS1}) in PBS solutions (black squares) fitted by the Langmuir Isotherm (red curve).

The Langmuir isotherm equation can be applied to our LSPR sensor to fit the data in Fig. 4. The Langmuir adsorption model is frequently used to fit adsorption data as a function of concentration or partial pressure at a fixed temperature [20]. Among several other applications, this model can be applied to describe the antibody-antigen binding interaction when characterizing a biosensor. The Langmuir model can be applied to our LSPR sensor to characterize the antibody/antigen (anti-NS1/NS1) interaction, assuming the following requirements apply: all adsorption sites are equivalent, the adsorption is limited to only one monolayer, there is only one monolayer involved in adsorption, and the probability of a molecule being adsorbed by a site is independent of neighboring sites. In this case, the wavelength shift measured by our optical fiber LSPR sensor as a function of NS1 antigen concentration can be approximated by the Langmuir isotherm equation expressed as [21],

$$\Delta\lambda = \Delta\lambda_{MAX}\left(\frac{KC_{NS1}}{1+KC_{NS1}}\right) \quad \text{Langmuir isotherm equation} \qquad (1)$$

#196103 - $15.00 USD Received 20 Aug 2013; revised 2 Oct 2013; accepted 7 Oct 2013; published 31 Oct 2013

where $\Delta\lambda$ is the LSPR wavelength shift due to binding of NS1 antigen to the layer of anti-NS1 antibody; $\Delta\lambda_{MAX}$ is the maximum value of the wavelength shift (at saturation level); K is the affinity constant between anti-NS1 antibody and NS1 antigen, equal to the ratio of bound to non-bound NS1 antigen at equilibrium (saturation); and the independent variable C_{NS1} is the concentration of NS1 antigen in PBS solution. Note that $\Delta\lambda$ and $\Delta\lambda_{MAX}$ are negative because the wavelength shifts are blue-shifts, as shown in Fig. 3(b).

The red curve in Fig. 4 shows the fitting of the experimental data obtained with Eq. (1). From the fitting, the maximum LSPR wavelength shift ($\Delta\lambda_{MAX}$ = –17.6 nm) and the affinity constant (K = 0.81 ml/μg = 0.039 nM^{-1}) were determined. This result is in accordance with K values presented in [17]: K = 0.029 nM^{-1} for the Mach-Zehnder interferometer sensor and K = 0.063 nM^{-1} for the Michelson interferometer sensor.

The sensitivity of the sensor for NS1 antigen detection is given by [22],

$$S = \frac{|\Delta\lambda_{MAX}|}{\sigma_{MAX}} \tag{2}$$

where σ_{MAX} is the surface density of NS1 antigen when immobilized anti-NS1 antibody have all binding sites occupied, and is given by [22],

$$\sigma_{MAX} = \frac{M_{NS1}}{N_A P_{NS1}^2} \tag{3}$$

where $N_A = 6.02\text{x}10^{23}$ is Avogadro's number, and M_{NS1} and P_{NS1} are the molecular mass and average molecular length of NS1 antigen, respectively. Using $M_{NS1} \approx 48$kg/mol [23] and $P_{NS1} \approx 14$nm [17, 24] in Eq. (3), the surface density is $\sigma_{MAX} \approx 0.41$ ng/mm^2. Using this result in Eq. (2), the sensor sensitivity is equal to S ≈43 nm/(ng/mm^2).

An important procedure to establish the viability of the sensor is the determination of the lowest NS1 antigen concentration that can be quantitatively analyzed with reasonable reliability, known as the limit of quantification. By rewriting the Langmuir isotherm equation (Eq. (1), the limit of quantification ($C_{NS1} \rightarrow C_{lim}$) is given by [17, 25],

$$C_{lim} = \frac{\Delta\lambda_{RES}}{K(\Delta\lambda_{MAX} - \Delta\lambda_{RES})} \tag{4}$$

where $\Delta\lambda_{RES}$ is the spectrometer resolution ($\Delta\lambda_{RES} \approx 1$nm). Using $\Delta\lambda_{MAX}$ and K obtained from fitting the experimental data, one can estimate that C_{lim} = 0.074 μg/ml = 1.54 nM. This quantification limit is in the range of NS1 antigen concentrations in serum samples of patients during the acute phase of the infection (up to 7 days) [10], which vary from 0.04 to 2 μg/ml. This result indicates that AuNP LSPR optical fiber sensor presents a real potential for dengue diagnosis.

3.3 Dengue NS1 antigen sensing: blank

To show that eventual changes in the value of the LSPR wavelength are negligible in absence of NS1 antigen, the fiber was immersed in a blank solution, i.e. a PBS solution without NS1 antigen (C_{NS1} = 0). Figure 5 shows the zoomed-in LSPR dip acquired with the fiber in air after Step 5 and after immersion in the blank solution (C_{NS1} = 0). The inset graph shows the full spectra.

#196103 - $15.00 USD Received 20 Aug 2013; revised 2 Oct 2013; accepted 7 Oct 2013; published 31 Oct 2013

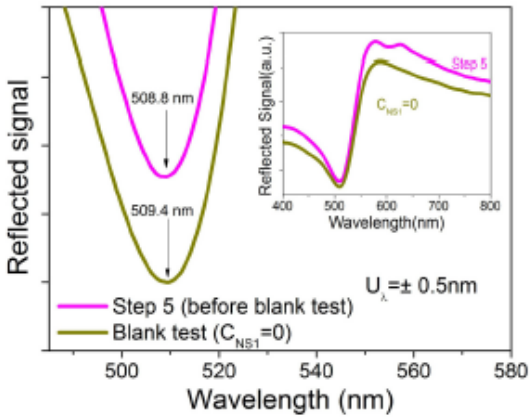

Fig. 5. Zoomed-in view of the LSPR dip after Step 5 (pink curve) and after a 60 min long immersion in PBS solution without NS1 antigen (C_{NS1} = 0, olive curve). Inset graph shows the full reflected spectra.

The uncertainty of measurement (U_λ = ± 0.5 nm) must be taken into account when calculating the wavelength shift in Fig. 5. After Step 5, the central wavelength is λ_{Step5} = 508.8nm ± 0.5 nm = [508.3 nm – 509.3 nm]. After immersion in the blank solution, the central wavelength is $\lambda_{NS1detection}$ = 509.4 nm ± 0.5 nm = [508.9 nm – 509.9 nm]. Since the intervals overlap considerably (40%), one can say that the wavelength shift for C_{NS1} = 0 was negligible or at least below our detection limit.

4. Conclusions

Dengue anti-NS1 antibody was immobilized on AuNPs to obtain an LSPR-based optical fiber sensor for NS1 antigen to be used during the acute phase of the infection. The sensor was shown to have good correlation between wavelength shifts and NS1 antigen concentration, as well as negligible wavelength shift when exposed to a blank solution (NS1 antigen concentration equal to zero). The sensing element is cheap and disposable, and was prepared in 5 straightforward steps. The NS1 antigen detection yields an accurate result in 1 hour, possibly less.

We showed that the sensor is able to detect and quantify dengue NS1 antigen with sensitivity of 43 nm/(ng/mm^2). The NS1 antigen concentration quantification limit (0.074 µg/ml = 1.54nM) was estimated. Considering that the level of secretory protein of dengue virus in the blood of an infected person in the acute phase is between 0.04 and 2.0 µg/ml, the proposed sensor can be a valuable tool for early diagnosis of the disease.

These results indicate that the sensor can be a powerful tool for sensing dengue NS1 antigen in samples from patients who exhibit symptoms that fit the clinical presentation of dengue. Future development of this sensor will involve attempting to use it to detect NS1 antigen in serum samples.

Acknowledgments

A. Camara and P. M. P Gouvêa thank the CAPES-STINT/Brazil-Sweden collaboration program for international doctorate and postdoctoral fellowships, respectively. A. Camara thanks the Brazilian Agency CNPq for national doctorate fellowship. I. C. S. Carvalho thanks CAPES-STINT, FAPERJ and CNPq for financial support. This study was also supported by the Center of Excellence in Nanophotonics and Biophotonics (PRONEX/FACEPE/CNPq) and INCT Fotonica (CNPq). The authors thank Hilton Betta Jr. and Eliane Correa for assistance with Figs. 1(a) and 2, respectively. The authors also wish to thank both referees for their insightful questions, comments and suggestions.

#196103 - $15.00 USD Received 20 Aug 2013; revised 2 Oct 2013; accepted 7 Oct 2013; published 31 Oct 2013

7.2 Apêndice B – Artigo publicado, ao longo do Doutorado, no periódico *Talanta*, com fator de impacto 3,511.

Talanta 128 (2014) 505–510

Contents lists available at ScienceDirect

Talanta

journal homepage: www.elsevier.com/locate/talanta

A thiophene-modified screen printed electrode for detection of dengue virus NS1 protein

M.M.S. Silva [a], A.C.M.S. Dias [a], M.T. Cordeiro [b], E. Marques Jr[b,c], M.O.F. Goulart [d], R.F. Dutra [a,*]

[a] Biomedical Engineering Laboratory, Federal University of Pernambuco, Av. Prof. Moraes Rego, 1235, Cidade Universitária, 50670-901 Recife, Brazil
[b] Aggeu Magalhães Research Center, FIOCRUZ-PE, Recife, Brazil
[c] Center for Vaccine Research, University of Pittsburgh, Pittsburgh, PA, USA
[d] Institute of Chemical and Biotechnology, Federal University of Alagoas, Maceió, Brazil

ARTICLE INFO

Article history:
Received 15 February 2014
Received in revised form
7 June 2014
Accepted 8 June 2014
Available online 14 June 2014

Keywords:
Screen printed electrode
Thiophene
Dengue virus
Immunosensor

ABSTRACT

A thiophene-modified screen printed electrode (SPE) for detection of the Dengue virus non-structural protein 1 (NS1), an important marker for acute phase diagnosis, is described. A sulfur-containing heterocyclic compound, the thiophene was incorporated to a carbon ink to prepare reproducible screen printed electrodes. After cured, the thiophene SPE was coated by gold nanoparticles conjugated to Protein A to form a nanostrutured surface. The Anti-NS1 antibodies immobilized via their Fc portions via Protein A, leaving their antigen specific sites free circumventing the problem of a random antibodies immobilization. Amperometric responses to the NS1 protein of dengue virus were obtained by cyclic voltammetries performed in presence of ferrocyanide/ferricyanide as redox probe. The calibration curve of immunosensor showed a linear response from 0.04 $\mu g\ mL^{-1}$ to 0.6 $\mu g\ mL^{-1}$ of NS1 with a good linear correlation ($r=0.991$, $p<0.05$). The detection limit (0.015 $\mu g\ mL^{-1}$ NS1) was lower than conventional analytical methods. In this work, thiophene monomers incorporated in the carbon ink enhanced the electroanalytical properties of the SPEs, increasing their reproducibility and sensitivity. This point-of-care testing represents a great potential for use in epidemic situations, facilitating the early diagnosis in acute phase of dengue virus.

1. Introduction

Dengue is a significant public health threat, with estimates of 50 to 100 million cases per year and around 3 billion people at risk of infection, mainly in tropical and subtropical regions [1]. Infection can result in a broad spectrum of disease syndromes ranging from an asymptomatic or mild infection, classical dengue fever (DF), to the potentially fatal dengue haemorrhagic fever (DHF) and dengue shock syndrome [2]. So far, there is no effective anti-viral therapeutic on the market and supportive therapy such as fluid replacement is the only treatment for severe forms of the disease. An early and accurate laboratory diagnosis of dengue could assist clinical management [3]. An ideal blood test for diagnostic should be affordable and easy to use with high performance and sensitivity to distinguish the acute-phase of dengue [4]. Additionally, it should not be costly and not require several steps, being adaptable at laboratory or at a point-of-care diagnostic without compromising its accuracy [5].

The most important development in dengue diagnostics in recent years is the advent of the specific detection of dengue virus NS1 antigen [6]. Enzyme-linked immunosorbent assays (ELISA) for detecting the NS1 were developed and demonstrated excellent sensitivity and specificity in detection of dengue infections [6–8]. NS1 glycoprotein is circulating mostly from days 1–6 after the onset of clinical symptoms, with the peak NS1 antigen detection occurring between days 3 and 5, in both primary and secondary infections, and hence is an excellent diagnostic target for acute dengue diagnosis [4,8]. Although the classical techniques are very powerful for monitoring, they are time consuming and are not adaptable for in situ and real time detection, beyond require skilled personnel [9,10]. Alternatively, rapid diagnostic test (RDT) for NS1 detection based on immunochromatography was proposed [11]. However, even if RDTs can provide opportunities for point-of-care, they have limitations regarding detectability, once their results are limited to a qualitative analyses (yes/no), becoming difficult the diagnostic of the acute-phase of dengue that is correlated with NS1 levels. Contrary, biosensors can supplier quantitative responses through a transducer that converts biochemical reactions in a measurable electric signal [12].

Electrochemical biosensors employing screen printed electrodes have emerged as adequate tools for point-of-care testings. They have

* Corresponding author. Tel.: +55 81 21268200.
E-mail address: rosa.dutra@ufpe.br (R.F. Dutra).

http://dx.doi.org/10.1016/j.talanta.2014.06.009
0039-9140/

innumerous advantages, such as ease of mass production and versatility [13]. Screen printed electrodes (SPEs) can combine good electrochemical proprieties and portability with simple and inexpensive fabrication techniques, thus being a good strategy to accomplish safety, disposable and quantitative immunonsensors [14]. In the fabrication of SPEs are used inks containing different chemical compounds, polymers or functional linking that can printed onto diverse type of plastic or ceramic substrates. The incorporation of compounds in the inks used for printing on the electrodes is a determinant factor for their selectivity and sensitivity required for each analysis [15].

Thiophene monomer derivatives have been pointed as attractive compounds to prepare electrochemical sensor, because they increase the conductivity, reduce the redox potential and improve the thermal and electrochemical stability [16]. Herein, thiophene monomers were incorporated into the carbon ink to form a homogenous and conductive composite, supplying a suitable signal amplification strategy to improve the electrochemical characteristics of the SPE increasing the sensitivity due to higher current densities and charge transfer across the interface electrode–electrolyte. Furthermore, sensitivity of immunosensors can be improved by increasing the amount of antibody immobilized on the electrode surface. Variety of nanostructures materials, with similar dimensions to biomolecules (antibodies, enzymes, DNA) owning different sizes, shapes and exceptional properties; such as metal nanoparticles (NP), quantum dots, carbon nanotubes and nanowires have employed for improvement of electrochemical biosensors. Nevertheless, NP which has capability for in situ synthesis onto the various composite films for antibody immobilization can improve the electrochemical signal and adsorption capacity of antibodies, and consequently enhance detection sensitivity. Therefore, the use of NPs represents a promising integration of electrochemical methods with new nanomaterials and electroactive complexes for electrochemical immunosensing [17].

It is well-known that way as antibodies are immobilized on the electrode surface affects the performance of an immunosensor. Fab portions of antibodies should be free for recognizing and binding to the epitopes of antigens. The Protein A extracted from Staphylococcus aureus has high affinity to the Fc portion of immunoglobulins from a variety of species, being widely used to promote an oriented antibody immobilization [18]. When the Protein A was used in a chromatographic assay, it was capable of binding antigen at over 80% of their theoretical capacity, because of the increased strength of the couple between the antibody Fc portion and protein A [19]. Stable and oriented immobilization of antibodies combined with the electrochemical advantages of thiophene as chemical modifying compound allowed a accurate detection of NS1. No labels were necessary when the antigen–antibody interactions were registered. The method described herein involves one-step preparation process and represents an advance in the production of SPEs for point-of-care testing.

2. Experimental

2.1. Materials and reagents

2.1.1. Chemical reagents and materials

Electrodag PF-407 C carbon ink with a density of 1.13 kg cm^{-3} was acquired from Acheson Henkel Corporation (Port Huron, MI, USA). Thiophene, protein A–conjugated gold nanoparticles (PtnA–AuNP) with approximately 20 nm (P6855), potassium ferricyanide ($K_3[Fe(CN)_6]$), potassium ferrocyanide ($K_4[Fe(CN)_6]$) and glycine, were acquired from Sigma-Aldrich (St. Louis, MO, USA). Phosphate buffer saline (PBS) (10 mmol L^{-1}, pH 7.4) used in all experiments was prepared by dissolving 0.2 g KCl, 8.0 g NaCl, 0.24 g KH_2PO_4 and 1.44 g Na_2HPO_4, in 1000 mL of deionized Milli-Q water from Millipore units (Bedford, MA, USA). All chemicals were of analytical grade.

2.1.2. Biological reagents

Mouse monoclonal antibodies against the NS1 glycoprotein of dengue virus (ab 138696) used to electrodes preparation and the dengue virus NS1 recombinant full-length protein (ab 64456) were purchased from Abcam (Cambridge, MA, USA). NS1 native protein was obtained from DENV-3 (strain 101.905/BR-PE/03) culture supernatant collected on the 5th day after inoculation in C6/36 cell monolayers, maintained in Leibovitz L-15 medium (GIBCO, Invitrogen, Grand Island, NY) containing 2% fetal calf serum. DENV-3 was detected and identified by RT-PCR [20]. In house ELISA, using anti-NS1 monoclonal antibodies, confirmed the presence of NS1 native protein in virus culture supernatant. As control was used supernatant from C6/36 cell culture (without virus) collected in the same conditions. Both supernatants were cleared by centrifugation for 10 min at 1.500 rpm (400 g).

2.2. Preparation of the thiophene-SPE

The electrodes were manufactured by squeezing a mixture containing carbon ink and thiophene onto a polyethylene terephtalate support to form a think conductive film. Four different concentrations of thiophene in relation to carbon ink were tested: 0.5% (w/V); 1% (w/V); 2.5% (w/V) and 10% (w/V). Prior printing, a plastic mold was used onto the PET rectangular surface (0.4 × 1.0 cm) to ensure electrodes with equal areas. After manufacturing, the electrodes were cured at 60 °C for 20 min. The manufactured thiophene-SPE consisted of with a circular area (Ø=4 mm) joined to a rectangular area (1 mm × 15 mm) used to electrical contact. After ready, the area of the electrode was delimited using a tape for galvanoplasty.

Prior to use, the thiophene-SPEs were pretreated by cyclic voltammetry (CV), scanning 30 cycles with a potential ranging from − 2.0 V to 2.0 V, at a scan rate of 0.1 V s^{-1} and step potential of 2.44 mV, using 0.1 mol L^{-1} of KCl solution as the supporting electrolyte [21].

2.3. Apparatus

All the electrochemical experiments were performed in an Ivium Compact Stat potentiostat/galvanostat from Ivium Technologies (Eindhoven, The Netherlands) interfaced with a microcomputer and controlled by Ivium Soft software. A three-electrode system was used, which consisted of a thiophene-SPE as the working electrode (4 mm diameter), an Ag/AgCl electrode as the reference electrode and a helical platinum wire as the counter electrode. The electrodes were set up in a glassy electrochemical cell with 5 mL volume.

Experiments for characterizing the assembling of the thiophene-SPE were performed by CV in presence of 5 mmol L^{-1} of K3Fe(CN)6/K4Fe(CN)6 prepared in 0.1 mol L^{-1} of KCl solution, with a potential ranging from − 0.6 V to 1.0 V, at 50 mV s^{-1} scan rate. Antigen–antibody interactions at the interface of the thiophene-SPE were also monitored by differential pulse voltammetry (DPV). DPV measurements were recorded from 0 V to 0.8 V, with pulse amplitude of 0.025 V, width of 0.05 s, and step potential of 0.05 V. The current signals were registered at a fixed potential (0.25 V) and the analytical response to NS1 was obtained taking into account the difference between the peak current (ΔI) of the thiophene-SPE with NS1 and the blank.

Fourier transform infrared (FTIR) spectra of samples were recorded by using a Bruker IFS 66 model FTIR spectrometer in

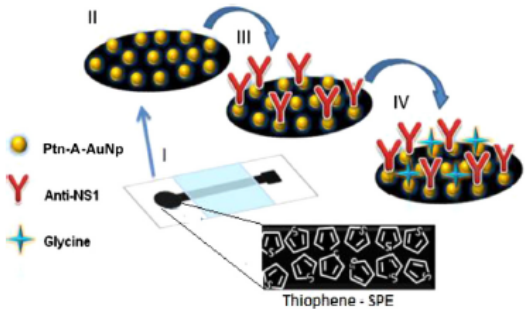

Fig. 1. Schematic illustration of the stepwise preparation of the NS1 immunosensor (I) bare thiophene-SPE; (II) AuNP–Ptn-A/thiophene-SPE; (III) anti-NS1/AuNP–Ptn-A/thiophene-SPE; and (IV) glycine/anti-NS1/AuNP–Ptn-A/thiophene-SPE.

the region of 4000 cm^{-1} to 400 cm^{-1}, by using the standard KBr pellet technique.

2.4. Immobilization of the anti-NS1

Anti-NS1 antibodies were immobilized via protein A–conjugated gold nanoparticle (AuNP–Ptn A), forming a nanostructured film on the electrode surface. 10 μL AuNP–Ptn A solution was pipetted onto the electrode surface of the thiophene-SPEs and left at 4 °C (overnight). Subsequently, 10 μL of anti-NS1 (10 μg mL^{-1}) prepared in 10 mmol L^{-1} of PBS was incubated on the electrode surface for 1 h. Non-specific bindings were blocked by incubating the electrode surface with 50 mmol L^{-1} of glycine solution for 40 min. For preservation of the anti-NS1, the immobilized thiophene-SPE was stored in a moist chamber in a refrigerator (approximately +4 °C). A schematic design of the thiophene-SPE is shown in Fig. 1.

2.5. Immunosensor response to NS1

Initially, the analytical responses of the immunosensor were evaluated by incubating the coated anti-NS1 thiophene-SPEs with NS1 samples in different concentrations. Then, 10 μL of NS1 solutions were pippeted on the electrode surface and left to react for 30 min in a moist chamber at room temperature (24 °C). Afterwards, the electrode was washed four times in PBS and water. The immunosensor response was also evaluated in real samples against the NS1 native protein by incubating the anti-NS1 thiophene-SPEs with culture supernatant collected on the 5th day after inoculation in C6/36 cell monolayers. The supernatant solution containing NS1 native antigen was 1:128, 1:64, 1:32, 1:16, 1:8, 1:4 and 1:1 serial diluted in PBS and 10 μL of supernatant was also pippeted on the electrode surface at the same conditions described. A culture supernatant of C6/36 cells monolayers without NS1 infected serum inoculation was used as control.

3. Results and discussion

3.1. Characterization of thiophene-SPE

Chemically modified screen-printed carbon electrodes may be produced by incorporating specific reagents into the screen-printing inks, thus increasing the selectivity and detectability of measurements [22]. Among the available electroanalytical techniques, the CV technique has been widely used to understand the electroactivity and the electrochemical properties of conducter films or organic salts because it can better describe the

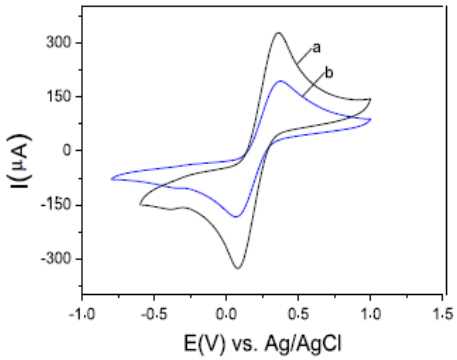

Fig. 2. (a) Cyclic voltammogram profiles of the carbon ink-printed electrode, with thiophene; and (b) without thiophene. The scans were performed in 5 mmol L^{-1} $K_3Fe(CN)_6/K_4Fe(CN)_6$, at a scanning rate of 50 mV s^{-1}.

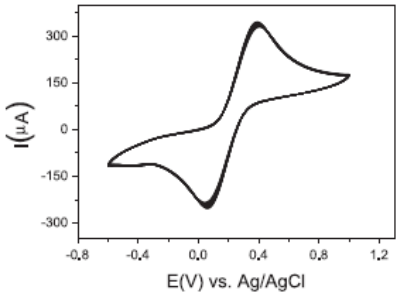

Fig. 3. Cyclic voltammograms of the thiophene-SPE from twenty replicate cycles performed in presence of 5 mmol L^{-1} of $K_3Fe(CN)_6/K_4Fe(CN)_6$ prepared in a 0.1 mol L^{-1} KCl solution, at a scanning rate of 50 mV s^{-1}.

characteristics of the electrochemical switching behavior between conducting and insulating states. Herein, the thiophene-SPE and the chemically-unmodified screen-printed carbon electrode were submitted to a CV technique in the presence of 5 mmol L^{-1} of $K_3Fe(CN)_6/K_4Fe(CN)_6$ prepared in 0.1 mol L^{-1} of KCl solution, at a 0.1 V s^{-1} scan rate and potential ranging from −0.6 V to 1.0 V (Fig. 2). The incorporation of the thiophene into the carbon ink resulted in an increase of approximately 40% of the current density. This behavior tell that the thiophene makes considerable contribution to higher charge transfer, improving the technical performance of carbon ink electrode.

The stability of the thiophene-SPE was also evaluated by setting the chemically- modified electrode to successive CVs. After 20 cycles performed in presence of 5 mmol L^{-1} of $K_3Fe(CN)_6/K_4Fe(CN)_6$ prepared in a 0.1 mol L^{-1} KCl electrolyte, at 0.1 V s^{-1} scanning rate and a potential ranging from −0.6 V to1.0 V, the redox peaks were practically constant. It was obtained a coefficient of variation of approximately 3.4% that is much more stable than the electrode without thiophene (9.2% coefficient of variation) (Fig. 3).

3.2. Effect of thiophene concentration

The influence of thiophene concentration on the electrode performance were performed by using CV in presence of $K_3Fe(CN)_6/K_4Fe(CN)_6$ as redox probe. The concentrations of thiophene varied from 0.5% to 10%, were analyzed according to maximal amplitude of the produced redox peaks. It was found that the redox peaks increased with the thiophene concentration, achieving

a plateau at 2.5% (m/v) thiophene. The use of 2.5% of thiophene resulted conductivities two times greater than for non-modified electrodes (Fig. 4) Thus, this concentration was used in all remaining experiments.

3.3. Fourier transform infra-red (FTIR) spectroscopy

FTIR spectra were used to investigate the modification of the carbon ink with thiophene. The FTIR spectra of the carbon ink layer without thiophene are shown in Fig. 5. Typical spectra for several concentrations of carbon black (ink component) are shown in Fig. 5(a). A band at 1634 cm^{-1} is probably a high conjugated C=O. O'Reilly and Mosher [23] discuss the assignment of the 1600 cm^{-1} band in carbon black and they attributed to aromatic ring stretching frequencies whose intensity is enhanced by the presence of oxygen atoms as phenol or ether groups. Two peaks are required in the 1400 cm^{-1} to1200 cm^{-1} region to reproduce the experimental curve. A band at 1400 cm^{-1} to 1450 cm^{-1} is assumed to be the C–O stretching frequency of the carboxylic acid groupand a band at 1120 cm^{-1} to 1190 cm^{-1}, probably due to the coupled C–O stretching frequency and OH bending modes of COOH and possibly the C–O stretching modes of ethers.

After the incorporation of thiophene in the carbon ink, the spectral analysis showed functional groups of the thiophene (Fig. 5(b)). Two bands at 2920 cm^{-1} and 2850 cm^{-1} corresponding to the C–H stretching; at cm^{-1} to the C=C stretching, at 1250 cm^{-1} to the CH2 stretching, at 1116 cm^{-1} to the bending vibrating peak of C–H, and 572 cm^{-1} to the feature peak of S. Also was observed at 1116 cm^{-1} and 1012 cm^{-1} peaks in the spectra attributed to S–O and S–phenyl bonds of sulfonic acid. Peaks of C,

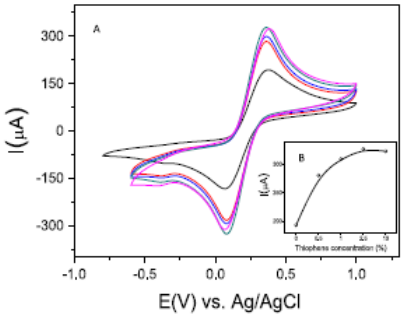

Fig. 4. Effect of the concentration of the thiophene monomer in the presence of 5 mmol L^{-1} of $K_3Fe(CN)_6/K_4Fe(CN)_6$ at a scanning rate of 50 mV s^{-1}.

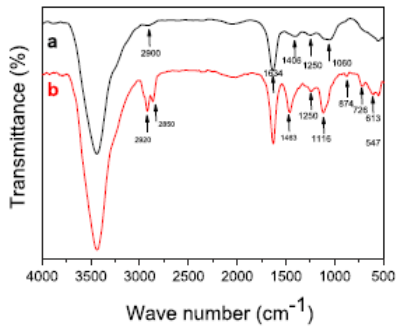

Fig. 5. ATR-FTIR spectra of the SPE—(a) without thiophene; and (b) with thiophene.

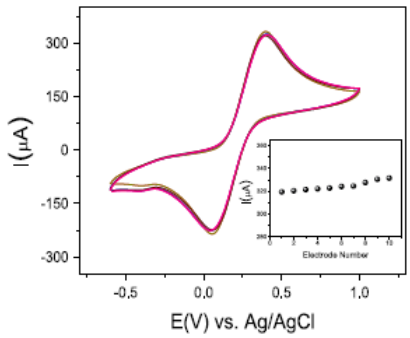

Fig. 6. Study of the reproducibility and stability of printed electrodes modified with thiophene. Ten screen-printed electrodes were tested in the presence of 5 mmol L^{-1} of $K_3Fe(CN)_6/K_4Fe(CN)_6$ at a scanning rate of 50 mV s^{-1}.

C–C, and C–S bonds in the thiophene backbone at 1463 cm^{-1}, 874 cm^{-1}, and 726 cm^{-1}, respectively, was also indicated [24]. Focusing on the 1450 cm^{-1} to1370 cm^{-1} range, the band at 1434 cm^{-1} is observed together with three other weak bands at 1418 cm^{-1}, 1408 cm^{-1}, and 1400 cm^{-1}, that are typically indicative of the thiophene in the carbon ink.

3.4. Reproducibility and stability of the thiophene-SPE

SPE not only answers the criterion of cost effectiveness, but also it satisfy the previously much sought after criteria of being highly reproducible and offering sensitive methods of detection towards target analytes, whilst maintaining low cost production through scales of economy. The adaptability of SPE is also of great benefit, due to mainly its ability to easily modify the electrode through different inks or chemical compounds allows for highly specific and finely calibrated electrode to be produced for specific target analytes [25,26]. To evaluate the reproducibility of the SPE, a series often electrodes were prepared (Fig. 6a). The relative standard deviation (RSD) of the measurements for the ten electrodes was 1.28%, suggesting an acceptable precision and reproducibility. These good results should be attributed to the use of ink with a thiophene Fig. 6). The electrodes from one series not only have the same sensitivities, but also nearly the same standard potentials, which is especially important in the case of disposable sensors.

3.5. Scan rate study

Information involving the electrochemical mechanisms can often be obtained by the relationship between the cathodic/anodic current peak and scanning rate of CV [27]. Fig. 7 shows the CVs of thiophene-SPEs at different scanning rates ranging from 10 mV s^{-1} to 100 mV s^{-1}, performed in 5 mmol L^{-1} of $K_3Fe(CN)_6/K_4Fe(CN)_6$ prepared in 0.1 mol L^{-1} of KCl solution, with potential ranging from −0.6 V to 1.0 V.

According to Fig. 7b, by increasing the scanning rates from 10 mV s^{-1} to 100 mV s^{-1}, the CVs of all redox couples showed a pair of symmetric peaks with a gradually increasing peak current. The currents of both the anodic and cathodic peaks increased linearly with the square root of the scanning rate, thus indicating that the process is controlled by diffusion. There was proportionality between the cathodic peak currents and the square root of the scanning rate, which shows that the charge transfer occurred reversibly. The electron transfer rate constant (ks) was calculated employing the Laviron equation [28]:

$ks = \alpha nFv/RT$;

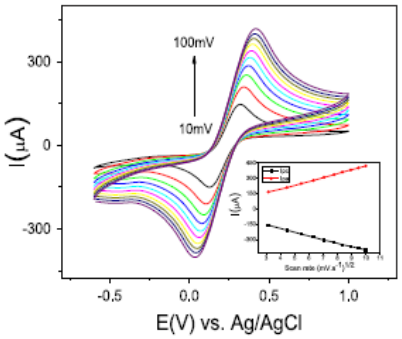

Fig. 7. (a) Cyclic voltammograms of the immunosensor in 5 mmol L^{-1} of $K_3Fe(CN)_6/K_4Fe(CN)_6$ at scanning rates (from inner to outer) of: 10 mV s^{-1}, 20 mV s^{-1}, 30 mV s^{-1}, 40 mV s^{-1}, 50 mV s^{-1}, 60 mV s^{-1}, 70 mV s^{-1}, 80 mV s^{-1}, 90 mV s^{-1}, and 100 mV s^{-1}; (b) Plots of current peak as a function of the square root of the scanning rate.

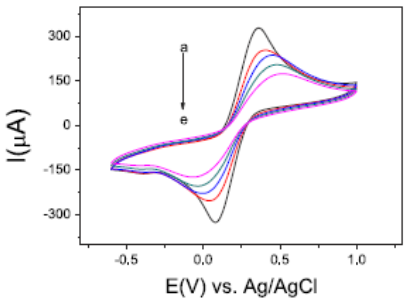

Fig. 8. Cyclic voltammograms of the immunosensor in each step of immobilization: (a) bare thiophene-SPE; (b) AuNP–Ptn-A/thiophene-SPE; (c) anti-NS1/AuNP–Ptn-A/thiophene-SPE; (d) glycine/anti-NS1/AuNP–Ptn-A/thiophene-SPE and (e) NS1/glycine/anti-NS1/AuNP–Ptn-A/thiophene-SPE. Scans were performed in 5 mmol L^{-1} of $K_3Fe(CN)_6/K_4Fe(CN)_6$, at a scanning rate of 0.1 V s^{-1}.

where α is the electron transfer coefficient, n is the number of electrons transferred, F is the Faraday constant, v is the scanning rate, R is the gas constant and T is the temperature. The ks was estimated to be 1.2×10^4 s^{-1}.

3.6. Immobilization of the anti-NS1

CV is a very versatile electrochemical technique which allows probing of the mechanics of redox reactions and transport properties of a system in solution. When well defined redox mediators are used, CV can be utilized to characterize the stepwise modifications of the occurred at the interface of electrode surface by changes on conductivity/reactivity properties. As shown at Fig. 8, when the thiophene-SPE was coated with gold-conjugated protein A film, a decrease of the anodic and cathodic peaks was observed. Although the presence of AuNP on the electrode surface increase the electroactive area, producing a nanostructured regions, the insulating nature of protein A is probably responsible by hindering the electronic transfer [19]. According to the area of the redox peaks, a decrease of electroactive area at approximately 23% was observed. Also was observed a decrease of redox peaks after anti-NS1 antibodies immobilization and glycine blocking as expected [16].

The role of nanogold layer onto the thiophene-modified screen printed electrode was not only to increase the amount of immobilized anti-NS1 antibodies [6], but also promote an oriented immobilization of antibodies by their Fc terminal. Therefhore, this simple strategy improves the sensitivity and selectivity of the immunosensor [29,30].

3.7. Analytical response of the immunosensor

Under optimized experimental conditions, the calibration curve of the immunosensor was obtained. The electrodes were incubated in different concentrations of NS1 and submitted to CV measurements in presence of $K_3[Fe(CN)_6]/K_4[Fe(CN)_6]$ (5 mmol L^{-1}) in KCL (0.1 mmol L^{-1}). The results show that the anodic peak current decreased with the increase of NS1 concentration in the incubation solution (Fig. 9a). Linearity in the calibration curve was obtained over

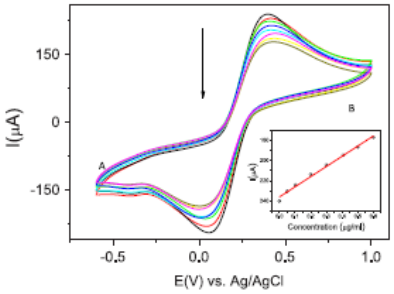

Fig. 9. (a) Cyclic voltammograms of the immunosensor in different NS1 concentrations (b) Calibration curve obtained by the anodic peaks from three replicated measurements.

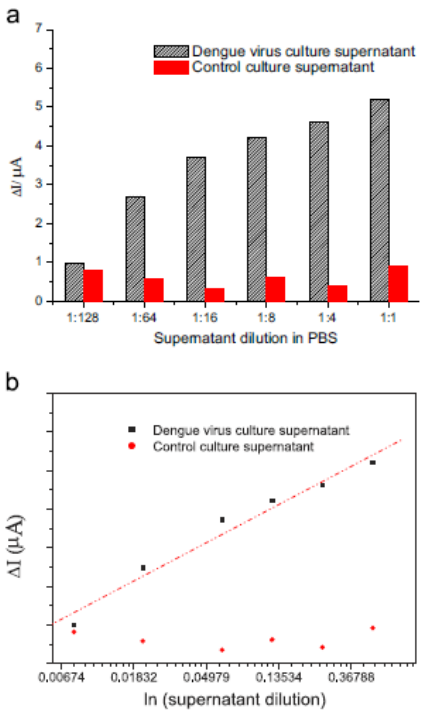

Fig. 10. (a) Analytical responses of thiophene-SPEs to the NS1 native protein f from dengue virus and control (CD4 cells) culture supernatant at serial dilutions. (b) Linear fit obtained by natural logarithm of supernatants dilutions. The amperometric responses obtained by DDP in 5 mmol L^{-1} of $K_3Fe(CN)_6/K_4Fe(CN)_6$.

the range of 0.05 g mL^{-1} to 0.6 g mL^{-1} of NS1 (r=0.991). The limit of detection (LOD) defined as three times the blank standard deviation signal was found to be 0.015 μg mL^{-1}, which was much lower than the other methods used to detect the NS1 antigen [16,31,32]. Alcon et al. [7] reported that the NS1 antigen was found circulating from the first day after onset of the illness up until the 9th day. In primary infections, NS1 levels range from 0.05 μg mL^{-1} to 0.6 μg mL^{-1} in serum samples of patients in the acute phase of the disease (up to 7 days). These clinical range for dengue diagnostic are matched with values detected by the gold nanoparticle thiophene-SPE developed.

3.8. Determination of NS1 in real samples

The proposed immunosensor was tested against real NS1 samples through culture supernatant collected on the 5th day after inoculation in C6/36 cell monolayers, period which the NS1 native protein reach maximal production [7]. The immunoelectrodes were incubated with 10 μL of a serial two-fold dilution of dengue virus culture supernatants in PBS for 30 min, at room temperature and specific responses were obtained regarding control supernatant (C6/36 cell culture). Immunosensor responses for all serial dilutions of the control culture (1:128, 1:64, 1:32, 1:16, 1:8, 1:4 to 1:1) were practically constant and similar to 1:128 dilution of control culture supernatants, whereas dengue virus supernatant responses increased inversely proportional to serial dilutions (Fig. 10a). Linear fit obtained by natural logarithm from curve shown in Fig. 9A, shows a correlation coefficient of 0.996 (n=6, p < <0,01) that is indicative of a good linearity (Fig. 10b). This label-free immunosensor is more practical than ELISA and also provide quantitative responses contrary to RDTs [33].

4. Conclusions

Thiophene monomers incorporated into the carbon ink resulted in more stable, sensible and reproducible screen printed electrodes. Moreover, nanolayer formed by gold conjugated to protein A resulted more antibodies immobilized on the electrode surface and non-random linkage. this encouraging results indicate that this chemically-modified carbon-based can be used to specific NS1 detection. Moreover, this developed immunosensor can easily become a point-of-care testing for early diagnostic of acute-phase.

Acknowledgements

The authors thank the National Council of Scientific and Technological Development (CNPq, Brazil) and the Pernambuco Research Foundation (FACEPE, PE, Brazil) for financial support.

References

[1] J.L. Kyle, E. Harris, Annu. Rev. Microbiol. 62 (2008) 71–92.
[2] A.T.A. Mairuhu, J. Wagenaar, D.P.M. Brandjes, E.C.M. van Gorp, Eur. J. Clin. Microbiol. Infect. Dis. (2004) 425–433.
[3] S.D. Blacksell, R.G. Jarman, R.V. Gibbons, A. Tanganuchitcharncha, M. P. Mammen, A. Nisalak, S. Kalayanarooj, M.S. Bailey, R. Premaratna, H.J. de Silva, N.P.J. Day, D.G. Lalloo, Clin. Vaccine Immunol. 19 (2012) 804–810.
[4] WHO, Special Programme for Research, Training in Tropical Diseases, Dengue: guidelines for diagnosis, treatment, prevention and control, World Health, 2009.
[5] M.L. Moi, T. Omatsu, S. Tajima, C.-K. Lim, A. Kotaki, M. Ikeda, F. Harada, M. Ito, M. Saijo, I. Kurane, T. Takasaki, J. Travel Med. 20 (2013) 185–193.
[6] S.D. Blacksell, J. Biomed. Biotechnol. (2012) 1–12 (Article ID 151967).
[7] S. Alcon, A. Talarmin, M. Debruyne, A. Falconar, V. Deubel, M. Flamand, J. Clin. Microbiol. 40 (2002) 376–381.
[8] S.R. Fry, M. Meyer, M.G. Semple, C.P. Simmons, S.D. Sekaran, J.X. Huang, C. McElnea, C.-Y. Huang, A. Valks, P.R. Young, M.A. Cooper, PLoS Negl.Trop. Dis. 5 (2011) e1199.
[9] G.-J. Zhang, L. Zhang, M.J. Huang, Z.H.H. Luo, G.K.I. Tay, E.-J.A. Lim, T.G. Kang, Y. Chen, Sens. Actuators, B 146 (2010) 138–144.
[10] T.Q. Huy, N.T.H. Hanh, N.T. Thuy, P. Van Chung, P.T. Nga, M.A. Tuan, Talanta 86 (2011) 271–277.
[11] S.D. Blacksell, R.G. Jarman, M.S. Bailey, A. Tanganuchitcharnchai, K. Jenjaroen, R.V. Gibbons, D.H. Paris, R. Premaratna, H.J. de Silva, D.G. Lalloo, N.P.J. Day, Clin. Vaccine Immunol. 18 (2011) 2095–2101.
[12] F. Ricci, G. Adornetto, G. Palleschi, Electrochim. Acta 84 (2012) 74–83.
[13] V. Somerset, J. Leaner, R. Mason, E. Iwuoha, A. Morrin, Electrochim. Acta 55 (2010) 4240–4246.
[14] A.C.M.S. Dias, S.L.R. Gomes-Filho, M.M.S. Silva, R.F. Dutra, Biosens. Bioelectron. 44 (2013) 216–221.
[15] O.D. Renedo, M.A. Alonso-Lomillo, M.J.A. Martínez, Talanta 73 (2007) 202–219.
[16] Y. Yoshioka, G.E. Jabbour, Synth. Met. 156 (2006) 779–783.
[17] J.E.N. Dolatabadi, M. Guardiab, Anal. Methods 6 (2014) 3891–3900.
[18] I.T. Cavalcanti, M.I.F. Guedes, M.D.P.T. Sotomayor, H. Yamanaka, R.F. Dutra, Biochem. Eng. J. 67 (2012) 225–230.
[19] T.H. Sisson, C.W. Castor, J. Immunol. Methods 127 (1990) 215–220.
[20] R.S. Lanciotti, C.H. Calisher, D.J. Gubler, G.J.Chang, A.V. Vorndam, J. Clin. Microbiol. 30 (1992) 545–551.
[21] M.A. Alonso-Lomillo, O. Domínguez-Renedo, L. Ferreira-Gonçalves, M.J. Arcos-Martínez, Biosens. Bioelectron. 25 (2010) 1333–1337.
[22] N.R. Stradiotto, H. Yamanaka, M.V.B. Zanoni, J. Braz. Chem. Soc. 14 (2003) 159–173.
[23] J.M. O'Reilly, R.A. Mosher, Carbon N. Y. 21 (1981) 47–51.
[24] Z. Wu, C. Li, Z. Wei, P. Ying, Q. Xin, J. Phys. Chem. B 106 (2002) 979–987.
[25] J.P. Metters, R.O. Kadara, C.E. Banks, Analyst 136 (2011) 1067–1076.
[26] R. Koncki, M. Mascini, Anal. Chim. Acta 351 (1997) 143–149.
[27] S.L.R. Gomes-Filho, A.C.M.S. Dias, M.M.S. Silva, B.V.M. Silva, R.F. Dutra, Microchem. J. 109 (2013) 10–15.
[28] E. Laviron, J. Electroanal. Chem. Interfacial Electrochem. 101 (1979) 19–28.
[29] Z. Pei, H. Anderson, A. Myrskog, G. Dunér, B. Ingemarsson, T. Aastrup, Anal. Biochem. 398 (2010) 161–168.
[30] S. Babacan, P. Pivarnik, S. Letcher, A.G. Rand, Biosens. Bioelectron. 15 (2000) 11–12.
[31] S. Datta, C. Wattal, Indian J. Med. Microbiol. 28 (2010) 107–110.
[32] D.H. Libraty, P.R. Young, D. Pickering, T.P. Endy, S. Kalayanarooj, S. Green, D. W. Vaughn, A. Nisalak, F.A. Ennis, A.L. Rothman, J. Infect. Dis. 186 (2002) 1165–1168.
[33] V.T. Hang, N.M. Nguyet, D.T. Trung, V. Tricou, S. Yoksan, N.M. Dung, T. Van Ngoc, T.T. Hien, J. Farrar, B. Wills, C.P. Simmons, PLoS Negl. Trop. Dis. 3 (1) (2009) e360.

7.3 Apêndice C – Artigo publicado, ao longo do Doutorado, no periódico *Journal of Chemical Technology and Biotechnology*, com fator de impacto 2,494.

Research Article

Received: 29 September 2013 Revised: 15 December 2013 Accepted article published: 6 January 2014 Published online in Wiley Online Library:

(wileyonlinelibrary.com) DOI 10.1002/jctb.4305

Electrochemical detection of dengue virus NS1 protein with a poly(allylamine)/carbon nanotube layered immunoelectrode

Mízia M. S. Silva,[a] Ana C. M. S. Dias,[a] Bárbara V. M. Silva,[a] Sérgio L. R. Gomes-Filho,[a] Lauro T. Kubota,[b,c] Marília O. F. Goulart[c,d] and Rosa F. Dutra[a]*

Abstract

BACKGROUND: A sensitive nanostructured immunoelectrode based on poly(allylamine) (PAH) sandwich is developed for non-structural 1 (NS1) of dengue virus. NS1 is a secretory protein abundant in the acute phase of disease associated to hemorrhagic fever. Anti-NS1 antibodies are immobilized on the electrode surface by a thin layer of PAH assembled on carboxylated carbon nanotubes (CNTs). PAH is cationic polymer acting as bi-functional agent to tightly attach CNTs to the electrode surface and anti-NS1 antibodies through their Fc terminal, avoiding random immobilization. Electrochemical responses of immunoassay are generated at a controlled potential by a reaction between H_2O_2 and peroxidase enzyme conjugated to anti-NS1 antibodies.

RESULTS: The immunosensor developed exhibited a linear range to NS1 varying between 0.1 μg mL^{-1} and 2.5 μg mL^{-1}, with clinical range for early diagnostic of acute dengue and a limit of detection of 0.035 μg mL^{-1} that is much lower than the concentration observed from the first day after the onset of fever up to the 9th day. Serum samples are also tested showing good accuracy and specificity.

CONCLUSIONS: An immunosensor for NS1 protein of dengue virus was developed. This versatile and reproducible PAH-sandwich platform can be applied to other immunoassays to give reliable and highly sensitive responses.

Keywords: poly(allylamine) film; carbon nanotubes; NS1; dengue virus; immunosensor

INTRODUCTION

Dengue fever is a disease causing successive epidemics in many tropical and subtropical regions of the world.[1] It is estimated that 50–100 million dengue cases occur annually, ranging from mild fever to life-threatening dengue hemorrhagic fever (DHF) and dengue shock syndrome (DSS).[2] DHF is associated with thrombocytopenia, coagulopathy, acute inflammation, frequent hepatomegaly, and, most importantly, plasma leakage, with which the risk of fatal hypovolemic shock (DSS) is associated.[3,4] Rapid and easy diagnosis of dengue can assist patient trials and care management. Recently, the non-structural 1 (NS1) protein of dengue virus has been proposed as a predictive marker of DHF.[5,6] Enzyme-linked immunosorbent assays (ELISA) for NS1 antigen in serum samples have demonstrated that NS1 is present in high concentrations during the early clinical phase of the disease[7] and can be detected from the first day of onset of the disease.[5] Moreover, the NS1 protein is prevalent in all four serotypes of dengue virus.[8] Recently, point-of-care rapid diagnostic tests (RDTs) have been proposed by offering a fast route to a presumptive dengue diagnosis.[9,10] However, the RDTs have limitations regarding their sensitivity since they offer only qualitative responses; so far they cannot differentiate stages of disease that are correlated with changes in serum levels of the NS1. Alternatively, biosensors can offer quantitative responses through a transducer that converts biochemical reactions to an electrical measurable signal; besides, they turn out to be a point-of-care assay.[11] Some biosensors based on electrochemical transduction have been proposed for the detection of NS1,[12,13] and have used the Cratylia mollis lectin as bioreceptor. However, due to the reaction with glycoproteins or carbohydrates, these biosensors present low specificity.

The development of a highly efficient antibodies immobilization method is essential to obtain biosensors with high sensitivity and specificity.[14] In particular, in immunosensors (i.e. biosensors for immunoassays), the way the antibodies are immobilized

* *Correspondence to: Rosa Fireman Dutra, Biomedical Engineering Laboratory, Federal University of Pernambuco, Av. Prof. Moraes Rego, 1235 - Cidade Universitária, 50670-901, Recife, PE, Brazil. E-mail: rfiremandutra@yahoo.com.br / rosa.dutra@ufpe.br*

a *Biomedical Engineering Laboratory, Federal University of Pernambuco, Av. Prof. Moraes Rego, 1235 - Cidade Universitária, 50670-901, Recife, PE, Brazil*

b *Chemical Institute, State University of Campinas, Rua Carlos Gomes, 241 - Cidade Universitária, 13083-970, Campinas, SP, Brazil*

c *National Institute of Science and Technology in Bioanalysis, Brazil*

d *Institute of Chemical and Biotechnology, Federal University of Alagoas, Av.Tabuleiro do Martins, 57072-970, Maceió, AL, Brazil*

leaving their active sites prone to react with epitopes and also a controlled and optimal amount of charge demanded are important criteria for good performance.[15] Herein, a strategy of non-random immobilization for anti-NS1 antibodies is presented. The orientation of anti-NS1 by the Fc terminal is carried out through the PAH, due to its ability to form amide bonds.[16,17] Its linear structure favors the building of thin films in the sub-nanometer range, which implies non-reducing electron transfer charge at electrochemical sensors.[18,19]

In recent years, possible applications for carbon nanotubes (CNTs) have excited scientists and engineers due to their excellent structural, electrical and mechanical properties.[19,20] For electrochemical biosensors, CNTs enhance the electrochemical reactivity of important electroactive species with faster ion-to-electron transfer.[21,22] Moreover, they increase the electroactive area permitting an increase of immobilized biomolecules on electrode surfaces.[23] Thus, it is possible to improve the amperometric responses through CNTs on the electrode surface, without any reinforcement of chemical mediators or other compounds which may interfere with the analysis.[24] When CNTs are simply deposited on the carbon electrode surface it is difficult to obtain reproducible and stable matrices due to leaching of CNTs because of their weak interactions with the electrode surface.[25,26] In attempting to circumvent these difficulties, an amine polymer film is assembled on the carbon nanotubes surface in order to ensure the CNTs are retained. In this assembly, PAH behaves as a bi-functional linker towards carboxylated carbon nanotubes on one side, and as anti-NS1 antibodies through their Fc portions, on the other side. In this immunoassay, it is possible to measure the NS1 present in serum samples at concentrations in the clinical range for dengue virus diagnosis with good reproducibility and sensitivity.

EXPERIMENTAL

Materials and reagents

Anti-dengue virus NS1 glycoprotein mouse monoclonal antibody (Anti-NS1) and dengue virus NS1 glycoprotein were purchased from Abcam (USA). COOH-functionalized multi-walled carbon nanotubes (COOH-MWCNT) with an average diameter of ~10 nm, average length 1–2 μm and 95% purity were obtained from DropSens (Spain) and the PAH polymer from Sigma-Aldrich (USA). Dimethylformamide (DMF), hydrogen peroxide (H_2O_2) (30% w/v) and ethanol (99.3% v/v) were obtained from F. Maia (Brazil). All the solutions used in the experiments were prepared in ultrapure water (>18 MΩ cm), obtained from a Milli-Q water purification system from Millipore (USA).

Anti-NS1 antibody was labelled with horseradish peroxidase (HRP) from Sigma (USA) according to Avrameas' method.[27] For the coupling of HRP to anti-NS1, 12 mg of peroxidase were dissolved in 1 mL of 0.1 mol L^{-1} phosphate buffer (pH 6.8) containing 5 mg of anti-NS1 antibody. While the solution was gently stirred, 0.05 mL of a 1% aqueous solution of glutaraldehyde was added. The reaction mixture was left for 2 h at room temperature and then dialyzed against two changes of 5 L of PBS at 4°C overnight. The precipitate was removed by centrifugation for 30 min at +4°C and 20 000 rpm. This stock solution of peroxidase labeled-antibody was kept at +4°C until use.

A pool of serum samples consisted of five serum samples from voluntary donors kindly provided by the Oswaldo Cruz Hospital of the Pernambuco University, Brazil, according to the ethics committee's recommendations. All voluntary donors were found negative for dengue virus. The serum samples were collected from venous blood and immediately centrifuged for 120 s at 3000g and stored at −20°C. The positive control was prepared by spiking NS1 antigens in concentrations similar to those detected in viremic dengue patients.[28]

Synthesis of the anti-NS1 nanostructured electrode surface

Prior to modifications, the glassy carbon electrode (GCE) was cleaned on a polishing cloth with 1.0, 0.3, 0.05 μm alumina powder, respectively, followed by sonication in water and 95% ethanol for 10 s to remove residual alumina particles. After cleaning, 10 μL of a COOH-MWCNT solution previously dispersed in DMF was pipetted onto the electrode surface and dried for 30 min at 40°C. The COOH-MWCNT solution consisted of 1 mg of COOH-MWCNT suspended in 1 mL of DMF and sonicated in an ultrasonic bath (40 kHz) for 2 h.[14] After this coating step, forming COOH-MWCNT/GCE, an aliquot (5 μL) of the 2% (v/v) PAH aqueous solution was dropped and left to react for 1 h at room temperature (~25°C) to promote strong bonds with COOH-MWCNT.

To immobilize the Anti-NS1 on the nanostructured electrode, an aliquot (5 μL) of the anti-NS1 solution (10 μg mL^{-1}) was dropped onto the electrode surface and incubated for 1 h at room temperature. Non-specific bindings were blocked by incubating the electrode surface in a solution of 50 mmol L^{-1} glycine, prepared in PB (pH 6.5, 10 mmol L^{-1}) for 40 min.

The stepwise modification of the electrode surface was accomplished by cyclic voltammetry (CV) at a potential ranging from −0.2 to 0.8 V, at 100 mV s^{-1} scan rate, in the presence of 5 mmol L^{-1} $K_3Fe(CN)_6/K_4Fe(CN)_6$ solution prepared in 0.1 mol L^{-1} KCl.

Analytical responses to the NS1

The analytical responses of the immunosensor were obtained by incubating the anti-NS1 nanostructured electrode surface with 10 μL of NS1 antigen samples for 30 min. For analytical responses, 10 μL of anti-NS1-HRP (10 μg mL^{-1}) were pippeted onto the NS1 coated electrode. Afterwards, amperometric responses were generated by reaction between H_2O_2 (0.75 mmol L^{-1}) and peroxidase conjugated to anti-NS1 in PB (pH 6.5, 10 mmol L^{-1}), at −0.2 V potential vs. Ag/AgCl

Anti-NS1 nanostructured electrode surface characterization and electrochemical measurement

Analyses using Fourier transform infrared (FTIR) spectra of the samples were recorded using a Bruker IFS 66 model FT-IR spectrometer at 4000 to 400 cm^{-1} by employing a standard KBr pellet technique.

Scanning electron microscopy (SEM) images were obtained in a JSM 5900 (JEOL Instruments, Japan) at an acceleration voltage of 20 kV and a working distance of 0.5 μm.

Cyclic voltammetry and amperometric experiments were carried out on an Ivium Compact Stat potentiostat/galvanostat (Ivium Technologies, Netherlands) coupled to a microcomputer and controlled by Ivium Soft software. A conventional three-electrode system using a glassy carbon electrode (GCE) with an area of 0.7 mm^2 as the working electrode, an Ag/AgCl electrode as reference and a platinum electrode as an auxiliary electrode.

RESULTS AND DISCUSSION

COOH-MWCNT film on the electrode surface

One of the most important requirements in developing regular and homogeneous COOH-MWCNT electrode surfaces, includes a uniform and reproducible dispersion.[25] Comparing five different

dispersing agents (DMF, ethanol, 5% nafion in ethanol, 1% SDS and water) after sonication, DMF dispersion resulted in a black and homogenous solution. Taking account that the stability of the dispersion is also very important for preparing the modified electrodes with high reproducibility, the stability was then checked by observing the mixture 24 h after sonication. In this case, DMF dispersion was also most satisfactory, preventing coalescence and aggregation. Except for DMF, all other dispersing agents yielded COOH-MWCTNs either glued to the walls of vials or having large aggregates. This fact can also be attributed to the anionic nature of DMF, which provokes a more repulsive electrostatic force against negatively charged carboxylated nanotubes.

Different methods to form a COOH-MWCNT film have been employed; among them drop coating is one of simplest and was chosen in this work. The morphology of CNT film mainly depends on the temperature used for solvent drying, solvent type and droplet size. Herein, solvent drying was fixed at 40°C due to limitations of the glass carbon electrode used. Then, the droplet size was investigated in order to yield a COOH-MWCNT coating with a desired thickness. Modification of the electrode surface was accomplished by CVs using $K_3Fe(CN)_6/K_4Fe(CN)_6$ as redox probe. A gradual increase of the redox peaks with increase of the COOH-MWCNT droplet size was observed (Fig. 1). However, analysis of the cathodic and anodic current peaks ratio (Ipc/Ipa) evidenced a decrease of the electrochemical reversibility applying a droplet size greater than 10 µL, which may represent a non-homogeneous CNT film (Fig. 1 inset). This non-homogeneity can be attributed to the capillary forces induced by drying droplets that ball up the CNTs or bundle and separate CNTs within the droplet creating noncongruent layers. Thus, 10 µL droplet size was adopted in all remaining experiments.

After preparation of the COOH-MWCNT/GCE film, the electroactive area of the modified electrode was calculated according to the Randles–Sevcik Equation.[29]

$$I_p = (2.69 \times 10^5)\ A\ D^{1/2} n^{3/2} v^{1/2} C$$

where, I_p is the peak current value, A represents the electroactive area of the electrode (cm^2), D is the diffusion coefficient of the probe molecule in solution ($cm^2\ s^{-1}$), n is the number of electrons involved in the redox reaction, ν is the potential scan rate ($V\ s^{-1}$) and C is the concentration of the probe molecule in solution. Under these conditions, an increase of 87.7% in the electroactive area was achieved in relation to the bare electrode, indicating a good COOH-MWCNT coating.

PAH film on the nanostructured electrode

The effect of film thickness on electrochemical response was evaluated changing the concentration of PAH solution (0.5, 1.0, 1.5, 2.0, 2.5, 3.0 and 3.5% v/v). The COOH-MWCNT/GCE modified with 2% PAH showed the best performance, reaching 29% increase of the anodic current and 23% of the cathodic one, when compared with COOH-MWCNT/GCE. Although the insulating nature of PAH can result in a decrease of redox peaks, herein, an increase of the redox peaks of the negatively charged hexacyanoferrate was possible due to the electrostatic attraction experienced with the positively charged polymer.[30] Thus, a concentration of 2.0% PAH was chosen for further experiments.

Scan rate studies were performed on the PAH/COOH-MWCNT/GCE varying from 10 mV s^{-1} to 120 mV s^{-1} (Fig. 2). The voltammograms presented highly symmetric redox peaks. The currents of cathodic and anodic peaks increased linearly with increase of the square root of the scan rate, indicating a diffusion controlled electron transfer (Fig. 2 inset).

The stability of the PAH film on the electrode was checked by performing 15 consecutive voltammetric cycles in the potential range from −0.2 V to 0.8 V in 5 mmol L^{-1} $K_3Fe(CN)_6/K_4Fe(CN)_6$ solution. The coefficients of variation were 0.04% and 0.09% for anodic and cathodic peaks, respectively, indicating good stability of PAH film. The results show a strong synergism between COOH-MWCNT and PAH. Presumably, interactions formed between carboxylated carbon nanotubes and PAH allowed a stable immobilization matrix.

To characterize the interaction of COOH-MWCNT with PAH and the consequent formation of the nanostructured film, analyses using FTIR were performed. Figure 3(A), curve (a) shows the CNTs FTIR spectrum with typical bands of the carboxylic groups at 3436 cm^{-1} corresponding to molecular stretching of O–H groups. Other peak was observed at 1633 cm^{-1}, corresponding to molecular stretching of C=O.[14,22,23] PAH spectra (curve (b)) show a remarkable band around 3400 cm^{-1}, which is associated with

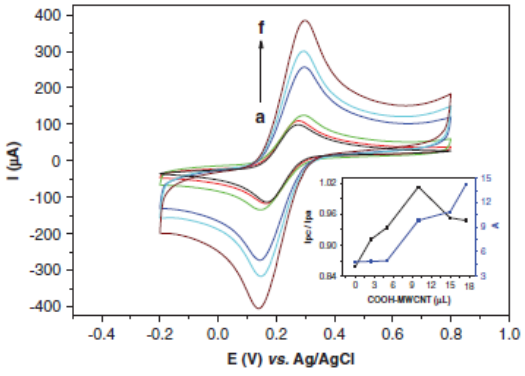

Figure 1. Cyclic voltammograms of the electrode modified with different COOH-MWCNT droplet size: (a) bare GCE; (b) 2.5 µL; (c) 5 µL; (d) 10 µL; (e) 15 µL; and (f) 17.5 µL, in the presence of 5 mmol L^{-1} $K_3Fe(CN)_6/K_4Fe(CN)_6$, at a scan rate of 100 mV s^{-1}. Inset: I_{pc}/I_{pa} (solid line) and area (dashed line) depending on the COOH-MWCNT droplet size.

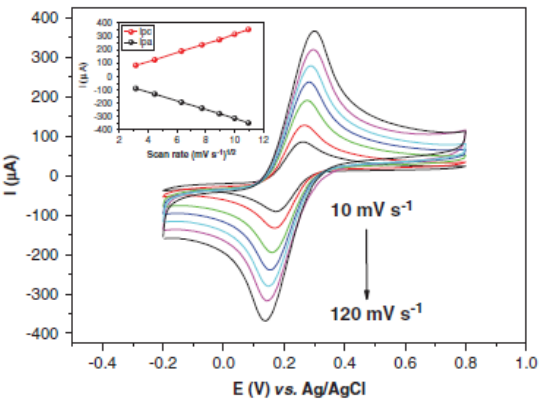

Figure 2. Voltammetric profile of the PAH/COOH-MWCNT/GCE in 5 mmol L^{-1} $K_3Fe(CN)_6/K_4Fe(CN)_6$ under different scan rates (10, 20, 40, 60, 80, 100 and 120 mV s^{-1}). Inset: Current at the anodic and cathodic peaks *vs.* square root of the scan rate.

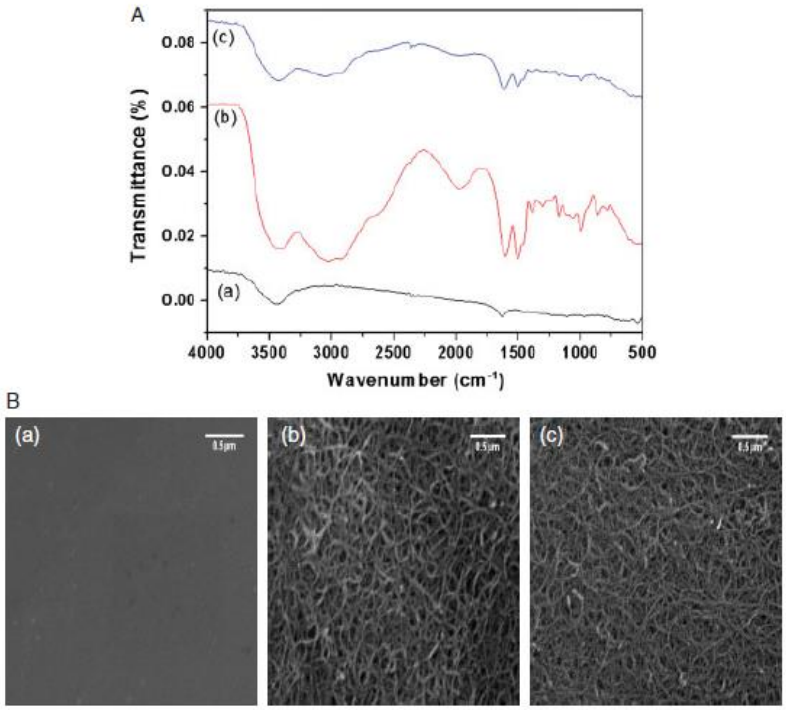

Figure 3. (A) FTIR spectra in transmission mode (a) COOH-MWCNT, (b) PAH, (c) PAH/COOH-MWCNT and c(B) SEM images of (a) bare GCE, (b) GCE modified with COOH-MWCNT and (c) GCE modified with COOH-MWCNT and PAH.

primary amine groups of the polymer. Further, bands observed at 1608 cm^{-1} and 1466 cm^{-1} that are associated with N–H asymmetric bending and C–H stretch.[24] The curve (c) shows the spectrum of COOH-MWCNT after deposition of the PAH film, displaying bands between 825 cm^{-1} and 1380 cm^{-1} which confirm the PAH–COOH-MWCNT linkage.[25,26]

The stepwise modification of the GCE surface with COOH-MWCNT and PAH film under optimal conditions was accomplished by SEM (Fig. 3(B)). Micrographs (a) and (b) show the bare GCE and the COOH-MWCNT modified electrode, respectively. It is observed that COOH-MWCNTs are deposited on the GCE forming an irregular surface composed of entangled cross-linked fibrils. COOH-MWCNT-modified electrode surface after the PAH film deposition is shown in micrograph (c). The image shows the COOH-MCWCNTs also distributed as spaghetti-like structures, however, brightness and contrast of the image were diminished, attributed to the reduction of backscattered electrons and secondary effects that are perturbed by the low-conductivity of polymer film.[31,32]

Immobilization of anti-NS1 on the PAH/COOH-MWCNT/GCE

A schematic illustration of the anti-NS1/PAH/COOH-MWCNT/GCE electrode assembling and principle of the immunoassay by H_2O_2–peroxidase reaction is shown in Fig. 4(A). PAH film is assembled between the carbon nanotubes and biomolecules. Due to its linear structure, the PAH permits bonds on both sides, one side with COOH-MWCNT and the other with the anti-NS1, thus, acting as a bi-functional linker.

In order to electrochemically characterize the anti-NS1 immobilization, cyclic voltammetric (CV) profiles of the electrode surface were carried out using the $K_3Fe(CN)_6/K_4Fe(CN)_6$ as redox probe (Fig. 4(B)). The electrochemical proprieties of the COOH-MWCNT and PAH resulted in an increase of the catalytic activity, confirmed by increase of the anodic and cathodic peaks compared with the bare GCE and PAH/COOH-MWCNT/GCE.[33] After anti-NS1 immobilization, a decrease in redox peak currents was observed. This same behaviour also occurred after blocking the non-specific bindings with incubation of the electrode in 50 mmol L^{-1} glycine solution.[34]

Optimization of experimental conditions

To investigate the optimum pH for enzyme activity of the anti-NS1-HRP conjugate, a study of the pH influence on the catalytic current was carried out. It was observed that the peak current gradually increased when changing the solution pH from 5.5 to 6.5, and then decreased when the pH value was higher than 6.5.

The effect of the incubation time of NS1 antigen on the amperometric response of the sensor was also investigated. This allowed one to analyse the time in which interactions between the NS1 antigen and previously immobilized anti-NS1 antibody are considered maximum, i.e. with the maximum number of occupied binding sites. It was observed that the amperometric signal gradually increased with incubation time, achieving a plateau at 60 min.

In order to obtain the maximum response, the work potential of electrode vs. Ag/AgCl for amperometric measurements was determined from catalytic response of the peroxidase. The presence of the enzyme conjugate (anti-NS1-HRP) was established by CVs in PB (pH 6.5, 0.1 mol L^{-1}) at a scan rate of 100 mV s^{-1}. Detection of the enzyme was based on the current produced by

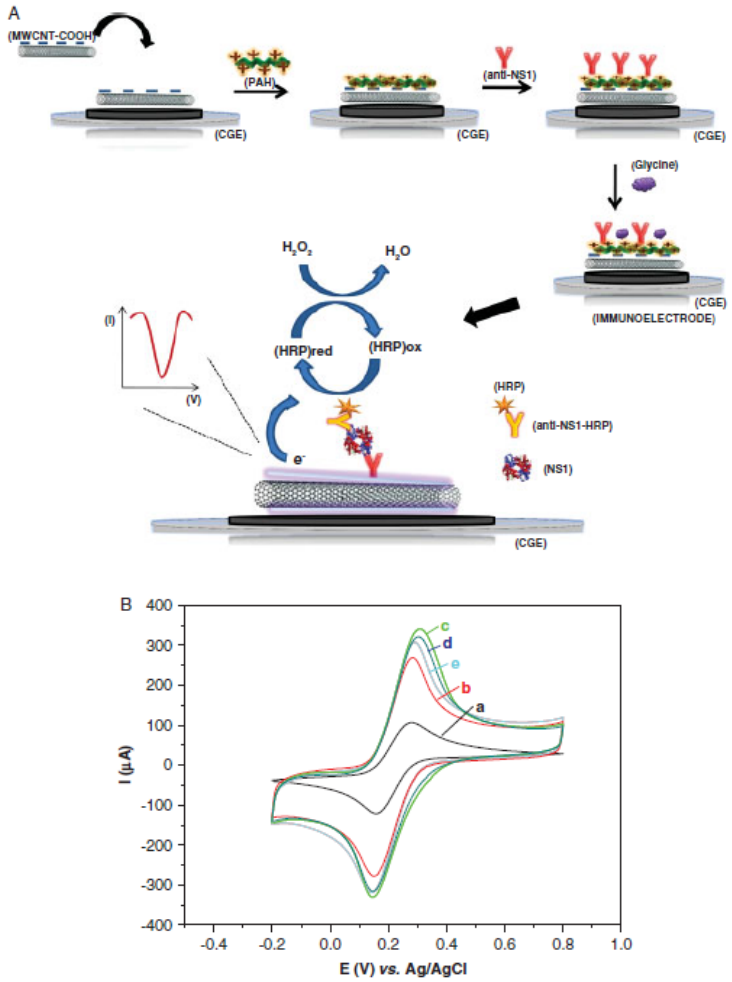

Figure 4. (A) Principle of the amperometric immunosensor showing the stepwise construction of immunoelectrode and principle of immunoassay. (B) Cyclic voltammograms at (a) bare GCE, (b) COOH-MWCNT/GCE, (c) PAH/COOH-MWCNT/GCE, (d) anti-NS1/PAH/COOH-MWCNT/GCE, (e) glycine/anti-NS1/PAH/COOH-MWCNT/GCE. The scans were performed in 5 mmol L^{-1} $K_3Fe(CN)_6/K_4Fe(CN)_6$, at 100 mV s^{-1} scan rate.

the displacement of ions from the redox process undergone by the iron atom present in its structure, which may undergo oxidation and reduction under certain conditions.[35] Comparing the CVs of NS1/anti-NS1/PAH/COOH-MWCNT/GCE in the presence of the anti-NS1-HRP, a slight alteration was observed in cathodic peak due to the process of iron charge transfer from the active centre of enzyme.[36] This slight alteration is observed even in the absence of its enzymatic substrate (H_2O_2) showing that HRP conjugated to anti-NS1 is present and has an electrocatalytic response. When 0.75 mmol L^{-1} H_2O_2 was used, a significant increase in the cathodic peak ($\Delta i = +20\%$) with a slight shift in potential $E_{pc} \approx -0.2$ V and a decrease of the anodic peak were observed, indicating an electrocatalytic reduction process of the enzyme with the substrate. Also observed was a smaller cathodic peak at potential of −0.1 V attributed to load transfer from the iron active centre of the HRP enzyme and the surface. The optimal condition was established at $E_{pc} \approx -0.2$ V.

Analytical response of the immunosensor

The calibration curve was performed in different NS1 concentrations. The amperometric responses were obtained from the cathodic peaks after the H_2O_2 reaction was subtracted from that of a blank (without H_2O_2). The reductions in the peak currents were proportional to the NS1 concentrations in a linear range from 0.1 to 2.5 μg mL^{-1} (Fig. 5(A)). The data adjusted by a linear regression equation showed a correlation coefficient of 0.997 ($P \ll 0.01$, $n = 8$) and a low relative error (≪1%). Based on the RSD of the blank sample and the slope of the calibration curve, the LOD can be calculated as: LOD = 3(RSD/slope). This immunosensor showed a LOD of 0.035 μg mL^{-1}. Alcon *et al.*[28] reported that the NS1 antigen is found circulating from the first day after the onset of fever up to the 9th day. In primary infection, NS1 levels ranged from 0.04 to 2 μg mL^{-1} in acute-phase serum samples (up to 7 days) and in secondary infection, NS1 levels ranged from 0.01 to 2 μg mL^{-1}.

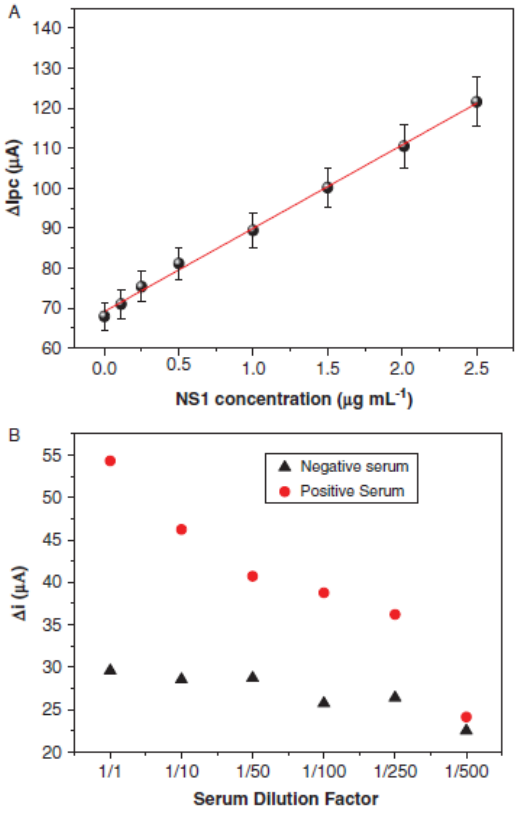

Figure 5. (A) Calibration curve of the immunosensor for NS1 antigen. (B) Response to the NS1 in negative and NS1 spiked serum samples at different PBS dilutions.

The matrix effect on the analytical anti-NS1/PAH/COOH-MWCNT/GCE responses was evaluated as shown in Fig. 5(B). A negative dengue serum was 1:1; 1:10; 1:50; 1:100; 1:250 and 1:500-fold diluted and compared with a spiked NS1 serum (with 5 μg mL^{-1} NS1). All the dilutions were carried out using PBS (10 mmol L^{-1}, pH 7.4). The dilution curve obtained from negative serum (curve I) was maintained practically constant demonstrating a non-matrix effect. The limit of detection to distinguish the serum was established at 1:250, which corresponds to approximately 0.02 μg mL^{-1} NS1. Therefore, this proposed immunosensor is suitable for NS1 detection in levels for diagnostic of dengue virus and has good selectivity.

CONCLUSIONS

An electrochemical immunosensor based on the synergic effect between PAH and carboxylated carbon nanotubes was developed for NS1 protein detection. The strategy of PAH film assembled on COOH-MWCNT ensured a stable nanostructured surface, and simultaneously promoted Fc-oriented immobilization of the anti-NS1. This uniform and homogeneous platform for antibodies immobilization could be capable of detecting NS1 protein at levels in the clinical range for an early acute dengue diagnosis.

ACKNOWLEDGEMENTS

The authors thank the National Council for Scientific and Technological Development - CNPq for supporting this work and Physics Department of Federal University of Pernambuco for performing the SEM images.

REFERENCES

1 Peeling RW, Artsob H, Pelegrino JL, Buchy P, Cardosa MJ, Devi S *et al.*, Evaluation of diagnostic tests: dengue. Nature Publishing Group, S30–S37 (2010).
2 Gurugama P, Garg P, Perera J, Wijewickrama A and Seneviratne SL, Dengue viral infections. *Indian J Dermatol* **55**:68–78 (2010).
3 Martina BEE, Koraka P and Osterhaus ADME, Dengue virus pathogenesis: an integrated view. *Clin Microbiol Rev* **22**:564–581 (2009).
4 Mairuhu ATA, Brandjes DPM and van Gorp ECM, Treating viral hemorrhagic fever. *IDrugs* **6**:1061–1066 (2003).
5 Singh MP, Majumdar M, Singh G, Goyal K, Preet K, Sarwal A *et al.*, NS1 antigen as an early diagnostic marker in dengue: report from India. *Diagn Microbiol Infect Dis* **68**:50–54 (2010).
6 Zainah S, Wahab AHA, Mariam M, Fauziah MK, Khairul AH, Roslina I *et al.*, Performance of a commercial rapid dengue NS1 antigen immunochromatography test with reference to dengue NS1 antigen-capture ELISA. *J Virol Methods* **155**:157–160 (2009).
7 Datta S and Wattal C, Dengue NS1 antigen detection: a useful tool in early diagnosis of dengue virus infection. *Indian J Med Microbiol* **28**:107–110 (2010).
8 Kumarasamy V, Wahab a HA, Chua SK, Hassan Z, Chem YK, Mohamad M *et al.*, Evaluation of a commercial dengue NS1 antigen-capture ELISA for laboratory diagnosis of acute dengue virus infection. *J Virol Methods* **140**:75–79 (2007).
9 Tontulawat P, Pongsiri P, Thongmee C, Theamboonlers A, Kamolvarin N and Poovorawan Y, Evaluation of rapid immunochromatographic NS1 test, anti-dengue IgM test, semi-nested PCR and IgM ELISA for detection of dengue virus. *Southeast Asian J Trop Med Public Health* **42**:570–578 (2011).
10 Chaterji S, Allen JC, Chow A, Leo Y and Ooi E, Evaluation of the NS1 rapid test and the WHO dengue classification schemes for use as bedside diagnosis of acute dengue fever in adults. *Am J Trop Med Hyg* **84**:224–228 (2011).
11 Vasconcelos EA, Peres NG, Pereira CO, da Silva VL, da Silva EF and Dutra RF, Potential of a simplified measurement scheme and device structure for a low cost label-free point-of-care capacitive biosensor. *Biosens Bioelectron* **25**:870–876 (2009).
12 Oliveira MDL, Correia MTS and Diniz FB, A novel approach to classify serum glycoproteins from patients infected by dengue using electrochemical impedance spectroscopy analysis. *Synth Met* **159**:2162–2164 (2009).
13 Oliveira MDL, Nogueira ML, Correia MTS, Coelho LCBB and Andrade CAS, Sensors and actuators B□: chemical detection of dengue virus serotypes on the surface of gold electrode based on Cratylia mollis lectin affinity. *Sensors Actuators B Chem* **155**:789–795 (2011).
14 Puertas S, de Gracia Villa M, Mendoza E, Jiménez-Jorquera C, de la Fuente JM, Fernández-Sánchez C *et al.*, Improving immunosensor performance through oriented immobilization of antibodies on carbon nanotube composite surfaces. *Biosens Bioelectron.* **43**:274–280 (2013).
15 Kausaite-Minkstimiene A, Ramanaviciene A, Kirlyte J and Ramanavicius A, Comparative study of random and oriented antibody immobilization techniques on the binding capacity of immunosensor. *Anal Chem* **82**:6401–6408 (2010).
16 Ruths J, Essler F, Decher G and Riegler H, Polyelectrolytes I: polyanion/polycation multilayers at the air/monolayer/water interface as elements for quantitative polymer adsorption studies and preparation of hetero-superlattices on solid surfaces. *Langmuir* **16**:8871–8878 (2000).
17 Stanton BW, Harris JJ, Miller MD and Bruening ML, Ultrathin, multilayered polyelectrolyte films as nanofiltration membranes. *Langmuir* **19**:7038–7042 (2003).
18 Kong B, Yoo H and Jung H, Electrical conductivity of graphene films with a poly(allylamine hydrochloride) supporting layer. *Langmuir* **25**:11008–11013 (2009).

19 Moreira FTC, Dutra RAF, Noronha JPC, Cunha AL and Sales MGF, Biosensors and bioelectronics artificial antibodies for troponin T by its imprinting on the surface of multiwalled carbon nanotubes□: its use as sensory surfaces. *Biosens Bioelectron* **28**:243–250 (2011).
20 Ahammad AJS, Lee J and Rahman A, Electrochemical sensors based on carbon nanotubes. *Sensors* **9**:2289–2319 (2009).
21 Lin J, He C, Zhang L and Zhang S, Sensitive amperometric immunosensor for a -fetoprotein based on carbon nanotube/gold nanoparticle doped chitosan film. *Anal Biochem* **384**:130–135 (2009).
22 Li N, Yuan R, Chai Y, Chen S and An H, Sensitive immunoassay of human chorionic gonadotrophin based on multi-walled carbon nanotube-chitosan matrix. *Bioprocess Biosyst Eng* **31**:551–558 (2008).
23 Dai Y and Shiu K, Glucose biosensor based on multi-walled carbon nanotube modified glassy carbon electrode. *Electroanalysis* **16**:1697–1703 (2004).
24 Kumar S, Vicente-Beckett V. Glassy carbon electrodes modified with multiwalled carbon nanotubes for the determination of ascorbic acid by square-wave voltammetry. *Beilstein J Nanotechnol*.**Jan**:3988-396 (2012).
25 Gavalas VG, Law SA, Christopher Ball J, Andrews R and Bachas LG, Carbon nanotube aqueous sol-gel composites: enzyme-friendly platforms for the development of stable biosensors. *Anal Biochem* **329**:247–52 (2004).
26 Jusoh N, Abdul-aziz A and Supriyanto E, Improvement of glucose biosensor performances using poly (hydroxyethyl methacrylate) outer membrane. *Int J Biol Biomed Eng Improv* **6**:77–86 (2012).
27 Avrameas S, Coupling of enzymes to proetins with glutaraldehyde. *Immunochemistry* **6**:43–52 (1969).
28 Alcon S, Talarmin A, Debruyne M, Falconar A, Deubel V and Flamand M, Enzyme-linked immunosorbent assay specific to dengue virus type 1 nonstructural protein ns1 reveals circulation of the antigen in the blood during the acute phase of disease in patients experiencing primary or secondary infections. Enzyme-linked Immunosorb. *J Clin Microbiol* **40**:1–7 (2002).
29 Bard AJ and Faulkner LR, *Electrochemical Methods: Fundamentals and Applications*, 2nd Edn. Wiley, New York (2001).
30 Park HJ, Kim J, Chang JY and Theato P, Preparation of transparent conductive multilayered films using active pentafluorophenyl ester modified multiwalled carbon nanotubes. *Langmuir* **24**:10467–10473 (2008).
31 Hua M, Chen H, Tsai R, Tseng S, Hu S, Chiang C *et al.*, Preparation of polybenzimidazole-carboxylated multiwalled carbon nanotube composite for intrinsic sensing of hydrogen peroxide. *J Phys Chem C* **115**:15182–15190 (2011).
32 Park J, Wook S, Mao J, Seob I and Yun Y, Recovery of Pd(II) from hydrochloric solution using polyallylamine hydrochloride-modified *Escherichia coli* biomass. *J Hazard Mater* **181**:794–800 (2010).
33 Hu Y, Zhao Z and Wan Q, Facile preparation of carbon nanotube-conducting polymer network for sensitive electrochemical immunoassay of Hepatitis B surface antigen in serum. *Bioelectrochemistry* **81**:59–64 (2011).
34 Kim J, Premkumar T, Lee K and Geckeler KE, A facile approach to single-wall carbon nanotube/poly(allylamine) nanocomposites. *Macromol Rapid Commun* **28**:276–280 (2007).
35 Lynam C, Gilmartin N, Minett AI, Kennedy RO and Wallace G, Carbon nanotube-based transducers for immunoassays. *Carbon* **47**:2337–2343 (2009).
36 Huang J and Tsai Y, Direct electrochemistry and biosensing of hydrogen peroxide of horseradish peroxidase immobilized at multiwalled carbon nanotube/alumina-coated silica nanocomposite modified glassy carbon electrode. *Sensors Actuators B Chem* **140**:267–272 (2009).

8 ANEXOS

Anexo A – Normas para publicação no periódico *Colloids and Surfaces B: Biointerfaces*, fator de impacto 4.287.

ELSEVIER

COLLOIDS AND SURFACES B: BIOINTERFACES

An International Journal Devoted to Fundamental and Applied Research on Colloid and Interfacial Phenomena in Relation to Systems of Biological Origin

AUTHOR INFORMATION PACK

TABLE OF CONTENTS

- **Description** p.1
- **Audience** p.2
- **Impact Factor** p.2
- **Abstracting and Indexing** p.2
- **Editorial Board** p.2
- **Guide for Authors** p.4

ISSN: 0927-7765

DESCRIPTION

Colloids and Surfaces B: Biointerfaces is an international journal devoted to fundamental and applied research on colloid and interfacial phenomena in relation to systems of biological origin, having particular relevance to the medical, pharmaceutical, biotechnological, food and cosmetic fields.

Each Editor of Colloids and Surfaces B has specific fields of expertise. To ensure a smooth and rapid refereeing process, please submit your article to the Editor related to the topic of your research (you can select the correct editor in the drop down menu in our online submission system: http://ees.elsevier.com/colsub):

John Brash
•Interactions of biomolecules (proteins, enzymes, peptides, polysaccharides, DNA) at the solid-solution and air-solution interfaces;
•Surface/interfacial interactions of tissue and blood; Biomaterials development and interfacial properties;
•Drug delivery/controlled release

Henk Busscher
•Physico-chemical mechanisms of microbial adhesion, biofilm formation and tissue cell interaction to surfaces
•Microbial adhesion and biofilm formation
•Role of surface characteristics, surface modification and protein adsorption on microbial adhesion and biofilm formation
•Physico-chemical mechanisms providing biolubrication to surfaces

Hong Chen
•Surface modification including structured surfaces;
•Biocompatible materials;
•Anti-fouling materials;
•Bio-detection/bio-imaging materials;
•Interactions of biomolecules and cells at interfaces.

Dganit Danino
•Self-assembly and molecular assemblies (proteins, polymers, peptides, surfactants)
•Structure of biological fluids
•Drug delivery vehicles at nano and meso scales

•1D structures - fibrils, ribbons, nanotubes
•Milk proteins

Submissions that: (1) deal solely with biological phenomena and do not describe the physico-chemical or colloid-chemical background and/or mechanism of the phenomena, and (2) deal solely with colloid/interfacial phenomena and do not have appropriate biological content or relevance, are outside the scope of the journal and will not be considered for publication.

The journal publishes regular research papers, reviews, short communications and invited perspective articles, called BioInterface Perspectives. The BioInterface Perspective provide researchers the opportunity to review their own work, as well as provide insight into the work of others that inspired and influenced the author. Regular articles should have a maximum total length of 6,000 words. In addition, a (combined) maximum of 8 normal-sized figures and/or tables is allowed (so for instance 3 tables and 5 figures). For multiple-panel figures each set of two panels equates to one figure. Short communications should not exceed half of the above. It is required to give on the article cover page a short statistical summary of the article listing the total number of words and tables/figures.

AUDIENCE

Colloid and Surface Chemists, Chemical Engineers, (Bio) Pharmaceutical, Cosmetic and Food Chemists, Physical Chemists, Polymer Chemists, Biological and Bioengineers, Organic Chemists, Microbiologists, Medicinal Chemists.

IMPACT FACTOR

2013: 4.287 © Thomson Reuters Journal Citation Reports 2014

ABSTRACTING AND INDEXING

Chemical Abstracts
Current Contents/Physics, Chemical, & Earth Sciences
EMBASE
INSPEC
PASCAL/CNRS
Applied Polymers Literature
APOLLIT
Scopus
EMBiology

EDITORIAL BOARD

Introduction

Colloids and Surfaces B: Biointerfaces is an international journal devoted to fundamental and applied research on colloid and interfacial phenomena in relation to systems of biological origin, having particular relevance to the medical, pharmaceutical, biotechnological, food and cosmetic fields.

Each Editor of Colloids and Surfaces B has specific fields of expertise. To ensure a smooth and rapid refereeing process, please submit your article to the Editor related to the topic of your research (you can select the correct editor in the drop down menu in our online submission system: http://ees.elsevier.com/colsub):

John Brash

•Interactions of biomolecules (proteins, enzymes, peptides, polysaccharides, DNA) at the solid-solution and air-solution interfaces;

•Surface/interfacial interactions of tissue and blood; Biomaterials development and interfacial properties;

•Drug delivery/controlled release

Henk Busscher

•Physico-chemical mechanisms of microbial adhesion, biofilm formation and tissue cell interaction to surfaces

•Microbial adhesion and biofilm formation

•Role of surface characteristics, surface modification and protein adsorption on microbial adhesion and biofilm formation

•Physico-chemical mechanisms providing biolubrication to surfaces

Hong Chen

•Surface modification including structured surfaces;

•Biocompatible materials;

•Anti-fouling materials;

•Bio-detection/bio-imaging materials;

•Interactions of biomolecules and cells at interfaces.

Dganit Danino

•Self-assembly and molecular assemblies (proteins, polymers, peptides, surfactants)

•Structure of biological fluids

•Drug delivery vehicles at nano and meso scales •1D structures - fibrils, ribbons, nanotubes

•Milk proteins

Submissions that: (1) deal solely with biological phenomena and do not describe the physico-chemical or colloid-chemical background and/or mechanism of the phenomena,

and (2) deal solely with colloid/interfacial phenomena and do not have appropriate biological content or relevance, are outside the scope of the journal and will not be considered for publication.

The journal publishes regular research papers, reviews, short communications and invited perspective articles, called BioInterface Perspectives. The BioInterface Perspective provide researchers the opportunity to review their own work, as well as provide insight into the work of others that inspired and influenced the author. Regular articles should have a maximum total length of 6,000 words. In addition, a (combined) maximum of 8 normal-sized figures and/or tables is allowed (so for instance 3 tables and 5 figures). For multiple-panel figures each set of two panels equates to one figure. Short communications should not exceed half of the above. It is required to give on the article cover page a short statistical summary of the article listing the total number of words and tables/figures.

Cover Letter

A cover letter is mandatory and should give the justification of the submission, highlights of the article, and a general impact statement. A short statistical summary of the article listing the total number of words and tables/figures is also required.

Before You Begin

Ethics in publishing

For information on Ethics in publishing and Ethical guidelines for journal publication seehttp://www.elsevier.com/publishingethics and http://www.elsevier.com/journal-authors/ethics.

Human and animal rights

If the work involves the use of animal or human subjects, the author should ensure that the work described has been carried out in accordance with The Code of Ethics of the World Medical Association (Declaration of Helsinki) for experiments involving humans http://www.wma.net/en/30publications/10policies/b3/index.html; EU Directive 2010/63/EU for animal experiments http://ec.europa.eu/environment/chemicals/lab_animals/legislation_en.htm; Uniform Requirements for manuscripts submitted to Biomedical journals http://www.icmje.org. Authors should include a statement in the manuscript that informed consent was obtained for experimentation with human subjects. The privacy rights of human subjects must always be observed.

Conflict of interest

All authors are requested to disclose any actual or potential conflict of interest including any financial, personal or other relationships with other people or organizations within three years of beginning the submitted work that could inappropriately influence, or be perceived to influence, their work. See alsohttp://www.elsevier.com/conflictsofinterest. Further information and an example of a Conflict of Interest form can be found at: http://help.elsevier.com/app/answers/detail/a_id/286/p/7923.

Submission declaration

Submission of an article implies that the work described has not been published previously (except in the form of an abstract or as part of a published lecture or

academic thesis or as an electronic preprint, seehttp://www.elsevier.com/sharingpolicy), that it is not under consideration for publication elsewhere, that its publication is approved by all authors and tacitly or explicitly by the responsible authorities where the work was carried out, and that, if accepted, it will not be published elsewhere including electronically in the same form, in English or in any other language, without the written consent of the copyright-holder.

Contributors

Each author is required to declare his or her individual contribution to the article: all authors must have materially participated in the research and/or article preparation, so roles for all authors should be described. The statement that all authors have approved the final article should be true and included in the disclosure.

Changes to authorship

This policy concerns the addition, deletion, or rearrangement of author names in the authorship of accepted manuscripts:
Before the accepted manuscript is published in an online issue: Requests to add or remove an author, or to rearrange the author names, must be sent to the Journal Manager from the corresponding author of the accepted manuscript and must include: (a) the reason the name should be added or removed, or the author names rearranged and (b) written confirmation (e-mail, fax, letter) from all authors that they agree with the addition, removal or rearrangement. In the case of addition or removal of authors, this includes confirmation from the author being added or removed. Requests that are not sent by the corresponding author will be forwarded by the Journal Manager to the corresponding author, who must follow the procedure as described above. Note that: (1) Journal Managers will inform the Journal Editors of any such requests and (2) publication of the accepted manuscript in an online issue is suspended until authorship has been agreed.

After the accepted manuscript is published in an online issue: Any requests to add, delete, or rearrange author names in an article published in an online issue will follow the same policies as noted above and result in a corrigendum.

Copyright

Upon acceptance of an article, authors will be asked to complete a 'Journal Publishing Agreement' (for more information on this and copyright, see http://www.elsevier.com/copyright). An e-mail will be sent to the corresponding author confirming receipt of the manuscript together with a 'Journal Publishing Agreement' form or a link to the online version of this agreement.

Subscribers may reproduce tables of contents or prepare lists of articles including abstracts for internal circulation within their institutions. Permission of the Publisher is required for resale or distribution outside the institution and for all other derivative works, including compilations and translations (please consulthttp://www.elsevier.com/permissions). If excerpts from other copyrighted works are included, the author(s) must obtain written permission from the copyright owners and credit the source(s) in the article. Elsevier has preprinted forms for use by authors in these cases: please consult http://www.elsevier.com/permissions.

For open access articles: Upon acceptance of an article, authors will be asked to complete an 'Exclusive License Agreement' (for more information see http://www.elsevier.com/OAauthoragreement). Permitted third party reuse of open access articles is determined by the author's choice of user license (seehttp://www.elsevier.com/openaccesslicenses).

Author rights

As an author you (or your employer or institution) have certain rights to reuse your work. For more information seehttp://www.elsevier.com/copyright.

Role of the funding source

You are requested to identify who provided financial support for the conduct of the research and/or preparation of the article and to briefly describe the role of the sponsor(s), if any, in study design; in the collection, analysis and interpretation of data; in the writing of the report; and in the decision to submit the article for publication. If the funding source(s) had no such involvement then this should be stated.

Funding body agreements and policies

Elsevier has established a number of agreements with funding bodies which allow authors to comply with their funder's open access policies. Some authors may also be reimbursed for associated publication fees. To learn more about existing agreements please visit http://www.elsevier.com/fundingbodies.

Open access

This journal offers authors a choice in publishing their research:

Open access

• Articles are freely available to both subscribers and the wider public with permitted reuse
• An open access publication fee is payable by authors or on their behalf e.g. by their research funder or institution

Subscription
• Articles are made available to subscribers as well as developing countries and patient groups through our universal access programs (http://www.elsevier.com/access).
• No open access publication fee payable by authors.

Regardless of how you choose to publish your article, the journal will apply the same peer review criteria and acceptance standards.

For open access articles, permitted third party (re)use is defined by the following Creative Commons user licenses:

Creative Commons Attribution (CC BY)

Lets others distribute and copy the article, create extracts, abstracts, and other revised versions, adaptations or derivative works of or from an article (such as a translation), include in a collective work (such as an anthology), text or data mine the article, even for commercial purposes, as long as they credit the author(s), do not represent the author as endorsing their adaptation of the article, and do not modify the article in such a way as to damage the author's honor or reputation.

Creative Commons Attribution-NonCommercial-NoDerivs (CC BY-NC-ND) For non-commercial purposes, lets others distribute and copy the article, and to include in a collective work (such as an anthology), as long as they credit the author(s) and provided they do not alter or modify the article.

The open access publication fee for this journal is **USD 2600**, excluding taxes. Learn more about Elsevier's pricing policy: http://www.elsevier.com/openaccesspricing.

Language (usage and editing services)

Please write your text in good English (American or British usage is accepted, but not a mixture of these). Authors who feel their English language manuscript may require editing to eliminate possible grammatical or spelling errors and to conform to correct scientific English may wish to use the English Language Editing service available from Elsevier's WebShop (http://webshop.elsevier.com/languageediting/) or visit our customer support site (http://support.elsevier.com) for more information.

Submission

Our online submission system guides you stepwise through the process of entering your article details and uploading your files. The system converts your article files to a single PDF file used in the peer-review process. Editable files (e.g., Word, LaTeX) are required to typeset your article for final publication. All correspondence, including notification of the Editor's decision and requests for revision, is sent by e-mail.

For submitting your manuscript to Colloids and Surfaces B: Biointerfaces please go to our Elsevier Editorial System (EES) Website at: http://ees.elsevier.com/colsub/ .

Referees

Please submit, as part of the covering letter with the manuscript, the names, affiliation and email addresses of four potential Referees. Appropriate Referees should be knowledgeable about the subject but have no close connection with any of the authors. In addition, Referees should be from institutions other than (and preferably countries other than) those of any of the Authors.

Preparation

Use of word processing software

It is important that the file be saved in the native format of the word processor used. The text should be in single-column format. Keep the layout of the text as simple as possible. Most formatting codes will be removed and replaced on processing the article. In particular, do not use the word processor's options to justify text or to hyphenate words. However, do use bold face, italics, subscripts, superscripts etc. When preparing tables, if you are using a table grid, use only one grid for each individual table and not a grid for each row. If no grid is used, use tabs, not spaces, to align columns. The electronic text should be prepared in a way very similar to that of conventional manuscripts (see also the Guide to Publishing with Elsevier: http://www.elsevier.com/guidepublication). Note that source files of figures, tables and text graphics will be required whether or not you embed your figures in the text. See also the section on Electronic artwork.

To avoid unnecessary errors you are strongly advised to use the 'spell-check' and 'grammar-check' functions of your word processor.

Subdivision - unnumbered sections

Divide your article into clearly defined sections. Each subsection is given a brief heading. Each heading should appear on its own separate line. Subsections should be used as much as possible when cross-referencing text: refer to the subsection by heading as opposed to simply 'the text'.

Introduction
State the objectives of the work and provide an adequate background, avoiding a detailed literature survey or a summary of the results.

Material and methods

Provide sufficient detail to allow the work to be reproduced. Methods already published should be indicated by a reference: only relevant modifications should be described.

Results
Results should be clear and concise.

Discussion
This should explore the significance of the results of the work, not repeat them. A combined Results and Discussion section is often appropriate. Avoid extensive citations and discussion of published literature.

Conclusions
The main conclusions of the study may be presented in a short Conclusions section, which may stand alone or form a subsection of a Discussion or Results and Discussion section.

Appendices
If there is more than one appendix, they should be identified as A, B, etc. Formulae and equations in appendices should be given separate numbering: Eq. (A.1), Eq. (A.2), etc.; in a subsequent appendix, Eq. (B.1) and so on. Similarly for tables and figures: Table A.1; Fig. A.1, etc.

Essential title page information

• **Title.** Concise and informative. Titles are often used in information-retrieval systems. Avoid abbreviations and formulae where possible.
• **Author names and affiliations.** Where the family name may be ambiguous (e.g., a double name), please indicate this clearly. Present the authors' affiliation addresses (where the actual work was done) below the names. Indicate all affiliations with a lower-case superscript letter immediately after the author's name and in front of the appropriate address. Provide the full postal address of each affiliation, including the country name and, if available, the e-mail address of each author.
• **Corresponding author.** Clearly indicate who will handle correspondence at all stages of refereeing and publication, also post-publication. **Ensure that the e-mail address is given and that contact details are kept up to date by the corresponding author.**
• **Present/permanent address.** If an author has moved since the work described in the article was done, or was visiting at the time, a 'Present address' (or 'Permanent address') may be indicated as a footnote to that author's name. The address at which the author

actually did the work must be retained as the main, affiliation address. Superscript Arabic numerals are used for such footnotes.

Abstract

A concise and factual abstract is required. The abstract should state briefly the purpose of the research, the principal results and major conclusions. An abstract is often presented separately from the article, so it must be able to stand alone. For this reason, References should be avoided, but if essential, then cite the author(s) and year(s). Also, non-standard or uncommon abbreviations should be avoided, but if essential they must be defined at their first mention in the abstract itself.

The abstract should be no longer than 250 words

Graphical abstract

A Graphical abstract is mandatory for this journal. It should summarize the contents of the article in a concise, pictorial form designed to capture the attention of a wide readership online. Authors must provide images that clearly represent the work described in the article. Graphical abstracts should be submitted as a separate file in the online submission system. Image size: please provide an image with a minimum of 531 × 1328 pixels (h × w) or proportionally more. The image should be readable at a size of 5 × 13 cm using a regular screen resolution of 96 dpi. Preferred file types: TIFF, EPS, PDF or MS Office files. See http://www.elsevier.com/graphicalabstracts for examples. Authors can make use of Elsevier's Illustration and Enhancement service to ensure the best presentation of their images also in accordance with all technical requirements: Illustration Service.

Highlights

Highlights are mandatory for this journal. They consist of a short collection of bullet points that convey the core findings of the article and should be submitted in a separate editable file in the online submission system. Please use 'Highlights' in the file name and include 3 to 5 bullet points (maximum 85 characters, including spaces, per bullet point). See http://www.elsevier.com/highlights for examples.

Keywords

Immediately after the abstract, provide a maximum of 6 keywords, using American spelling and avoiding general and plural terms and multiple concepts (avoid, for example, 'and', 'of'). Be sparing with abbreviations: only abbreviations firmly established in the field may be eligible. These keywords will be used for indexing purposes.

Acknowledgements

Collate acknowledgements in a separate section at the end of the article before the references and do not, therefore, include them on the title page, as a footnote to the title or otherwise. List here those individuals who provided help during the research (e.g., providing language help, writing assistance or proof reading the article, etc.).

Nomenclature and Units

The use of nomenclature and symbols adopted by IUPAC is recommended (Quantities, Units and Symbols in Physical Chemistry, Blackwell Scientific, Oxford, 1988).

Math formulae

Please submit math equations as editable text and not as images. Present simple formulae in line with normal text where possible and use the solidus (/) instead of a horizontal line for small fractional terms, e.g., X/Y. In principle, variables are to be presented in italics. Powers of e are often more conveniently denoted by exp. Number consecutively any equations that have to be displayed separately from the text (if referred to explicitly in the text).

Footnotes

Footnotes should be used sparingly. Number them consecutively throughout the article. Many word processors can build footnotes into the text, and this feature may be used. Otherwise, please indicate the position of footnotes in the text and list the footnotes themselves separately at the end of the article. Do not include footnotes in the Reference list.

Artwork

Electronic artwork

General points

• Make sure you use uniform lettering and sizing of your original artwork.
• Embed the used fonts if the application provides that option.
• Aim to use the following fonts in your illustrations: Arial, Courier, Times New Roman, Symbol, or use fonts that look similar.
• Number the illustrations according to their sequence in the text.
• Use a logical naming convention for your artwork files.
• Provide captions to illustrations separately.
• Size the illustrations close to the desired dimensions of the published version.
• Submit each illustration as a separate file.
A detailed guide on electronic artwork is available on our website: http://www.elsevier.com/artworkinstructions
You are urged to visit this site; some excerpts from the detailed information are given here.

Formats
If your electronic artwork is created in a Microsoft Office application (Word, PowerPoint, Excel) then please supply 'as is' in the native document format. Regardless of the application used other than Microsoft Office, when your electronic artwork is finalized, please 'Save as' or convert the images to one of the following formats (note the resolution requirements for line drawings, halftones, and line/halftone combinations given below):

EPS (or PDF): Vector drawings, embed all used fonts.

TIFF (or JPEG): Color or grayscale photographs (halftones), keep to a minimum of 300 dpi.

TIFF (or JPEG): Bitmapped (pure black & white pixels) line drawings, keep to a minimum of 1000 dpi.

TIFF (or JPEG): Combinations bitmapped line/half-tone (color or grayscale), keep to a minimum of 500 dpi.

Please do not:

• Supply files that are optimized for screen use (e.g., GIF, BMP, PICT, WPG); these typically have a low number of pixels and limited set of colors;

• Supply files that are too low in resolution;

• Submit graphics that are disproportionately large for the content.

Color artwork

Please make sure that artwork files are in an acceptable format (TIFF (or JPEG), EPS (or PDF), or MS Office files) and with the correct resolution. If, together with your accepted article, you submit usable color figures then Elsevier will ensure, at no additional charge, that these figures will appear in color online (e.g., ScienceDirect and other sites) regardless of whether or not these illustrations are reproduced in color in the printed version. **For color reproduction in print, you will receive information regarding the costs from Elsevier after receipt of your accepted article**. Please indicate your preference for color: in print or online only. For further information on the preparation of electronic artwork, please see http://www.elsevier.com/artworkinstructions.

Please note: Because of technical complications that can arise by converting color figures to 'gray scale' (for the printed version should you not opt for color in print) please submit in addition usable black and white versions of all the color illustrations.

Figure captions

Ensure that each illustration has a caption. Supply captions separately, not attached to the figure. A caption should comprise a brief title (**not** on the figure itself) and a description of the illustration. Keep text in the illustrations themselves to a minimum but explain all symbols and abbreviations used.

Tables

Please submit tables as editable text and not as images. Tables can be placed either next to the relevant text in the article, or on separate page(s) at the end. Number tables consecutively in accordance with their appearance in the text and place any table notes below the table body. Be sparing in the use of tables and ensure that the data presented in them do not duplicate results described elsewhere in the article. Please avoid using vertical rules.

Citation in text

Please ensure that every reference cited in the text is also present in the reference list (and vice versa). Any references cited in the abstract must be given in full. Unpublished results and personal communications are not recommended in the reference list, but may be mentioned in the text. If these references are included in the reference list they should follow the standard reference style of the journal and should include a substitution of the publication date with either 'Unpublished results' or 'Personal

communication'. Citation of a reference as 'in press' implies that the item has been accepted for publication.

Reference links

Increased discoverability of research and high quality peer review are ensured by online links to the sources cited. In order to allow us to create links to abstracting and indexing services, such as Scopus, CrossRef and PubMed, please ensure that data provided in the references are correct. Please note that incorrect surnames, journal/book titles, publication year and pagination may prevent link creation. When copying references, please be careful as they may already contain errors. Use of the DOI is encouraged.

Reference management software

This journal has standard templates available in key reference management packages EndNote (http://www.endnote.com/support/enstyles.asp) and Reference Manager (http://refman.com/support/rmstyles.asp). Using plug-ins to wordprocessing packages, authors only need to select the appropriate journal template when preparing their article and the list of references and citations to these will be formatted according to the journal style which is described below.

Reference formatting

There are no strict requirements on reference formatting at submission. References can be in any style or format as long as the style is consistent. Where applicable, author(s) name(s), journal title/book title, chapter title/article title, year of publication, volume number/book chapter and the pagination must be present. Use of DOI is highly encouraged. The reference style used by the journal will be applied to the accepted article by Elsevier at the proof stage. Note that missing data will be highlighted at proof stage for the author to correct. If you do wish to format the references yourself they should be arranged according to the following examples:

Reference Style

1. All references made to publications in the text should be presented in a list of references following the text of the manuscript. The manuscript should be carefully checked to ensure that the information given in the text is exactly the same as that given in the reference list.

References to the literature should be made according to the numerical system described below.
2. In the text refer to the subject or to the author's name (without initial), followed by the reference number in square brackets.

3. If reference is made in the text to publications written by more than two authors, the name of the first author should be used, followed by "et al.". Note that in the reference list the names of authors and co-authors should be given in full.
4. References should be arranged in the order in which they appear in the text.
5. Use the following system for arranging the references:
(i) For journals

N. Levy, N. Garti and S. Margdassi, Colloids Surfaces A: Physicochem. Eng. Aspects, 97 (1995) 91.

(ii) For monographs

B.E. Conway, Ionic Hydration in Chemistry and Biophysics, Elsevier, Amsterdam, 1981.
(iii) For edited books

R.D. Thomas, in E. Buncel and J.R. Jones (Eds.), Isotopes in the Physical and Biomedical Sciences, Vol. 2, Elsevier, Amsterdam, 1991, Chapter 7.
For conference proceedings, symposia etc.

A.G. Marshall, in P.G. Kistemaker and N.M.M. Nibbering (Eds.), Advances in Mass Spectrometry, Proc. 12th International Mass Spectrometry Conference, Amsterdam, 26-30 August 1991, Elsevier, Amsterdam, 1992, p. 37.

6. Abbreviations of journal titles should conform to those adopted by the Chemical Abstract Service (Bibliographic Guide for Editors and Authors, The American Chemical Society, Washington, DC, 1974). If the correct abbreviation is not known, the title should be given in full.

7. Reference to a personal communication should be followed by the year, e.g. A.N. Other, personal communication, 1989.

Journal abbreviations source

Journal names should be abbreviated according to the List of Title Word Abbreviations:http://www.issn.org/services/online-services/access-to-the-ltwa/.

Video data

Elsevier accepts video material and animation sequences to support and enhance your scientific research. Authors who have video or animation files that they wish to submit with their article are strongly encouraged to include links to these within the body of the article. This can be done in the same way as a figure or table by referring to the video or animation content and noting in the body text where it should be placed. All submitted files should be properly labeled so that they directly relate to the video file's content. In order to ensure that your video or animation material is directly usable, please provide the files in one of our recommended file formats with a preferred maximum size of 50 MB. Video and animation files supplied will be published online in the electronic version of your article in Elsevier Web products, including ScienceDirect: http://www.sciencedirect.com. Please supply 'stills' with your files: you can choose any frame from the video or animation or make a separate image. These will be used instead of standard icons and will personalize the link to your video data. For more detailed instructions please visit our video instruction pages at http://www.elsevier.com/artworkinstructions. Note: since video and animation cannot be embedded in the print version of the journal, please provide text for both the electronic and the print version for the portions of the article that refer to this content.

AudioSlides

The journal encourages authors to create an AudioSlides presentation with their published article. AudioSlides are brief, webinar-style presentations that are shown next to the online article on ScienceDirect. This gives authors the opportunity to summarize their research in their own words and to help readers understand what the paper is about. More information and examples are available at http://www.elsevier.com/audioslides. Authors of this journal will automatically receive an invitation e-mail to create an AudioSlides presentation after acceptance of their paper.

Supplementary data

Elsevier accepts electronic supplementary material to support and enhance your scientific research. Supplementary files offer the author additional possibilities to publish supporting applications, high-resolution images, background datasets, sound clips and more. Supplementary files supplied will be published online alongside the electronic version of your article in Elsevier Web products, including ScienceDirect: http://www.sciencedirect.com. In order to ensure that your submitted material is directly usable, please provide the data in one of our recommended file formats. Authors should submit the material in electronic format together with the article and supply a concise and descriptive caption for each file. For more detailed instructions please visit our artwork instruction pages athttp://www.elsevier.com/artworkinstructions.

3D molecular models

You can enrich your online articles by providing 3D molecular models (optional) in PDB, PSE or MOL/MOL2 format, which will be visualized using the interactive viewer embedded within the article. Using the viewer, it will be possible to zoom into the model, rotate and pan the model, and change display settings. Submitted models will also be available for downloading from your online article on ScienceDirect. Each molecular model will have to be uploaded to the online submission system separately, via the '3D molecular models' submission category. For more information see: http://www.elsevier.com/3DMolecularModels.

Interactive plots

This journal encourages you to include data and quantitative results as interactive plots with your publication. To make use of this feature, please include your data as a CSV (comma-separated values) file when you submit your manuscript. Please refer to http://www.elsevier.com/interactiveplots for further details and formatting instructions.

Submission checklist

The following list will be useful during the final checking of an article prior to sending it to the journal for review. Please consult this Guide for Authors for further details of any item.

Ensure that the following items are present:

One author has been designated as the corresponding author with contact details:

• E-mail address

• Full postal address

All necessary files have been uploaded, and contain:

• Keywords

• All figure captions

• All tables (including title, description, footnotes)

Further considerations

• Manuscript has been 'spell-checked' and 'grammar-checked'

• References are in the correct format for this journal

• All references mentioned in the Reference list are cited in the text, and vice versa

• Permission has been obtained for use of copyrighted material from other sources (including the Internet)

Printed version of figures (if applicable) in color or black-and-white
• Indicate clearly whether or not color or black-and-white in print is required.
• For reproduction in black-and-white, please supply black-and-white versions of the figures for printing purposes.

For any further information please visit our customer support site at http://support.elsevier.com.

After Acceptance

Use of the Digital Object Identifier

The Digital Object Identifier (DOI) may be used to cite and link to electronic documents. The DOI consists of a unique alpha-numeric character string which is assigned to a document by the publisher upon the initial electronic publication. The assigned DOI never changes. Therefore, it is an ideal medium for citing a document, particularly 'Articles in press' because they have not yet received their full bibliographic information. Example of a correctly given DOI (in URL format; here an article in the journal *Physics Letters B*):
http://dx.doi.org/10.1016/j.physletb.2010.09.059
When you use a DOI to create links to documents on the web, the DOIs are guaranteed never to change.

Online proof correction

Corresponding authors will receive an e-mail with a link to our online proofing system, allowing annotation and correction of proofs online. The environment is similar to MS Word: in addition to editing text, you can also comment on figures/tables and answer questions from the Copy Editor. Web-based proofing provides a faster and less error-prone process by allowing you to directly type your corrections, eliminating the potential introduction of errors.
If preferred, you can still choose to annotate and upload your edits on the PDF version. All instructions for proofing will be given in the e-mail we send to authors, including alternative methods to the online version and PDF.
We will do everything possible to get your article published quickly and accurately. Please use this proof only for checking the typesetting, editing, completeness and correctness of the text, tables and figures. Significant changes to the article as accepted for publication will only be considered at this stage with permission from the Editor.It is important to ensure that all corrections are sent back to us in one communication. Please check carefully before replying, as inclusion of any subsequent corrections cannot be guaranteed. Proofreading is solely your responsibility.

Offprints

The corresponding author, at no cost, will be provided with a personalized link providing 50 days free access to the final published version of the article

on ScienceDirect. This link can also be used for sharing via email and social networks. For an extra charge, paper offprints can be ordered via the offprint order form which is sent once the article is accepted for publication. Both corresponding and co-authors may order offprints at any time via Elsevier's WebShop (http://webshop.elsevier.com/myarticleservices/offprints). Authors requiring printed copies of multiple articles may use Elsevier WebShop's 'Create Your Own Book' service to collate multiple articles within a single cover (http://webshop.elsevier.com/myarticleservices/booklets).

Author Inquiries

You can track your submitted article

at http://help.elsevier.com/app/answers/detail/a_id/89/p/8045/. You can track your accepted article at http://www.elsevier.com/trackarticle. You are also welcome to contact Customer Support viahttp://support.elsevier.com.